

AD \_\_\_\_\_

Award Number: DAMD17-02-1-0435

TITLE: The Design, Synthesis, and Biological Evaluation of New Paclitaxel Analogs with the Ability to Evade Efflux by P- glycoprotein

PRINCIPAL INVESTIGATOR: Brandon J. Turunen, Ph.D.

CONTRACTING ORGANIZATION: University of Kansas  
Lawrence, KS 66047

REPORT DATE: May 2005

TYPE OF REPORT: Annual Summary

PREPARED FOR: U.S. Army Medical Research and Materiel Command  
Fort Detrick, Maryland 21702-5012

DISTRIBUTION STATEMENT: Approved for Public Release;  
Distribution Unlimited

The views, opinions and/or findings contained in this report are those of the author(s) and should not be construed as an official Department of the Army position, policy or decision unless so designated by other documentation.

<b>REPORT DOCUMENTATION PAGE</b>				<i>Form Approved</i> <b>OMB No. 0704-0188</b>	
Public reporting burden for this collection of information is estimated to average 1 hour per response, including the time for reviewing instructions, searching existing data sources, gathering and maintaining the data needed, and completing and reviewing this collection of information. Send comments regarding this burden estimate or any other aspect of this collection of information, including suggestions for reducing this burden to Department of Defense, Washington Headquarters Services, Directorate for Information Operations and Reports (0704-0188), 1215 Jefferson Davis Highway, Suite 1204, Arlington, VA 22202-4302. Respondents should be aware that notwithstanding any other provision of law, no person shall be subject to any penalty for failing to comply with a collection of information if it does not display a currently valid OMB control number. <b>PLEASE DO NOT RETURN YOUR FORM TO THE ABOVE ADDRESS.</b>					
<b>1. REPORT DATE</b> 01-05-2005		<b>2. REPORT TYPE</b> Annual Summary		<b>3. DATES COVERED</b> 1 May 2002 – 30 Apr 2005	
<b>4. TITLE AND SUBTITLE</b> The Design, Synthesis, and Biological Evaluation of New Paclitaxel Analogs with the Ability to Evade Efflux by P- glycoprotein				<b>5a. CONTRACT NUMBER</b>	
				<b>5b. GRANT NUMBER</b> DAMD17-02-1-0435	
				<b>5c. PROGRAM ELEMENT NUMBER</b>	
<b>6. AUTHOR(S)</b>  Brandon J. Turunen, Ph.D.				<b>5d. PROJECT NUMBER</b>	
				<b>5e. TASK NUMBER</b>	
				<b>5f. WORK UNIT NUMBER</b>	
<b>7. PERFORMING ORGANIZATION NAME(S) AND ADDRESS(ES)</b>  University of Kansas Lawrence, KS 66047				<b>8. PERFORMING ORGANIZATION REPORT NUMBER</b>	
<b>9. SPONSORING / MONITORING AGENCY NAME(S) AND ADDRESS(ES)</b> U.S. Army Medical Research and Materiel Command Fort Detrick, Maryland 21702-5012				<b>10. SPONSOR/MONITOR'S ACRONYM(S)</b>	
				<b>11. SPONSOR/MONITOR'S REPORT NUMBER(S)</b>	
<b>12. DISTRIBUTION / AVAILABILITY STATEMENT</b> Approved for Public Release; Distribution Unlimited					
<b>13. SUPPLEMENTARY NOTES</b> Original contains colored plates: ALL DTIC reproductions will be in black and white.					
<b>14. ABSTRACT</b> Regioisomeric, functional group, and one-carbon homologs of the semi-synthetic paclitaxel compound TX-67 (C10 hemi-succinate) have been prepared to investigate its lack of interaction with P-glycoprotein (Pgp). In accord with Seelig's model and our previous reports, all carboxylic acid analogs had no apparent interactions with Pgp. Furthermore, it is demonstrated that hydrogen-bonding properties were significant with respect to Pgp interactions. This anionic introduction strategy may allow for delivery of paclitaxel into the CNS as well as establishing an alternative strategy for delivery of other, non-CNS permeable drugs.					
<b>15. SUBJECT TERMS</b> Paclitaxel, Taxol, P-glycoprotein, MDR					
<b>16. SECURITY CLASSIFICATION OF:</b>			UU	<b>18. NUMBER OF PAGES</b>  54	<b>19a. NAME OF RESPONSIBLE PERSON</b> USAMRMC
<b>a. REPORT</b> U	<b>b. ABSTRACT</b> U	<b>c. THIS PAGE</b> U			<b>19b. TELEPHONE NUMBER</b> (include area code)

**Table of Contents**

**Cover.....1**

**SF 298.....2**

**Introduction.....4**

**Body.....5**

**Key Research Accomplishments.....20**

**Reportable Outcomes.....20**

**Conclusions.....20**

**References.....21**

**Appendices.....23**

# The Design, Synthesis, and Biological Evaluation of New Paclitaxel Analogs with the Ability to Evade Efflux by P-glycoprotein

## 1. Introduction

P-glycoproteins are non-specific transmembrane transporters that are present in normal cells and in tumors. They are associated with specialized normal tissue barriers such as the blood brain barrier (BBB), and are generally over expressed in tumor cells. It is believed that active P-glycoprotein efflux of highly lipophilic anti-cancer drugs such as paclitaxel is responsible for the development of drug resistance and also lack of brain uptake.<sup>1,2</sup> The problems in effectively treating drug resistant breast cancer and primary/metastatic brain cancer clearly indicate there is a need for the development of new drug delivery strategies. At the outset, the primary focus of this research entailed the covalent linkage of endogenous substances to paclitaxel or analogs. Transport carriers exist in the capillary endothelial cells of the blood brain barrier and also in drug resistant breast cancer cells to bring these substances into the cell. By attaching essential hydrophilic molecules such as amino acids, carboxylic acids, amines, and biotin, these paclitaxel analogs may circumvent the P-glycoprotein efflux via active transport into cells/past the BBB. This approach leaves the P-glycoprotein transporters intact and capable of performing their physiological role, potentially a factor for normal tissue survival.<sup>3</sup>

During the early stages of this research it was uncovered that the proposed carboxylic acid analogs were particularly promising. In addition, it was found that the analogs covalently bound to large molecules (ex. biotin) lost nearly all of the parent molecules activity in preliminary cytotoxicity assays (see previous annual report for details). Because of this, a modest redirection of the proposed research was undertaken focusing largely upon the carboxylic acid analogs. In addition, this aimed our studies toward other C3'N and C10 structural modifications to circumvent P-gp efflux (Section 3).

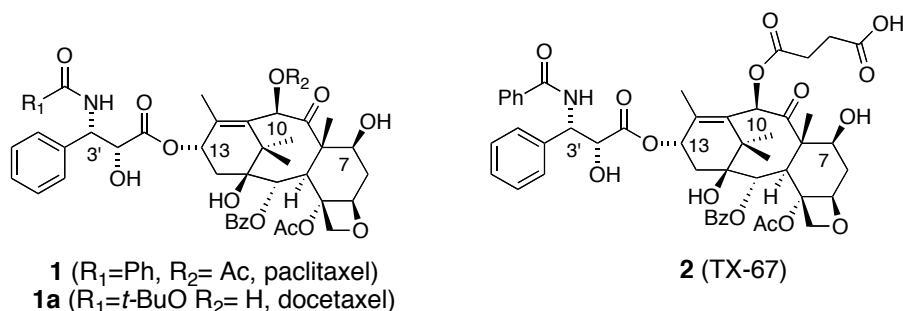


**Figure 1.** Paclitaxel, Docetaxel and TX-67

## 1.1 Seelig model vs. Active Transport

Seelig observed that compounds which carry a negative charge at physiological pH, such as those that contain a carboxylic acid, sulphonate, or nitro group, with few exceptions, *are not substrates for Pgp efflux*.<sup>4</sup> One caveat to this observation was that chemical structures that contain additional recognition elements, much like TX-67, will maintain their affinity for Pgp. Figure 16 illustrates the Pgp recognition elements (both type I and type II units) present in TX-67. As can be seen, TX-67 contains multiple recognition elements as well as a carboxylic acid, and appears to be an exception to this model. Our studies suggest that Pgp efflux mechanisms are substantially reduced or absent completely with respect to TX-67.<sup>5</sup> Our group and others have shown that particular modifications to C10 of taxanes provide analogs with increased effectiveness in controlling growth of Pgp expressing cancer cell lines.<sup>6</sup> These studies indicate the importance of this region of the molecule toward Pgp recognition.

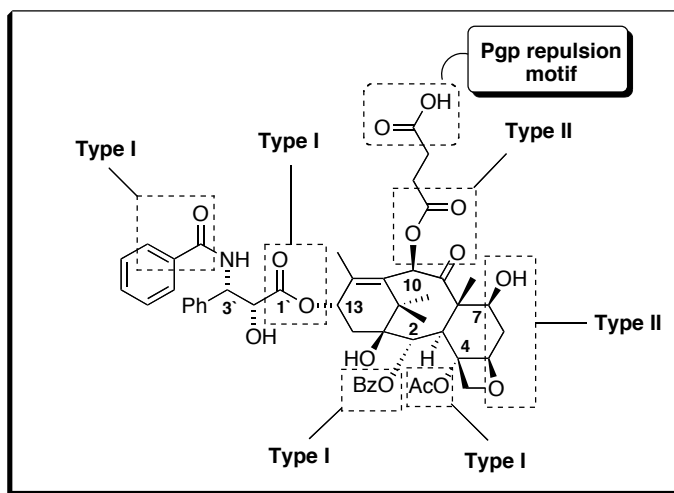


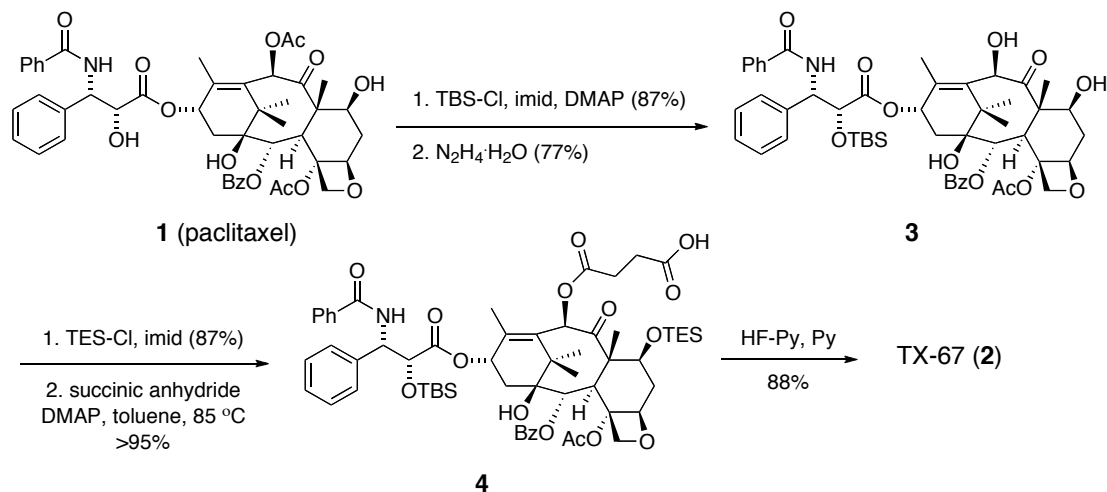
**Figure 2.** TX-67 recognition elements and acid moiety

It should also be considered that this carboxylic acid functionality may be serving as a surrogate for an influx pump, in a similar fashion that paclitaxel acts as a substrate for cellular eviction. Carboxylic acid transporters are known to exist within the BBB and it is possible that this transport system is shuttling TX-67 into the cell, past the Pgp efflux system, allowing for the observed increase in BBB permeation.<sup>7,8</sup>

## 2. C7 and C10 Analog Synthesis

To further investigate this phenomenon we proposed the preparation of a focused library of TX-67 analogs. The compounds prepared include functional group, regioisomeric, and one-carbon homologs. The acid functionality is

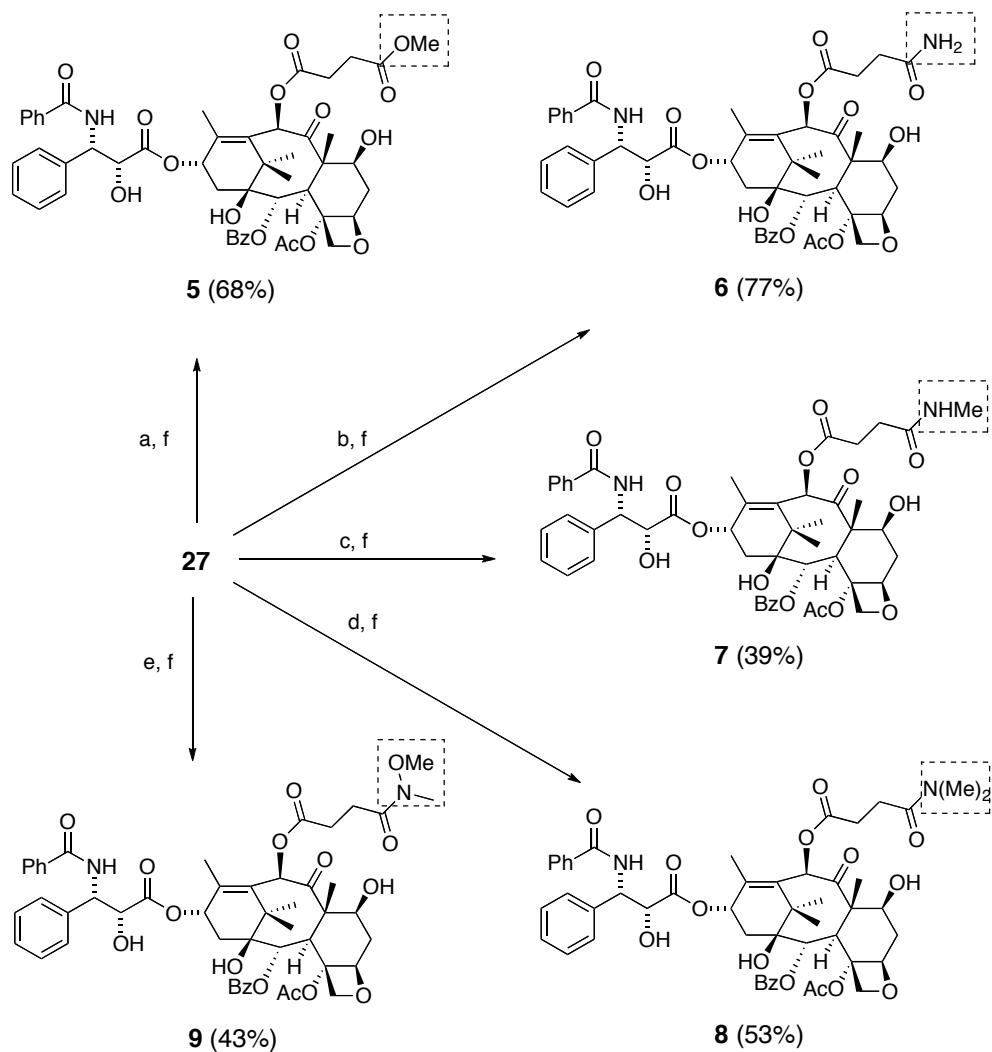
transformed to the ester as well as to a series of amides. These were made to evaluate the necessity for an anionic species as well as to investigate hydrogen-bonding effects. In addition, C7 analogs of the same are prepared as well as one carbon homologs (glutaric vs. succinic acid).



**Scheme 1.** TX-67 synthesis

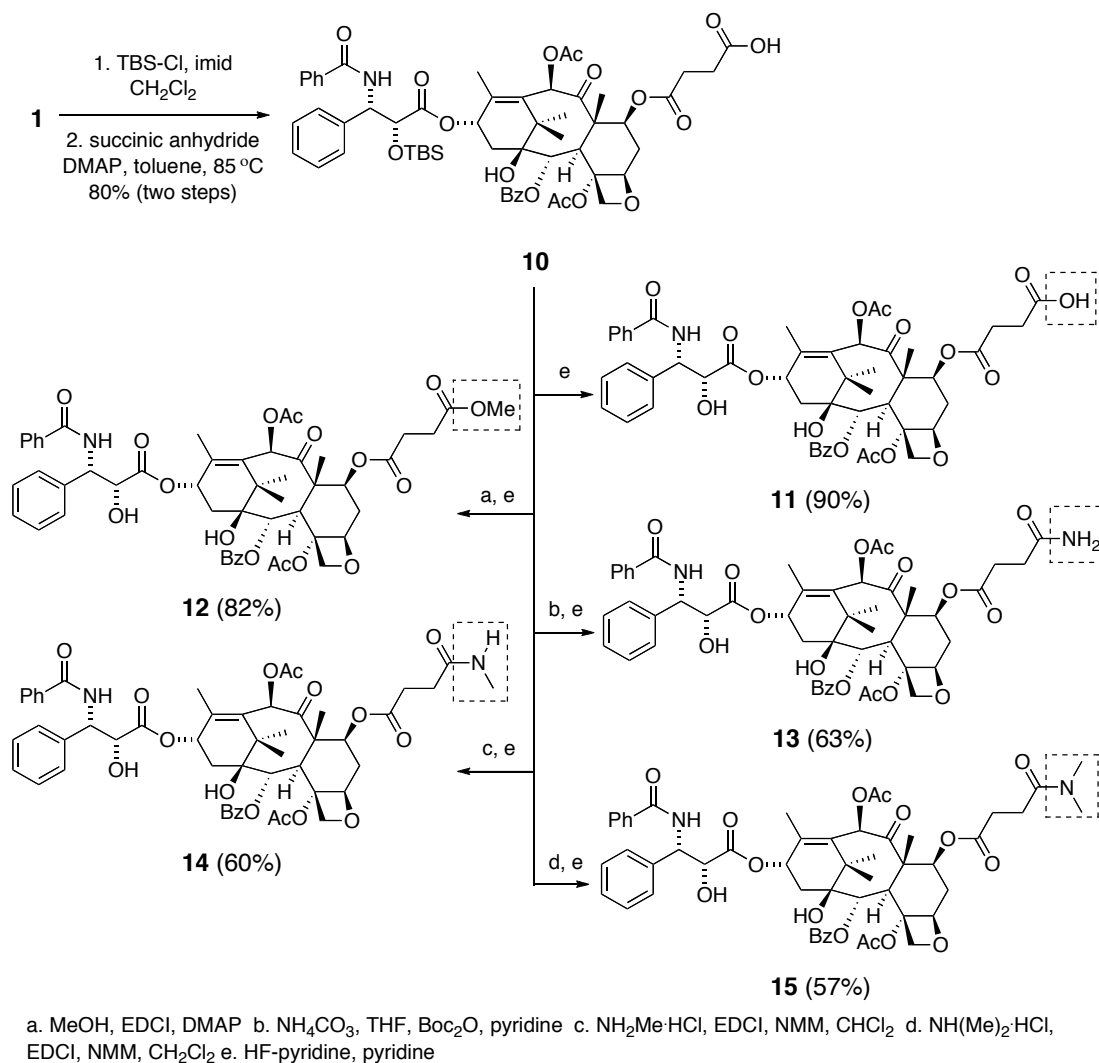
TX-67 (2), is prepared from paclitaxel by first selectively protecting the C2' alcohol as the *t*-butyldimethylsilyl ether (Scheme 1). Taking advantage of a method developed previously in our laboratory, the C10 acetyl ester is then discriminately cleaved, providing 3.<sup>9</sup> The C7 alcohol is protected as the triethylsilyl ether and the C10 hydroxyl succinylated, giving 4. Both compounds 3 and 4 will be critical intermediates in analog preparation. After removal of the silyl protecting groups, TX-67 (2) is arrived at in five steps and 49% overall yield.<sup>10</sup>

Many of the C10 functional group analogs can be prepared from common intermediate 4 (Scheme 2). The acid of 4 is cleanly and quantitatively converted to the methyl ester via treatment with diazomethane (Scheme 2), which, after treatment with HF-pyridine solution provides methyl ester 5 in good yield. The required primary amide (6) is prepared via mixed anhydride formation with  $\text{Boc}_2\text{O}$  followed by amide formation via ammonium bicarbonate ( $\text{NH}_4\text{CO}_3$ ) under basic conditions. The *N*-methyl, *N,N*-dimethyl, and Weinreb amides can all be accessed via standard coupling procedures employing EDCI as the coupling agent. It should be noted that although the yields are poor to moderate for examples 7-9, these yields were not optimized. Fluoride anion assisted protecting group removal then provides the desired analogs in reasonable yield.



a.  $\text{CH}_2\text{N}_2$ , THF    b.  $\text{NH}_4\text{CO}_3$ , THF,  $\text{Boc}_2\text{O}$ , pyridine    c.  $\text{NH}_2\text{Me}\cdot\text{HCl}$ , EDCI, NMM,  $\text{CHCl}_2$     d.  $\text{NH}(\text{Me})_2\cdot\text{HCl}$ , EDCI, NMM,  $\text{CH}_2\text{Cl}_2$     e.  $\text{NH}(\text{Me})\text{OMe}\cdot\text{HCl}$ , EDCI, NMM,  $\text{CH}_2\text{Cl}_2$     f. HF-pyridine, pyridine

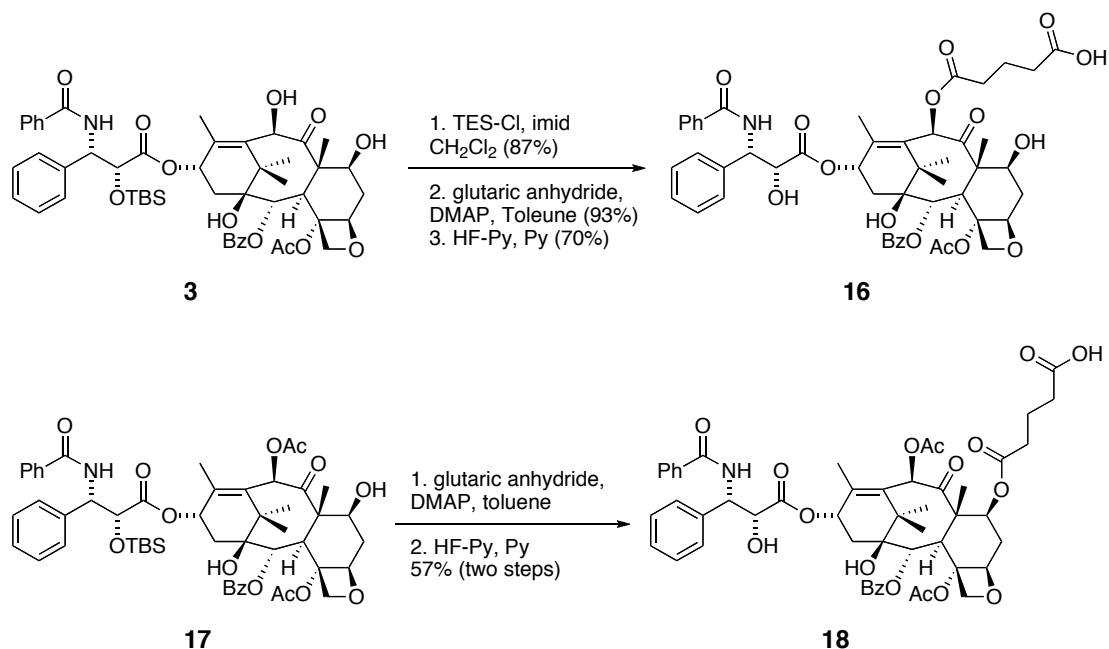
**Scheme 2.** C10 functional group analogs



**Scheme 3.** C7 Functional group analogs

The C7 analogs are accessed in short synthetic sequences from common intermediate **10** (Scheme 3); this compound is derived from paclitaxel in two steps in excellent yield. The C7 succinnic acid analog (**11**) is prepared by simply removing the 2'OTBS protecting group while the methyl ester analog (**12**) is generated from a DCC coupling between acid **10** and MeOH followed by the same deprotection. The same conditions for formation of the C10 primary amide are employed to provide the C7 analog (**13**). Standard coupling conditions employing EDCI to form amides **14** and **15** were uneventful and provided the targets in reasonable yield.

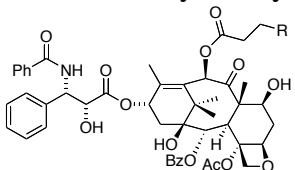




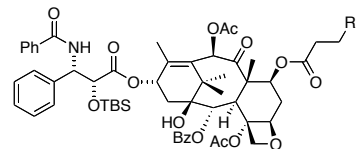
**Scheme 4.** One-carbon homologs of TX-67

The one carbon homolog of TX-67 was next prepared at both the C7 and C10 positions (Scheme 4). The C10 variant is generated from 2'-OTBS-10-deacetylpaclitaxel (**3**) by first protection of the C7 hydroxyl followed by acylation with glutaric anhydride. This intermediate is then treated with HF-pyridine complex to provide the desired compound **16**. The C7 glutaric acid analog **18** is prepared by the acylation of 2'-OTBS paclitaxel and silyl group removal.

**Table 1.** Tubulin assembly and cytotoxicity results



C10 Analogs



C7 Analogs

TX-67 Analog	Tubulin Assembly	MCF7	NCI/ADR-RES
paclitaxel ( <b>1</b> )	1.0	1.0	1.0
TX-67 ( <b>2</b> – C10 CO <sub>2</sub> H)	1.7	13.3	1.3
C10 CO <sub>2</sub> Me ( <b>5</b> )	1.0	2.5	0.4
C10 CONH <sub>2</sub> ( <b>6</b> )	0.4	10	6.0
C10 CONHMe ( <b>7</b> )	0.8	7.9	6.0
C10 CONMe <sub>2</sub> ( <b>8</b> )	1.6	2.1	2.7
C10 CON(OMe)Me ( <b>9</b> )	1.86	1.1	3.3
C10 CH <sub>2</sub> CO <sub>2</sub> H ( <b>16</b> )	1.8	27.9	5.8
C7 CO <sub>2</sub> H ( <b>11</b> )	3.8	>30.0	5.8
C7 CO <sub>2</sub> Me ( <b>12</b> )	1.2	0.54	0.5
C7 CONH <sub>2</sub> ( <b>13</b> )	0.6	3.2	0.6
C7 CONHMe ( <b>14</b> )	0.8	2.2	1.0
C7 CONMe <sub>2</sub> ( <b>15</b> )	1.1	10.8	0.8
C7 CH <sub>2</sub> CO <sub>2</sub> H ( <b>18</b> )	1.0	8.8	13.6

## 2.2 Biological Evaluation

We first screened the synthetic analogs in cytotoxicity and tubulin assembly assays. It was critical that our analogs maintain effectiveness against cancer cell lines to be of any utility. In addition, we screened our compounds against a drug resistant breast cancer cell line (NCI/ADR-RES). As with the epimeric paclitaxel analogs described in the previous chapter we reasoned that compounds which do not interact with Pgp would be more effective against these MDR cell lines. The results of these assays can be seen in Table 1.

In the tubulin assembly assay, all analogs maintained similar activity to the parent compound. Although not surprising since modifications at both the C7 and C10 OH are tolerated well, this result was pleasing. Their effectiveness against the breast cancer cell line (NCI/ADR-RES) compared well with paclitaxel with most analogs, however, two compounds (**16** and **11**) showed a significant reduction in activity while methyl ester **12** showed a modest improvement. Although we had hypothesized an increase in effectiveness of these analogs against the MDR breast cancer cell line (MCF7-ADR [Pgp over-expressing]) we were disappointed to find this was not the case. Although we see a modest increases in potency in several analogs (**5**, **12**, **13** and **15**), it should be reiterated that *paclitaxel is not an effective*

*anti-proliferative agent against this MDR cell line.* Therefore, an analog must exhibit potency on the order of 1000-times that of paclitaxel to be considered effective.

Our next biological screen was the rhodamine 123 uptake assay.<sup>11</sup> This assay is a preliminary screen to evaluate a compounds interaction with Pgp in bovine brain microvessel endothelial cells (BMECs). Audus et al., have developed this assay to determine a compounds ability to bind Pgp in the presence of a rhodamine dye. Our compounds have been evaluated in this assay and the results can be seen in Figure 3.

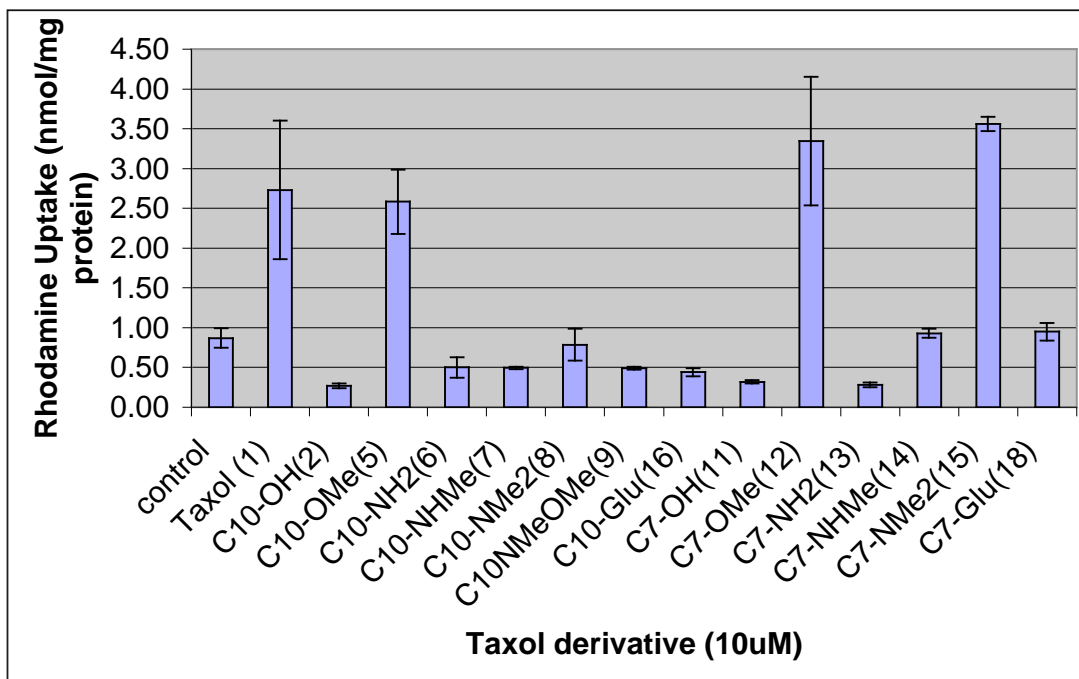


**Figure 3.** C7 and C10 TX-67 analogs rhodamine assay results

As anticipated all analogs containing a carboxylic acid functionality (**2**, **11**, **16** and **18**) showed no apparent interaction with Pgp in this assay. When the carboxylic acid is capped with a methyl group (**5** and **12**), in both the C7 and C10 series, a marked increase in rhodamine accumulation is observed. This is not surprising since the anionic character of the molecule is removed as well as adding an additional type I recognition element to paclitaxel. Somewhat surprisingly, none of the C10 amides (**5-8**) exhibited characteristics of a Pgp substrate. These examples are contrary to our hypothesis that an anion is required and suggest that other factors may play a role in recognition by Pgp. We speculate that the C10 region of paclitaxel is particularly important in the recognition by Pgp and may have steric requirements not met by these analogs. This would suggest however that any large group on this position should inhibit Pgp interactions, which is not the case. The C7 amide series displays an interesting, near linear trend. As the functional group on these analogs is

converting from a hydrogen bond donor to a hydrogen bond acceptor, we see transformation from a molecule that shows no interactions with Pgp to one which is an apparent substrate. This is in accord with Seelig's hypothesis that H-bond donors will not interact with Pgp and H-bond acceptors will serve as substrates. This may suggest that these particular analogs have a very intimate relationship with Pgp.

### 3. 3'N and C10 modifications, synthesis

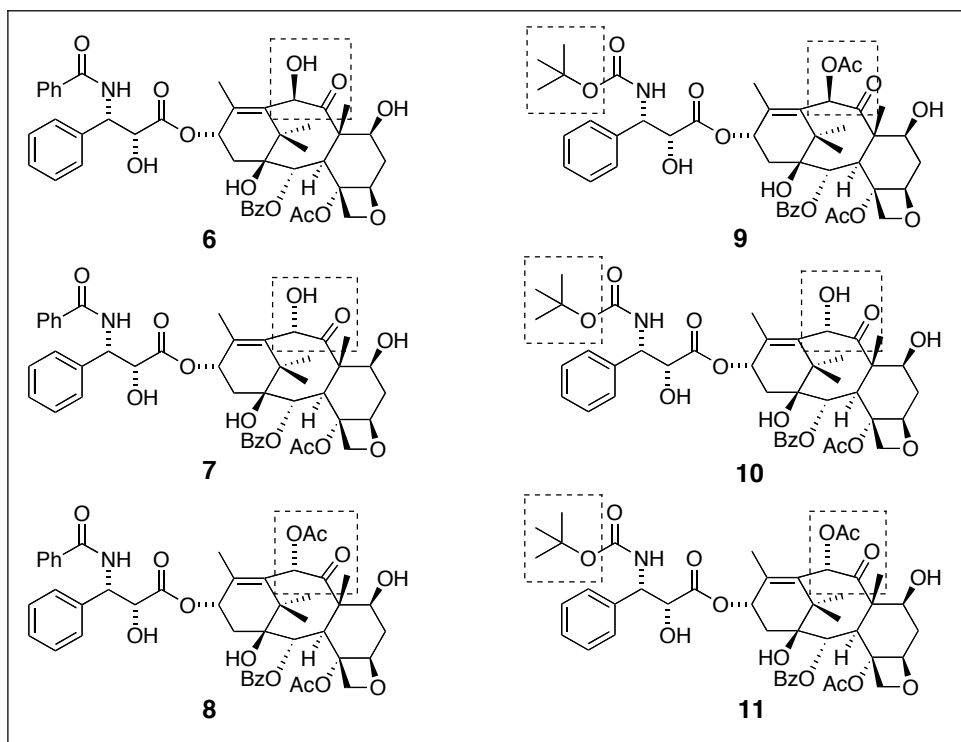


**Figure 4.** Proposed analogs to explore BBB permeation

To further probe the Pgp/paclitaxel structure-activity relationship we proposed a systematic study of the C10 and C3'N regions of select taxoids. The most apparent, and readily accessible are those directly obtained from the paclitaxel molecule (**6-8**). We reasoned, based upon Seelig's model and preliminary data, that simple hydrolysis of the C10 ester of paclitaxel (converting a type II unit into a type I) providing target compound **6** (Figure 4), should show a decreased interaction with Pgp. In addition we wanted to explore modifications to the spatial relationship of these recognition elements, which is key in the Seelig model. It was proposed to invert the stereochemistry of the C10 OH in order to change the spatial arrangement of H-bond acceptor groups (analog **7** and **8**).<sup>12</sup> The paclitaxel molecule is unique in that epimerization of C10 converts the much more accessible acetate on the "outer

surface” of its cup-shaped molecule to a group hidden within the confines of paclitaxel’s molecular architecture (Figure 5).<sup>12</sup> We therefore wanted to investigate placement of groups upon the epimerized derivative. The orientation of this type II unit may be inaccessible for interaction with Pgp and may allow us an avenue to install acyl groups, which have been shown to increase potency, without the detriment of creating a Pgp substrate.

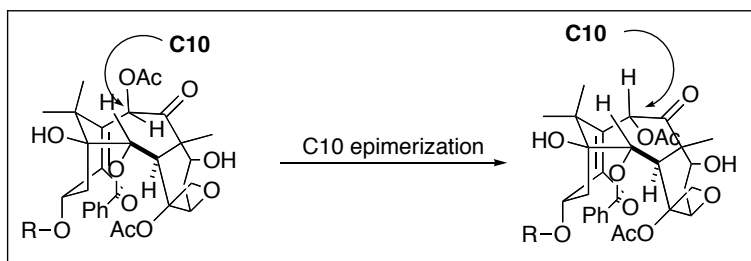
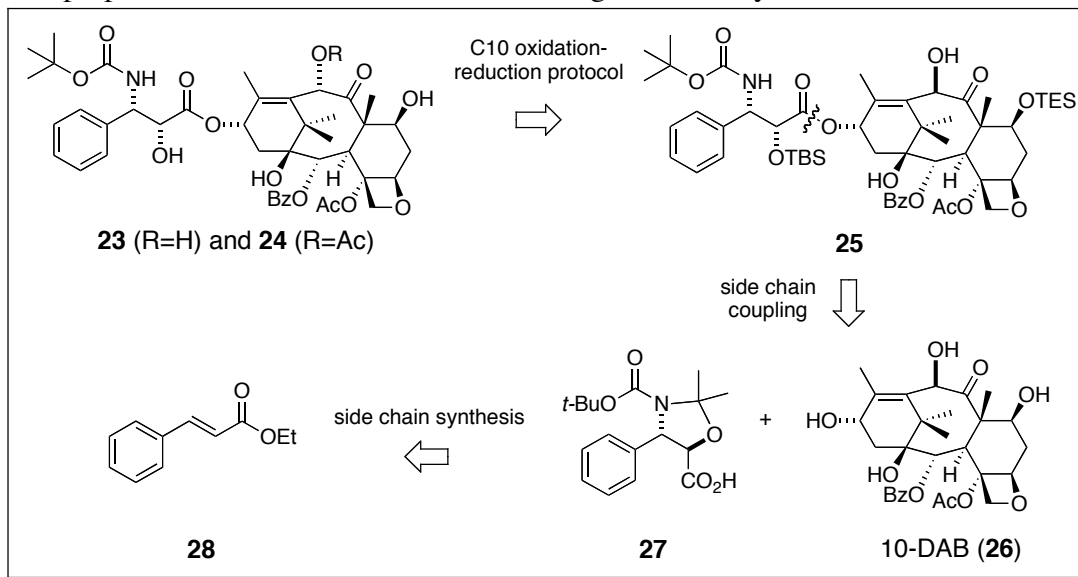


**Figure 5.** C10 epimer conformation

As a negative control, we reasoned that acylation of docetaxel (**22**, Figure 4), thus converting a weak interacting type I unit into a strong binding type II unit, should have an *increased interaction with Pgp* in comparison with docetaxel. Much like our proposed paclitaxel analogs, we planned to make the C10 docetaxel epimers, **23** and **24**, which lack the Type I recognition element of the paclitaxel side chain (at the 3’N) and replace it with a Boc group. We were particularly interested in these analogs as they incorporate the desirable characteristics from each of our leads into the same molecule.

Compounds **19-22** have been previously prepared by our group or others and the literature procedure was followed to access them.<sup>12</sup> Compounds **23** and **24**, potentially the most promising, are also the most difficult to access. We envisaged their preparation as seen in Scheme 5, outlining their retrosynthesis.

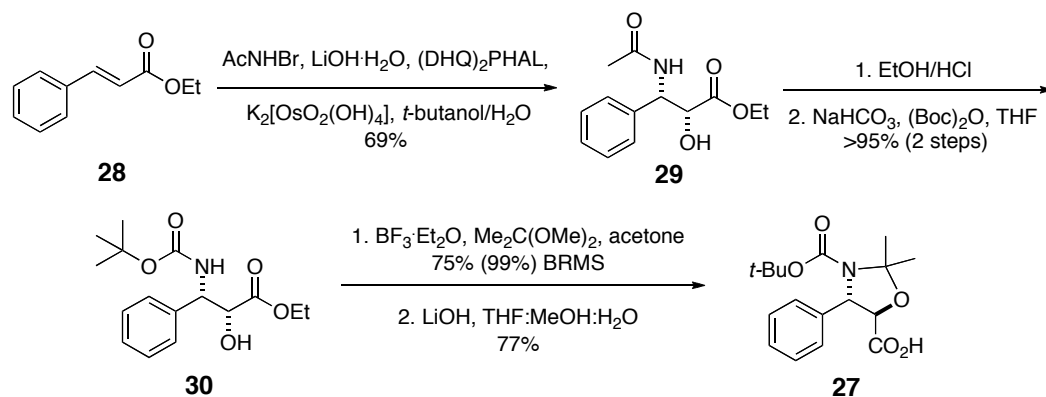


**Scheme 5.** Retrosynthesis of *epi*-docetaxel analogs

### 3.1 Docetaxel Analogs

In a retrosynthetic direction (Scheme 5) we envisioned the application of our groups oxidation-reduction protocol for the inversion of C10 which will allow us access to both target compounds **23** and **24**.<sup>13</sup> Intermediate **25** will be arrived at via coupling of acid **27** with a suitably protected variant of commercially available 10-DAB (**26**). The desired phenylisoserine side chain (**13**) will be prepared utilizing the Sharpless asymmetric amino-hydroxylation methodology as a key step.<sup>14</sup> From synthetic intermediate **25** we are also granted access to target compound **22**, following an existing protocol (vide infra).

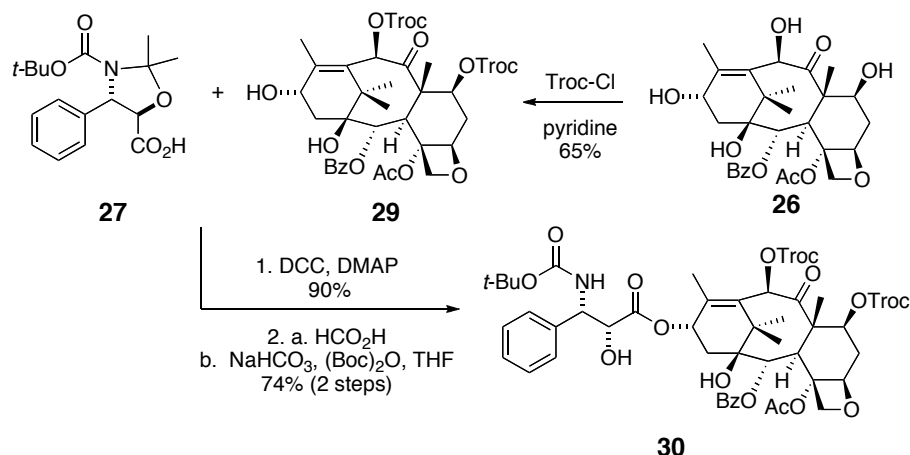
In a forward direction, the side chain is prepared utilizing the Sharpless asymmetric amino-hydroxylation methodology on commercially available ethyl *trans*-cinnamate (**28**) providing the desired amido alcohol, **29** (Scheme 6).<sup>14</sup> This reaction could be carried out on multigram scale with the only noticeable side product being the diol (10-15%). The acetyl group of the C3' nitrogen is then removed under acidic conditions and the nitrogen subsequently protected using *t*-butoxycarbonyl anhydride (Boc<sub>2</sub>O) to give **30** in near quantitative yield over two steps.<sup>15</sup> An acetonide group was then installed to protect the C2'O and the C3'N under Lewis acidic conditions followed by saponification of the ethyl ester to deliver the desired side chain acid **27**. The spectral data of acid **27** were identical to that reported in the literature with a small deviation in specific rotation (literature value:  $[\alpha]_D^{20}$  5.3, experimental value:  $[\alpha]_D^{20}$  7.5; taken at same concentration).<sup>15</sup> In attachment of our side chain to the chiral Baccatin III moiety, we were hopeful that if a mixture of side chain enantiomers persists, they would be resolved via this diastereomer formation.



**Scheme 6.** Side chain synthesis

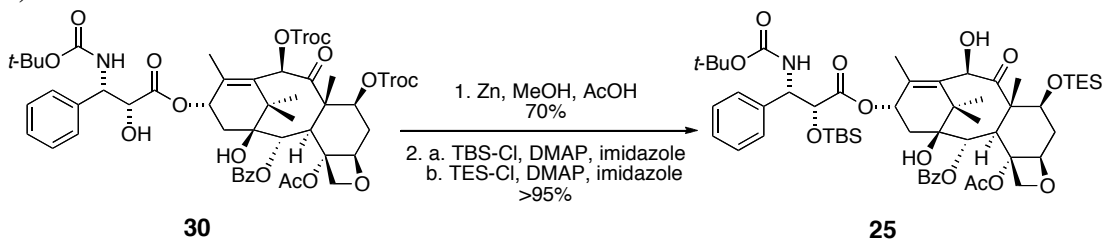
Acid **27** was next coupled to the 7,10-troc(2,2,2-trichloroethylformate) protected baccatin III derivative **29**, which was prepared in one step from 10-DAB (**26**, Scheme 7). The resultant coupled product (90% isolated yield) gave no evidence of the presence of diastereomers via TLC or <sup>1</sup>H NMR (<sup>1</sup>H NMR taken after flash column purification) and all spectral data matched that of the reported values.<sup>15</sup> The

coupled product was then treated with formic acid to remove the acetonide protecting group. This also removed the acid labile Boc group that was immediately put back onto the crude amine to provide the bis-troc protected analog **30** in good chemical yield.

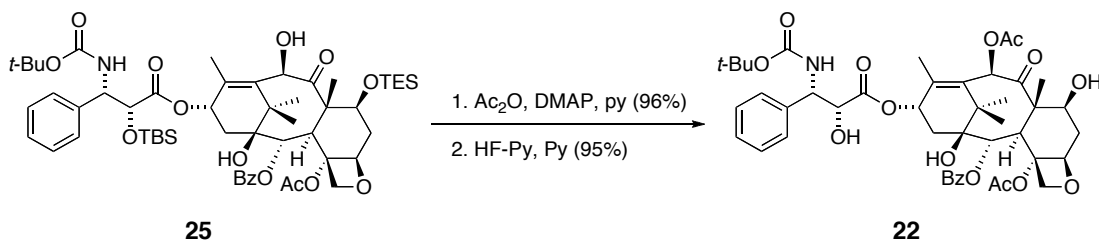


**Scheme 7.** Side chain coupling

The C7 and C10 Troc protecting groups were next removed utilizing zinc and acetic acid in methanol to provide the semi-synthetic taxoid, docetaxel (Scheme 8). Next, in a two-step, one-pot procedure, the 2' OH is chemoselectively protected as the TBS ether followed by protection of the C7 OH as the TES ether. These synthetic steps made available the required intermediate (**25**) for our epimerization strategy as well as the precursor to 10-acetyldocetaxel (**22**). From **25**, simple acetylation of the C10 hydroxy followed by global deprotection garnered target compound **22** (Scheme 9)



**Scheme 8.** 2'-OTBS-7OTES-docetaxel



**Scheme 9.** 10-Acetyldocetaxel

The stage was now set for our oxidation-reduction protocol for the epimerization of the C10 alcohol. This method has been employed successfully on the parent compound, however it has not been investigated on other synthetic derivatives.

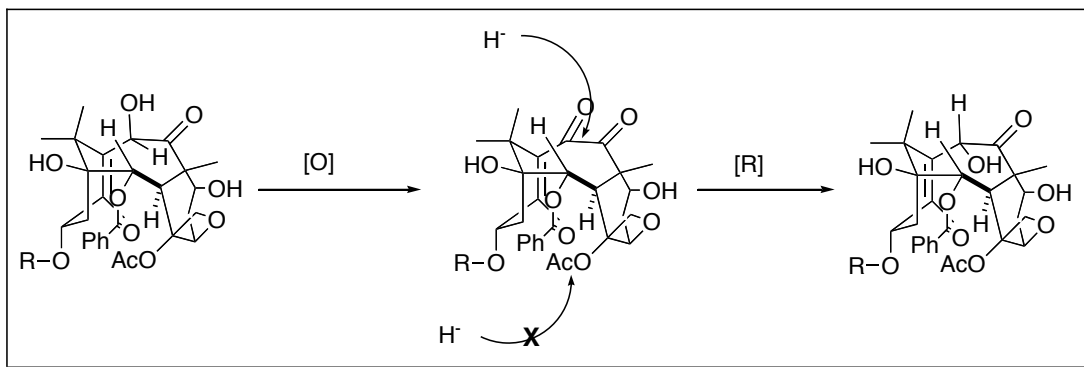
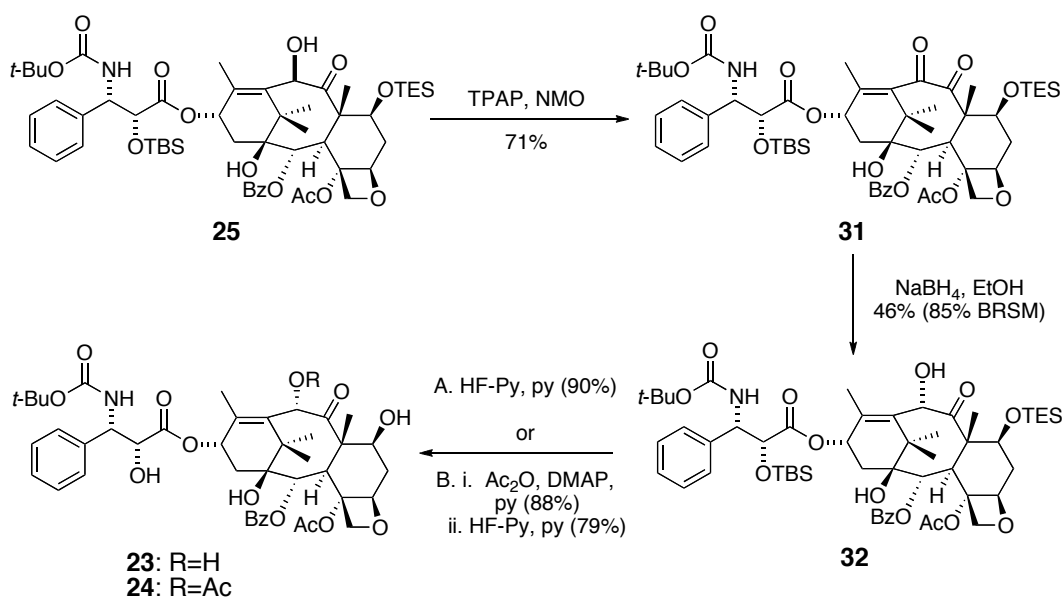


**Figure 6.** Oxidation-reduction protocol

As mentioned previously, the unique conformation of paclitaxel allows substrate controlled hydride addition to the C10 ketone (after subsequent oxidation of the alcohol) to deliver the antipode of the natural orientation at this center (Figure 6). From **25** (Scheme 10), as in the paclitaxel case, the C10 alcohol is oxidized with catalytic tetrapropylammonium perruthenate (TPAP) and stoichiometric 4-methylmorpholine *N*-oxide (NMO) to deliver the C9, C10 dicarbonyl compound **31**.<sup>16</sup> The reduction of the C10 carbonyl, as expected, gave rise to the opposite absolute stereochemistry as that of the natural product at C10 (**32**, Scheme 10). Although the yield of this reduction is modest (46%), combined with recovered, recyclable starting material, the overall yield is acceptable (85%). Attempts to push the reaction resulted in over reduction to the C9, C10 diol and ester cleavage products. Removal of the protecting groups via fluoride anion generates target molecule **23** (R=H). Alternatively, acetylation of the newly formed alcohol on intermediate **32** followed by the same deprotection gives target molecule **24** (R=Ac).

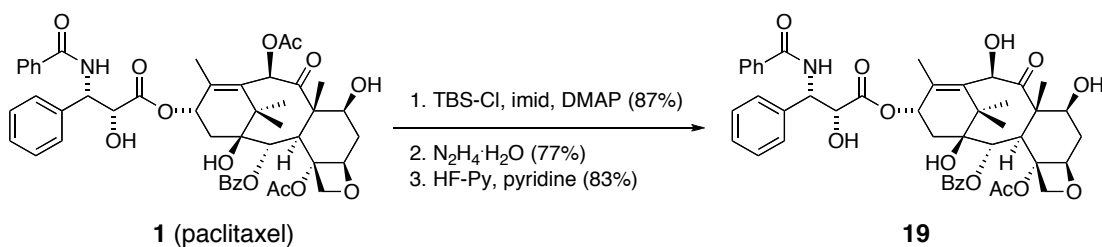




**Scheme 10.** Target compounds **23** and **24**

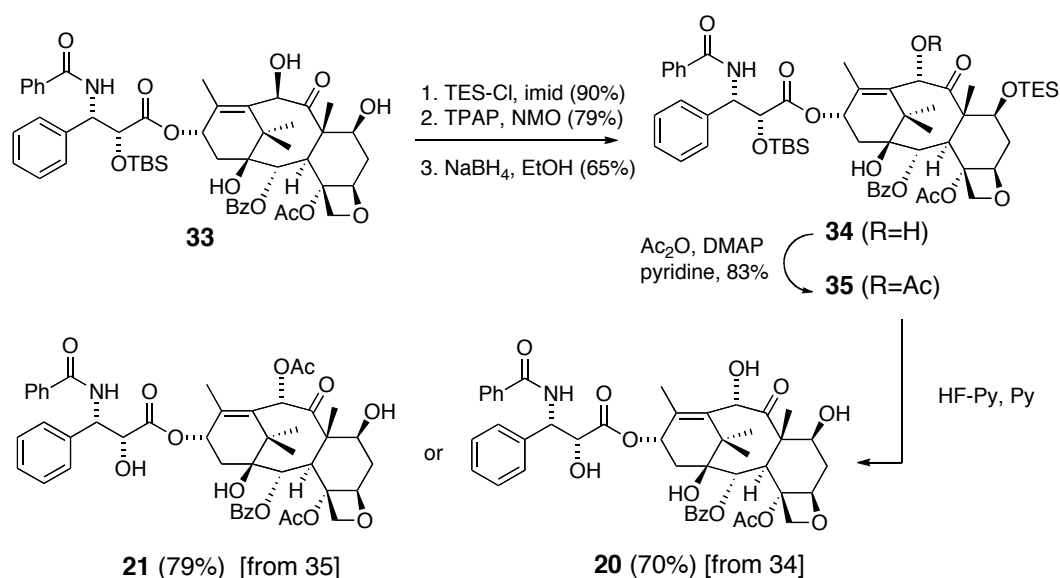
### 3.2 Paclitaxel analogs

A three-step sequence of reactions allowed access to 10-deacetylpaclitaxel **19** (Scheme 11). Preparation of this compound was accomplished via TBS protection of the 2' alcohol, chemoselective hydrazine cleavage of the C10 acetate,<sup>8</sup> and protecting group removal.



**Scheme 11.** 10-deacetyl paclitaxel

The preparation of the C10 epimers **20** and **21** was accomplished as seen in Scheme 12. From 2'TBS-10-deacetylpaclitaxel (**33**), prepared as shown in scheme 7, the C7 alcohol is protected, followed by C10 OH oxidation and subsequent reduction, as reported.<sup>12,13</sup> This intermediate (**34**) was deprotected to provide target compound 10-deacetyl-10-epipaclitaxel (**20**). In addition, intermediate **34** was acetylated then deprotected giving the last of our biological probes, 10-epi-paclitaxel (**21**).



**Scheme 12.** C10 Epi-Paclitaxel Analogs

### 3.3 Biological Evaluation

Our first tier biological screen entailed cytotoxicity and tubulin assembly assays. It was critical that our analogs maintain effectiveness against cancer cell lines to be of any utility. In addition, we further screened our compounds against a drug resistant breast cancer cell line (NCI/ADR-RES). We reasoned that compounds which do not interact with Pgp would be more effective against these NCI/ADR cell lines as it is proposed that paclitaxel is ineffective versus these NCI/ADR cell lines as a direct result of Pgp efflux. The results of these assays can be seen in Table 1.

**Table 2.** Tubulin assembly and cytotoxicity results

Analog	Tubulin Assembly <sup>a</sup>	MCF7 <sup>a</sup>	NCI/ADR-RES <sup>a</sup>
paclitaxel ( <b>1</b> )	1.0	1.0	1.0
10-deacylpaclitaxel ( <b>19</b> )	2.1	7.5	6.6
10- <i>epi</i> -deacylpaclitaxel( <b>20</b> )	0.75	1.4	0.7
10- <i>epi</i> -paclitaxel ( <b>21</b> )	0.42	0.7	1.3
docetaxel ( <b>1a</b> )	0.4	0.7	1.3
10-acetyldocetaxel ( <b>22</b> )	2.2	1.0	0.058
10- <i>epi</i> -docetaxel ( <b>23</b> )	1.7	1.5	0.44
10- <i>epi</i> -acetyldocetaxel ( <b>24</b> )	1.1	0.44	0.88

<sup>a</sup>ED<sub>50</sub>analog/ED<sub>50</sub>paclitxel

In the tubulin assembly assay, all analogs maintained similar activity to the parent compound. Although not surprising since modifications at both the 3'N and C10 OH are known to be tolerated well, this result was pleasing. Their effectiveness against the breast cancer cell line (MCF7) compared well with paclitaxel with several analogs performing better and only one (**19**), demonstrating a marked loss in activity. Although we had hypothesized an increase in effectiveness of these analogs against the NCI/ADR-RES breast cancer cell line (Pgp overexpressing) we found this was not the case. Although we see a modest increases in potency in several analogs, it should be pointed out to the reader that *paclitaxel is not an effective anti-proliferative agent against this MDR cell line*. An analog must exhibit potency in the order of 1000-times that of paclitaxel to be considered effective. It should be noted that compound **22** (10-acetyldocetaxel, Table 1), contrary to our hypothesis, demonstrated a 58-fold increase in activity against the MDR cell line.

Our second tier biological screen is the rhodamine 123 uptake assay.<sup>17</sup> This assay is a preliminary screen to evaluate a compounds interaction with Pgp in bovine brain microvessel endothelial cells (BMECs). Audus et al., have developed this assay to determine a compound's ability to bind Pgp in the presence of a rhodamine dye. Paclitaxel and rhodamine 123 are substrates for the MDR1 efflux system that is found in endothelial cells of the blood-brain barrier and in certain MDR cancer cell lines. Our compounds have been evaluated in this assay and the results can be seen in Figure 7. All new compounds generated displayed reduced interactions with Pgp compared with paclitaxel. Docetaxel (**1a**), which also demonstrated increased permeation in the BBB permeation assay, exhibited the same level of rhodamine as the control (indicating it is not interacting with Pgp). Simple acetylation of **1a** giving 10-acetyldocetaxel (**22**) increased the compounds interactions with Pgp as anticipated as this converts a type I unit into a type II. A similar phenomenon is noted with a significant drop in rhodamine levels when the C10 acetate on paclitaxel (**1**) is cleaved providing the C10 alcohol (**19**, 10-deacylpaclitaxel). Somewhat unexpectedly, none of the C10 epimeric compounds ( $\alpha$ -orientation) seem to perform significantly better than the  $\beta$  compounds. It should be pointed out that the C10 epi-paclitaxel (**21**), shows much less rhodamine accumulation then the parent compound suggesting that, at least with the parent molecule, this type II unit is less available for interaction with Pgp once confined within the baccatin core.

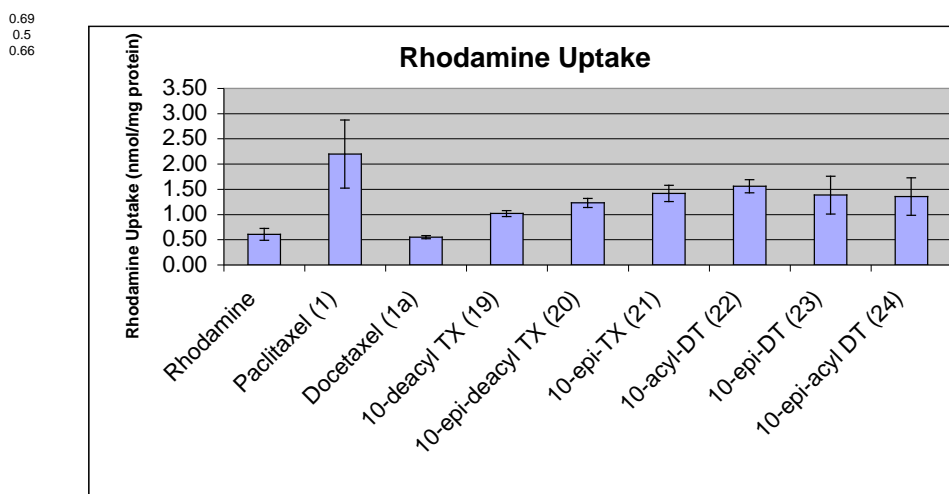


**Figure 7.** Rhodamine assay results

### Key Research Accomplishments

- Preparation of C7 and C10 carboxylic acid analogs
- Preparation of C7 and C10 functional group analogs
- Preparation of C7 and C10 biotin analog
- Preparation of protected variant of C7 and C10 phenylalanine analog
- Asymmetric synthesis of docetaxel side chain as well as docetaxel
- Synthesis of 3'N analogs
- Synthesis of select carboxylic analogs
- Systematic study of C10 paclitaxel and docetaxel epimeric taxanes
- Tubulin assembly and cytotoxicity data obtained for described analog
- Rhodamine 123 uptake studies completed for identified analogs

### Reportable Outcomes

- *Journal of Neurochemistry*, 2003, **84**, 347-362 (see attached)
- *Journal of Molecular Neuroscience*, 2003, **3**, 339-344 (see attached)
- *Journal of Organic Chemistry*, 2004, **69**, 2573-2576 (see attached)
- *Bioorganic and Medicinal Chemistry Letters*, 2006, **16**, 495-498 (see attached)
- *Journal of the American Chemical Society*, 2006, **128**, 8702-8703 (see attached)
- M. S. Medicinal Chemistry, University of Kansas, 2003
- Ph. D. in Medicinal Chemistry (*Honors*), September 2005
- Currently a NIH post-doctoral fellow in the laboratory of Barry M. Trost, Department of Chemistry, Stanford University (September 2005)

### Conclusions

We have developed novel paclitaxel analogs that can be easily prepared in short synthetic sequences from the parent molecule. This focused library of analogs

indicates that the placement of a carboxylic acid functionality on either the C7 or C10 position inhibits interactions with Pgp found in bovine BBB. Furthermore, we have illustrated that the length of linker between paclitaxel and the anionic species is able to be modified. Unexpectedly, we have uncovered that the acid functionality *is not required in all cases* and that hydrogen bonding character of the particular analog plays a major role.

A systematic investigation of C3'N and C10 analogs of paclitaxel and their structure-activity relationship to Pgp has been realized. This study represents an approach to rationally design paclitaxel analogs that demonstrate reduced interactions with Pgp in comparison with the parent compound based upon a model proposed by Seelig. The concept and data presented illustrate a simple and accessible method for the delivery of taxoids across the blood-brain barrier. This is in contrast to current strategies for brain delivery of non-CNS permeable drugs, including Pgp inhibition, and BBB disruption. Our data verifies our hypothesis that structurally modified analogs can be rationally designed, based on the Seelig model, to reduce interactions with Pgp in the BBB. These modifications had little effect on potency against MDR cancer cell lines and may suggest a different form of Pgp is present in the BBB as compared to MDR cells or alternative resistance mechanisms persist. Long-term application of this research has the potential to lead to effective agents for CNS cancer treatment

## References

1. Schinkel, A. H.; Smit, J. J. M.; van Tellingen, O.; Beijnen, J. H.; Wagenaar, E.; van Deemter, L.; Mol, C. A. A. M.; van der Valk, M. A.; Robanus-Maandag, E. C.; te Riele, H. P. J.; Berns, A. J. M.; Borst, P. Disruption of the Mouse *mdr1a* P-Glycoprotein Gene Leads to a Deficiency in the Blood-Brain Barrier and to Increased Sensitivity to Drugs. *Cell* **1994**, *77*, 491-502.
2. Schinkel, A. H.; Wagenaar, E.; Mol, C. A. A. M.; van Deemter, L. P-Glycoprotein in the Blood-Brain Barrier of Mice Influences the Brain Penetration and Pharmacological Activity of Many Drugs. *Journal of Clinical Investigation* **1996**, *97*, 2517-2524.
3. Burton, P. S.; Conradi, R. A.; Hilgers, A. R.; Ho, N. F. H. Evidence for a Polarized Efflux System for Peptides in the Apical Membrane of Caco-2 Cells. *Biochemical and Biophysical Research Communications* **1993**, *190*, 760-766.
4. Seelig, A.; Landwojtowicz, W.; Fisher, H.; Blatter, X. L. Towards P-Glycoprotein Structure-Activity Relationships. *Methods and Principles in Medicinal Chemistry* **2003**, *18*, 461-492.
5. Rice, A.; Liu, Y.; Michaelis, M. L.; Himes, R. H.; Georg, G. I.; Audus, K. Chemical Modification of Paclitaxel (Taxol) Reduces P-Glycoprotein Interactions and Increases Permeation across the Blood-Brain-Barrier in Vitro and in Situ. *Journal of Medicinal Chemistry* **2005**, *48*, 832-838.
6. Ojima, I.; Slater, J. C.; Michaud, E.; Kuduk, S. D.; Bounaud, P.-Y.; Vrignaud, P.; Bissery, M. C.; Veith, J. M.; Pera, P.; Bernacki, R. J. Syntheses and Structure-

Activity Relationships of the Second-Generation Antitumor Taxoids: Exceptional Activity Against Drug-resistant Cancer Cells. *Journal of Medicinal Chemistry* **1996**, 39, 3889-3896.

7. Aigner, A.; Wolf, S.; Gassen, H. G. Transport and Detoxication: Principles, Approaches and Perspectives for Research on the Blood-Brain Barrier. *Angewandte Chemie, International Edition in English* **1997**, 36, 24-41.
8. Terasaki, T.; Tsuji, A. Oligopeptide Drug Delivery to the Brain. In *Peptide Based Drug Design. Controlling Transport and Metabolism*, Taylor, M. D.; Amidon, G. L., Eds. American Chemical Society: Washington, DC, 1995; pp 297-316.
9. Datta, A.; Hepperle, M.; Georg, G. I. Selective Deesterification Studies on Taxanes: Simple and Efficient Hydrazinolysis of C-10 and C-13 Ester Functionalities. *Journal of Organic Chemistry* **1995**, 60, 761-763.
10. Liu, Y.; Boge, T. C.; Victory, S.; Ali, S. M.; Zygmunt, J.; Georg, G. I.; Marquez, R. T.; Himes, R. H. A Systematic SAR Study of C10 Modified Paclitaxel Analogues Using a Combinatorial Approach. *Combinatorial Chemistry and High Throughput Screening* **2002**, 5, 39-48.
11. Audus, K. L.; Borchardt, R. T. Characterization of an in vitro blood-brain barrier model system for studying drug transport and metabolism. *Pharmaceutical Research* **1986**, 3, 81-87.
12. Datta, A.; Vander Velde, D. G.; Georg, G. I. Syntheses of Novel C-9 and C-10 Modified Bioactive Taxanes. *Tetrahedron Letters* **1995**, 36, 1985-1988.
13. Georg, G. I.; Harriman, G. C. B.; Datta, A.; Ali, S.; Cheruvallath, Z.; Dutta, D.; Velde, D. G. V.; Himes, R. H. The Chemistry of the Taxane Diterpene: Stereoselective Reductions of Taxanes. *Journal of Organic Chemistry* **1998**, 63, 8926-8934.
14. Bruncko, M.; Schlingloff, G.; Sharpless, K. B. N-Bromoacetamide - a new nitrogen source for the catalytic asymmetric aminohydroxylation of olefins. *Angewandte Chemie, International Edition in English* **1997**, 36, 1483-1486.
15. Commercon, A.; Bezard, D.; Bernard, F.; Bourzat, J. D. Improved protection and esterification of a precursor of the Taxotere and taxol side chains. *Tetrahedron Letters* **1992**, 33, 5185-5188.
16. Ley, S. V.; Norman, J.; Griffith, W. P. Tetrapropylammonium Perruthenate,  $\text{Pr}_4\text{N}^+\text{RuO}_4^-$ , TPAP: A Catalytic Oxidant for Organic Synthesis. *Synthesis* **1994**, 639-666.
17. Audus, K. L.; Borchardt, R. T. Characterization of an in vitro blood-brain barrier model system for studying drug transport and metabolism. *Pharmaceutical Research* **1986**, 3, 81-87.

## Stabilization of the cyclin-dependent kinase 5 activator, p35, by paclitaxel decreases $\beta$ -amyloid toxicity in cortical neurons

Guibin Li,\* Alexander Faibushevich,\* Brandon J. Turunen,‡ Sung Ok Yoon,† Gunda Georg,‡ Mary L. Michaelis\* and Rick T. Dobrowsky\*

\*Department of Pharmacology and Toxicology, ‡Department of Medicinal Chemistry, University of Kansas, Lawrence, Kansas

†Neurobiotech Center and Department of Neuroscience, Ohio State University, Columbus, Ohio, USA

### Abstract

One hallmark of Alzheimer's disease (AD) is the formation of neurofibrillary tangles, aggregated paired helical filaments composed of hyperphosphorylated tau. Amyloid- $\beta$  (A $\beta$ ) induces tau hyperphosphorylation, decreases microtubule (MT) stability and induces neuronal death. MT stabilizing agents have been proposed as potential therapeutics that may minimize A $\beta$  toxicity and here we report that paclitaxel (taxol) prevents cell death induced by A $\beta$  peptides, inhibits A $\beta$ -induced activation of cyclin-dependent kinase 5 (cdk5) and decreases tau hyperphosphorylation. Taxol did not inhibit cdk5 directly but significantly blocked A $\beta$ -induced calpain activation and decreased formation of the cdk5 activator, p25, from p35. Taxol specifically inhibited the A $\beta$ -induced activation of the cytosolic cdk5-p25 complex, but not the membrane-associated cdk5-p35 complex. MT-stabilization was neces-

sary for neuroprotection and inhibition of cdk5 but was not sufficient to prevent cell death induced by overexpression of p25. As taxol is not permeable to the blood–brain barrier, we assessed the potential of taxanes to attenuate A $\beta$  toxicity in adult animals using a succinylated taxol analog (TX67) permeable to the blood–brain barrier. TX67, but not taxol, attenuated the magnitude of both basal and A $\beta$ -induced cdk5 activation in acutely dissociated cortical cultures prepared from drug treated adult mice. These results suggest that MT-stabilizing agents may provide a therapeutic approach to decrease A $\beta$  toxicity and neurofibrillary pathology in AD and other tauopathies.

**Keywords:** amyloid- $\beta$ , calpain, cyclin-dependent kinase 5, microtubules, paclitaxel, tau.

*J. Neurochem.* (2003) **84**, 347–362.

Alzheimer's disease (AD) is characterized by the loss of specific groups of neurons and the presence of two brain lesions, amyloid plaques and neurofibrillary tangles (NFTs) (Lee *et al.* 2001; Selkoe 2001b). NFTs are composed of intracellular aggregates of highly insoluble paired helical filaments (PHFs) made up of fibrils of the MT-associated protein tau (Goedert 1997). Although the relationship between these two principal lesions is unclear, the discovery that multiple *tau* gene mutations occur in frontotemporal dementia and parkinsonism linked to chromosome 17 (FTDP-17) has provided strong evidence that tau abnormalities are sufficient to promote neurodegeneration (Scheuner *et al.* 1996; Goedert *et al.* 1998; Spillantini *et al.* 1998). Abnormal phosphorylation of tau by A $\beta$  peptides promotes the loss of its microtubule (MT) stabilizing ability (Busciglio *et al.* 1995) and contributes to neurite degeneration and the formation of PHFs (Lee *et al.* 2001). These observations led to the hypothesis that MT-stabilizing agents, such as

paclitaxel (taxol), might help overcome the inadequate binding of hyperphosphorylated tau to MTs and slow the progression of neurofibrillary pathology and cell death (Lee *et al.* 1994). We have reported previously that taxol can protect primary cortical neurons from A $\beta$ -induced cell death (Michaelis *et al.* 1998). However, whether the neuroprotective action of taxol resulted solely from increased

Received August 13, 2002; revised manuscript received October 8, 2002; accepted October 11, 2002.

Address correspondence and reprint requests to Rick T. Dobrowsky, Department of Pharmacology and Toxicology, University of Kansas, 5064 Malott Hall, 1251 Wescoe Hall Dr, Lawrence, KS 66045, USA. E-mail: dobrowsky@ku.edu

**Abbreviations used:** A $\beta$ , amyloid-beta; AD, Alzheimer's disease; cdk5, cyclin-dependent kinase 5; CNS, central nervous system; DAB, 10-deacetylbaecatin III; JNK, c-jun N-terminal kinase; MTs, microtubules; NFTs, neurofibrillary tangles; PHFs, paired helical filaments; TX67, 10-succinyl paclitaxel.

MT-stabilization or had contributions from other effects, such as regulating tau phosphorylation, was unclear. The cascade of events that lead to tau hyperphosphorylation may be a critical step in the pathogenesis of tauopathies (Goedert *et al.* 1998). Although tau is phosphorylated by numerous kinases *in vivo* (Billingsley and Kincaid 1997), recent attention has focused upon the role of cdk5 as an important tau kinase whose activity is enhanced in response to A $\beta$  in cultured neurons (Alvarez *et al.* 1999, 2001) and in AD brain (Lee *et al.* 1999; Patrick *et al.* 1999). Cdk5 is a 33-kDa serine/threonine kinase that is active primarily in neurons (Ino *et al.* 1994) and can associate with MTs indirectly (Sobue *et al.* 2000). Cdk5 activity is regulated through association with the specific cyclin-related activator molecules, p35, p39, p25 and p29 (Dhavan *et al.* 2001). The calpain-directed proteolysis of p35/p39 (Kusakawa *et al.* 2000; Lee *et al.* 2000; Nath *et al.* 2000; Patzke and Tsai 2002a) releases p25/p29 from an N-terminal membrane tether and may delocalize cdk5/p25 (cdk5/p29) complexes from the plasma membrane and decrease phosphorylation of physiologic membrane substrates (Niethammer *et al.* 2000; Zukerberg *et al.* 2000). p35 has a short cellular half-life (Patrick *et al.* 1998, 1999) and its increased degradation can lead to cytoplasmic accumulation of cdk5/p25 complexes (Dhavan *et al.* 2001). As overexpression of cdk5/p25 in cells (Patrick *et al.* 1999) or transgenic mice (Ahlijanian *et al.* 2000) enhances tau phosphorylation, the ability of cdk5/p25 but not cdk5/p35 to serve as a tau kinase has led to the concept that tau is a pathological substrate for cdk5 (Dhavan *et al.* 2001). Thus, treatments that affect the turnover and/or production of p35 should indirectly impact on cdk5 activity. In this report, we demonstrate that taxol inhibits an A $\beta$ -induced pathway that links increased calpain activity to enhanced p25 production, cdk5 activation and tau phosphorylation. Although MT-stabilization by taxol was necessary for neuroprotection and inhibition of cdk5 activity, it was not sufficient to protect neurons from constitutive cdk5 activation following overexpression of p25 in primary cortical neurons. As the therapeutic potential of taxol in AD is limited by its bioavailability to the brain, we show that administration to adult mice of a taxol analog permeant to the blood-brain barrier inhibits A $\beta$ -induced cdk5 activation. Collectively, our data suggest that MT-stabilization is tightly linked to the regulation of tau phosphorylation and that MT-stabilizing drugs may be potential therapeutic agents to slow the development of neurofibrillary pathologies.

## Experimental procedures

### Materials

Polyclonal antibodies directed against cdk5 (C-8), the C-terminus of p35 (C-19) and the N-terminus of p35 (N-20) were obtained from Santa Cruz Biotechnology (Santa Cruz, CA, USA). AT-8 antibody

was purchased from Endogen and the Tau-5 and PHF-1 antibodies were provided by Dr Peter Davies (Albert Einstein College of Medicine). The pAdTrack-CMV (cytomegalovirus) shuttle vector and pAdEASY-1 adenoviral backbone vector were generous gifts from Dr T. C. He (Johns Hopkins University Medical School). Dr L-H. Tsai (Harvard Medical School) kindly provided the p35 cDNA construct. Taxol was purchased from Dabur India, Ltd. and the succinylated taxol analog (TX67) was prepared by parallel solution phase synthesis (Liu *et al.* 2002). Histone H1, bovine brain tau, N-succinyl-leu-tyr-7-amido-4-methylcoumarin, and A $\beta$ <sub>1–42</sub> peptides were purchased from Sigma/Aldrich Chemicals (St Louis, MO, USA). A $\beta$ <sub>25–35</sub> was synthesized by the Biochemical Research Services Laboratory at the University of Kansas. [ $\gamma$ -<sup>32</sup>P]ATP was from DuPont-NEN, Boston, MA, USA.

### Cell culture and drug administration

Primary cortical neurons were prepared from embryonic day 18 Sprague-Dawley rat pups as described previously (Michaelis *et al.* 1994). Following trituration, the cells were resuspended in Dulbecco's modified Eagle's medium/F12 (DMEM/F12) containing 15 mM KHCO<sub>3</sub>, 10% fetal calf serum and plated onto 35 or 60 mm poly D-lysine-coated dishes at a density of  $6.5 \times 10^5$  or  $2 \times 10^6$  cells/dish for viability and biochemical assays, respectively. Twenty-four hours after plating, the cells were washed and placed in defined medium (DMEM/F12, 0.1 g/L transferrin-APO form, 5 mg/L insulin, 0.1 mM putrescine, 10 nM progesterone, 30 nM sodium selenite, and 1 mM sodium pyruvate) for the duration of the experiment. After 4 days *in vitro*, the cells were treated with 10  $\mu$ M A $\beta$  peptides in the absence or presence of 100 nM taxol. Taxol was stored as a 1 mM stock solution in dimethyl sulfoxide (DMSO) and diluted to 25  $\mu$ M in H<sub>2</sub>O prior to the experiment. The final concentration of DMSO in all cultures was 0.01%.

TX67 is a substituted taxol analog that replaces the C-10 acetyl group of taxol with succinic acid (Liu *et al.* 2002). Adult mice received intraperitoneal injections (0.1 mL) of 8 mg/kg TX67 every 2 days over 16 days. TX67 was dissolved in a (1 : 1) solution of ethanol/Cremephor EL (polyethoxylated castor oil that is used clinically for taxol injections) and diluted 1 : 6 with 133 mM sterile saline immediately prior to injection. Animals receiving taxol were treated similarly. The dosing schedule appeared to have little effect on the general health of the animals, as all gained weight and displayed no obvious behavioral or physical anomalies. All animal procedures were performed in accordance with protocols approved by the Institutional Animal Care and Use Committee and in compliance with standards and regulations for care and use of laboratory rodents set by the National Institutes of Health.

Cultures of acutely dissociated neurons from the control and drug-treated animals were prepared after killing the animals with CO<sub>2</sub>. The brains were rapidly excised and placed in ice-cold isotonic buffer (5.0 mM HEPES, pH 7.4, 132 mM NaCl, 5.36 mM KCl, 0.21 mM Na<sub>2</sub>HPO<sub>4</sub>, 0.22 mM KH<sub>2</sub>PO<sub>4</sub>, 2.77 mM glucose and 58.4 mM sucrose). The cerebral cortices were dissected, the grey matter minced into small pieces and the tissue incubated with 0.25% trypsin in calcium and magnesium free Hank's solution for 1 h at 37°C. The tissue fragments were triturated to disperse the cells and placed into 20 mL of DMEM/F12 medium containing 10% fetal calf serum and 15 mM KHCO<sub>3</sub>. The cell suspension was filtered through a sterile 41  $\mu$ m nylon mesh filter to remove large clumps, the cells



collected by centrifugation and resuspended in pre-warmed DMEM/F12 medium containing 10% fetal calf serum. The cells were treated immediately with 20  $\mu$ M A $\beta_{25-35}$  for 24 h and both adherent and non-adherent cells were harvested, resuspended in lysis buffer and *ex vivo* cdk5 activity assessed as described below.

#### Immunoprecipitation of Cdk5 and *in vitro* kinase assay

Cells were harvested in lysis buffer (20 mM Tris-HCl pH 7.4, 140 mM NaCl, 1 mM PMSF, 1 mM Na<sub>3</sub>NO<sub>4</sub>, 10 mM NaF, 0.1% Nonidet-40, 1 mM EDTA, 1  $\times$  complete protease inhibitors (Roche Diagnostics, Indianapolis, IN, USA) and 26  $\mu$ M *N*-acetyl-leu-leu-norleucinal, ALLN) and cell debris was removed by centrifugation at 10 000 *g* for 10 min at 4°C. Protein concentration was determined using the Bio-Rad dye and bovine serum albumin as the standard. Protein (200  $\mu$ g) was incubated with 2  $\mu$ g of Cdk5 antibody (C-8) or p35 antibodies (N-20 or C-19) for 2 h at 4°C. Protein A-Sepharose beads (40  $\mu$ L of a 50% slurry) were added to the samples and immune complexes were formed by incubation for 1 h at 4°C. The beads were sedimented by centrifugation, washed two times with lysis buffer and one time with kinase buffer (50 mM Tris-HCl, pH, 7.4, 80 mM  $\beta$ -glycero-phosphate, 20 mM EGTA, 15 mM MgCl<sub>2</sub>, and 1 mM dithiothreitol). The beads were resuspended in 30  $\mu$ L of kinase buffer containing 50  $\mu$ M ATP, 1.25  $\mu$ Ci of [ $\gamma$ -<sup>32</sup>P]ATP, and 1  $\mu$ g of histone H1 or purified tau protein. The samples were incubated at 24°C for 30 min (histone H1) or 37°C for 30 min (tau) and the reaction was stopped by adding 10  $\mu$ L of 4  $\times$  sodium dodecyl sulfate–polyacrylamide gel electrophoresis (SDS–PAGE) loading buffer. Proteins were separated by SDS–PAGE and the radioactive bands were quantified using a phosphorimager.

In some experiments, cdk5 was immunoprecipitated from cytosolic and particulate fractions. Neurons were treated with A $\beta$  in the absence and presence of taxol and scraped into detergent-free lysis buffer to avoid solubilizing membrane bound cdk5/p35. The cells were sonicated and debris was removed by centrifugation at 10 000 *g* for 5 min. An aliquot of the whole cell lysate was removed (100  $\mu$ g) and 100  $\mu$ g was centrifuged at 100 000 *g* for 1 h at 4°C in a table top Optima-Max ultracentrifuge. The supernatant (cytosol) was transferred to a fresh tube and Nonidet-40 was added to a final concentration of 0.1%. The pellet (membrane) was washed and then solubilized in lysis buffer containing 0.1% Nonidet-40. Cdk5 was immunoprecipitated from the cytosolic and membrane fractions with 2  $\mu$ g of the C-19 p35 antibody and kinase activity assessed as described above.

#### Cell viability measurements

A $\beta_{25-35}$  (1.3 mg/mL) and A $\beta_{1-42}$  (4.5 mg/mL) were prepared by resuspending the peptides in H<sub>2</sub>O followed by dilution with 10 mM Tris-HCl, pH 7.4, to 1 mM. The peptides were then aged at 37°C for 24 h to induce aggregation. Cell viability was determined using the live/dead assay as described previously (Michaelis *et al.* 1998). The cells were stained with 10  $\mu$ M propidium iodide (PI) and 150 nM calcein-acetoxymethylester (calcein-AM, Molecular Probes, Eugene, OR, USA) for 30 min at 37°C and imaged by fluorescence microscopy. Six images were captured from each dish on marked fields with a CCD camera and all the cells in each field were counted to determine total cell number. Calcein-AM labels the viable cells (green) and PI stains the dead cells (red). Cell viability was calculated as a percentage of viable cells to total cell number.

#### Protein half-life assay

Neurons were treated with vehicle or taxol for 4 days followed by the addition of 30  $\mu$ g/mL cycloheximide for 0–480 mins (Patrick *et al.* 1998). At the indicated time, the cells were scraped into lysis buffer, cell debris was removed by centrifugation at 10 000 *g* for 10 min at 4°C and an equal amount of protein from each time point was subjected to SDS–PAGE. In assessing the effect of A $\beta$  and taxol treatment on p35/p25 levels, complete protease inhibitors and 26  $\mu$ M ALLN were always added to the lysis buffer immediately before harvesting and the samples were processed directly for SDS–PAGE without freezing and thawing of the lysates. The proteins were transferred to nitrocellulose and p35/p25 detected by immunoblot analysis using a C-terminal antibody. The blot was stripped and re-probed for the presence of tau (tau-5 antibody) and cdk5. The amount of p35 expression at each time point was quantified by densitometry and expressed as per cent remaining relative to that present at time 0.

#### Calpain activity assay

Neurons were harvested after 4 days of treatment in calpain lysis buffer (20 mM Tris pH 7.4, 140 mM NaCl, 0.1% Nonidet-40) and cell debris was removed by centrifugation as described above. Protein (30  $\mu$ g) from each sample was loaded in quadruplicate to a 96-well plate and the reaction initiated with 130  $\mu$ M substrate without the addition of exogenous calcium. The substrate for this assay, *N*-succinyl-leu-tyr-7-amido-4-methylcoumarin, is a non-fluorescent peptide which strongly fluoresces after cleavage by calpain (Xie and Johnson 1997). The increase in fluorescence intensity was recorded at 30°C for 3 h in a Bio-Tek FL600 microplate fluorometer and normalized to total protein. In some assays, 100 nM taxol was added directly to the reaction mix containing 0.4 units of purified calpain 1 (Calbiochem, San Diego, CA, USA) and 5 mM Ca<sup>2+</sup> in lysis buffer.

#### Generation of p25 recombinant adenovirus

p35-pcDNA3 served as a template for amplifying p25 by PCR. The forward primer (5'-GTCGACGGTACCATTGGCCAGCCCC-CACCG-3') incorporated a *Kpn*I site and an ATG start codon upstream of the N-terminal alanine for p25 (amino acid 98 of p35) (Tsai *et al.* 1994). The reverse primer (5'-CTCGAGTTACCGA TCCAGGCCTAG-3') was engineered with a *Xho*I site. The amplified PCR product was subcloned directly into TOPO2.1 (Invitrogen, Carlsbad, CA, USA) and sequenced in both directions for errors. The p25-TOPO2.1 cDNA was digested with *Kpn*I and *Xho*I, the approximate 0.6-kb p25 fragment was gel purified and subcloned into the pAdTrack-CMV shuttle vector (He *et al.* 1998). p25-AdTrack-CMV was linearized with *Pme*I and electroporated into RecA<sup>+</sup> bacteria (BJ5183) with 1  $\mu$ g of pAdEASY-1 as described (He *et al.* 1998). Bacterial clones containing recombinant adenoviral DNA were verified by restriction mapping and recombinant viruses were generated by transfection of HEK293 cells. Virus was amplified by four rounds of infection and purified from 20  $\times$  15 cm plates of HEK293 cells using two rounds of centrifugation through CsCl gradients. The residual CsCl was removed by dialysis against 10 mM Tris-HCl, pH 8.0, 100 mM NaCl, 0.1% bovine serum albumin, 20% glycerol in a Slide-a-Lyzer cassette. Recombinant adenoviruses were titered based upon number of green fluorescent foci in an agar-overlay assay as described (He *et al.* 1998). Cortical neurons were infected with blank or

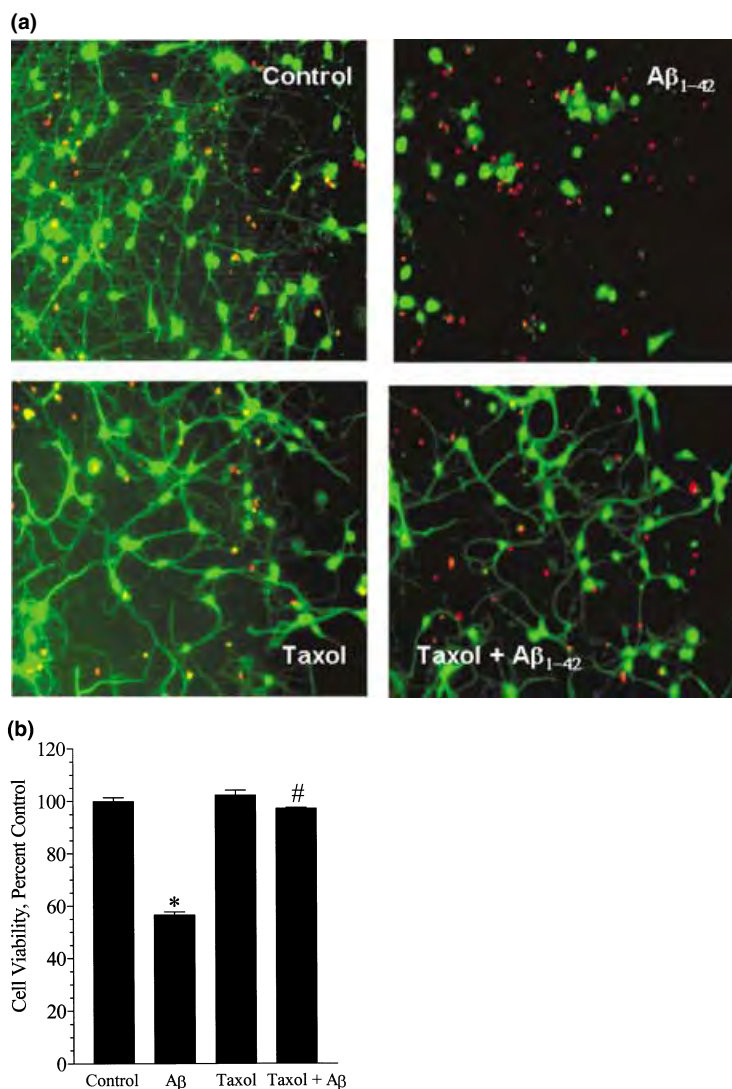


**Fig. 1** Cell death induced by Aβ<sub>1-42</sub> is prevented by taxol pre-treatment. (a) Neurons were treated with buffer, 100 nM taxol or 10 μM Aβ<sub>1-42</sub> in the absence or presence of taxol for 4 days. The cells were stained with calcein-AM and propidium iodide, photographed and cell viability determined. (b) The results from the quantitative analysis of neuronal viability from three experiments. \*,  $p < 0.001$  compared with control; #,  $p < 0.001$  compared with Aβ only. At least 200 cells per treatment were counted in each experiment.

p25-recombinant adenoviruses at 100–400 pfu/cell. The infection efficiency as monitored by cells expressing the green fluorescent protein ranged from 40 to 50%.

#### Statistical analysis

All results are presented as means ± SEM and statistically relevant differences between treatments within a data set were determined using a one-way ANOVA with subsequent post hoc analysis using Tukey's test.

## Results

### Taxol protects against cell death induced by Aβ peptides

Primary neuronal cell cultures derived from the brains of embryonic rat pups (Michaelis *et al.* 1994) were used to demonstrate the protective effect of taxol against Aβ-induced toxicity. Taxol pre-treated cells were minimally

distinguishable from control cells, indicating that the MT-stabilizing properties of the drug did not affect neuronal morphology (Fig. 1a). Our previous studies solely used the Aβ<sub>25-35</sub> peptide to assess the effect of taxol on cell death (Michaelis *et al.* 1998), but this Aβ peptide fragment is not produced in AD. Therefore, we assessed the effect of taxol against neuronal toxicity induced by Aβ<sub>1-42</sub>, the physiologically relevant Aβ peptide that accumulates in AD (Selkoe 2001a). Whereas cells treated with Aβ<sub>1-42</sub> were pyknotic with fragmented and degenerating neurites, taxol preserved neurite morphology and overall appearance in the presence of Aβ<sub>1-42</sub> (Fig. 1a). Further, quantitation of cell survival indicated that 100 nM taxol afforded significant protection against cell death induced by 10 μM Aβ<sub>1-42</sub> (Fig. 1b). As taxol rescues neurons against cell death induced by Aβ<sub>1-42</sub> with results qualitatively similar to Aβ<sub>25-35</sub>, most remaining studies used this shorter Aβ peptide.

**Table 1** TX67 but not 10-deacetylbaccatin III protects cortical neurons against A $\beta$  toxicity

	Cell viability	Per cent control
	Minus A $\beta$	Plus A $\beta$
Vehicle	100	57.6 $\pm$ 4.6 <sup>a</sup>
10-deacetylbaccatin III	91.3 $\pm$ 1.2	60.5 $\pm$ 3.2 <sup>a</sup>
10-succinyl taxol (TX-67)	93.7 $\pm$ 3.4	85.3 $\pm$ 2.9 <sup>b</sup>

Neurons were pre-treated for 2 h with 100 nM of the indicated drug and the cells were stimulated with 10  $\mu$ M A $\beta_{25-35}$ . After 4 days, cell viability was determined with the live/dead assay. <sup>a</sup> $p$  < 0.001 compared with vehicle minus A $\beta$ , <sup>b</sup> $p$  < 0.001 compared with vehicle plus A $\beta$ .

To assess whether the neuroprotective effects of taxol required MT-stabilization, cells were treated with 10-deacetylbaccatin III, a taxol precursor that is ineffective at stabilizing MTs (Wang *et al.* 1998). 10-Deacetylbaccatin III provided no significant protection against A $\beta_{25-35}$  toxicity (Table 1) which strongly supports that the MT-stabilizing properties of taxol are indeed necessary for neuroprotection. As neurons undergoing A $\beta$ -induced degeneration exhibit increased phosphorylation of the MT-interacting protein tau which leads to MT destabilization (Busciglio *et al.* 1995), taxol may help maintain MT stability and consequently regulate the interaction of tau with A $\beta$ -activated tau kinases. Therefore, we addressed the possibility that taxol may decrease A $\beta$  toxicity by stabilizing MTs and interfering with mechanisms regulating A $\beta$ -induced tau hyperphosphorylation.

### Taxol inhibits A $\beta$ -induced tau phosphorylation

To assess the *in vivo* effect of A $\beta_{25-35}$  and taxol treatment on tau phosphorylation in primary neurons, we used the AT-8, PHF-1 and Tau-5 antibodies. AT-8 recognizes an epitope phosphorylated at Ser202 and Thr205 while PHF-1 recognizes tau phosphorylated on Ser396 and Ser404 (Busciglio *et al.* 1995). The Tau-5 antibody recognizes total tau levels independent of phosphorylation state.

Neurons were pre-treated with 100 nM taxol for 2 h and challenged with 10  $\mu$ M A $\beta_{25-35}$ . After an additional 4 days, cell lysates were prepared and the proteins present in a post-nuclear supernatant fraction were resolved by SDS-PAGE. After transferring the proteins to nitrocellulose, tau phosphorylation and total tau levels were determined by immunoblot analysis. A $\beta_{25-35}$  significantly increased the amount of hyperphosphorylated tau detected by both the AT-8 and PHF-1 antibodies (Fig. 2a). Increased hyperphosphorylation was completely prevented by taxol which had no effect on total tau levels as determined using the Tau-5 antibody. Moreover, the Tau-5 antibody also recognizes phosphorylated tau species as indicated by the presence of a mobility shift in the tau band from cells treated with A $\beta_{25-35}$ . This species of tau was also abolished in the taxol-treated cells. The expression of cdk5 also remained the same in all the treatments and provides an additional control for protein loading. Densitometric quantitation of the PHF-1 immunoreactive bands from several experiments indicated that taxol significantly decreased both basal and A $\beta$ -induced tau phosphorylation (Fig. 2b).

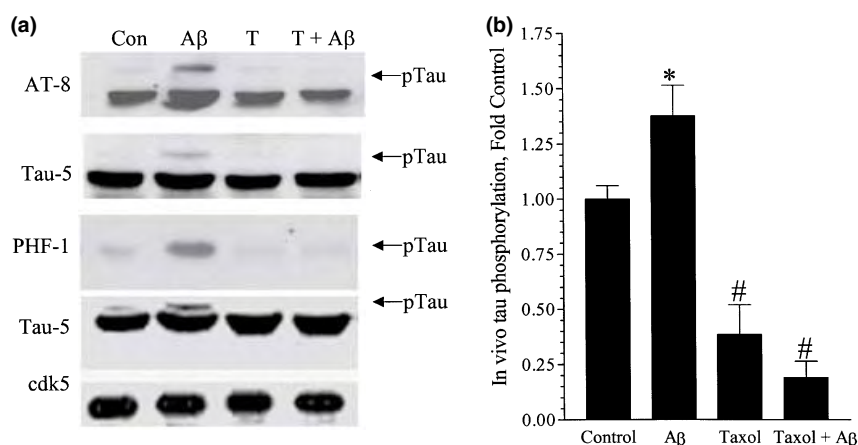


**Fig. 2** Taxol blocks A $\beta$ -induced tau hyperphosphorylation. (a) Neurons were exposed to buffer (Con), 100 nM taxol (T) or 10  $\mu$ M A $\beta_{25-35}$  in the absence (A $\beta$ ) or presence of taxol (T + A $\beta$ ) for 4 days. Whole cell lysates were prepared and total protein was separated by SDS-PAGE (20  $\mu$ g/lane). After transfer to nitrocellulose, the membrane was probed for phosphorylated tau (AT-8 or PHF-1 antibodies), stripped

and re-probed for total tau using the Tau-5 antibody. Phosphorylated tau (pTau) is indicated by the arrows. Bottom panel shows the expression level of cdk5 from the same samples. (b) Tau phosphorylation detected with the PHF-1 antibody was quantitated by densitometry from five experiments. \*,  $p$  < 0.05 compared with control; #,  $p$  < 0.001 compared with A $\beta_{25-35}$  only.

### Taxol blocks A $\beta$ -induced activation of cdk5/p25 complexes

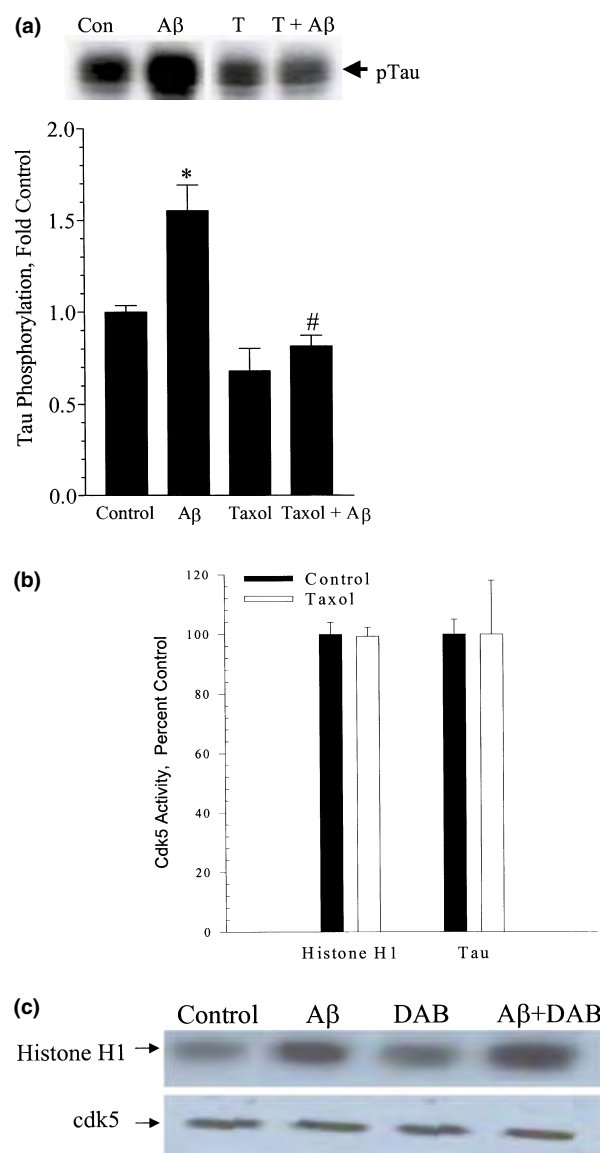
Tau is phosphorylated by numerous kinases *in vivo* including glycogen synthase kinase 3 $\beta$ , MT-affinity regulated kinases, protein kinase A and cdk5 (Billingsley and Kincaid 1997; Lee *et al.* 2001; Maccioni *et al.* 2001). A $\beta_{25-35}$  slightly stimulated glycogen synthase kinase 3 $\beta$  (~1.2-fold) under our culture conditions and taxol inhibited this activation (data not shown). However, A $\beta_{25-35}$  more robustly and reproducibly activated cdk5 (Fig. 3a). Because cdk5 is active primarily in neurons (Ino *et al.* 1994), associates with MTs indirectly through interactions with a MT-binding repeat of non-phosphorylated tau (Sobue *et al.* 2000), and its phosphorylation of tau directly leads to MT destabilization (Evans *et al.* 2000), we primarily focused upon the potential of taxol in regulating the activity of this tau kinase.

Neurons were treated with A $\beta_{25-35}$  in the absence and presence of 100 nM taxol for 4 days, whole cell lysates were prepared and cdk5 was immunoprecipitated. To assess cdk5 activity, the isolated immune-complexes were incubated in kinase buffer in the presence of [ $\gamma$ - $^{32}$ P]ATP and either histone H1 or bovine brain tau as an *in vitro* substrate. A $\beta_{25-35}$  induced a 1.5-fold increase in cdk5-mediated tau phosphorylation that was completely prevented by taxol treatment (Fig. 3a); it is important to note that the modest increase in total cdk5 activity in whole cell lysates is likely due to A $\beta_{25-35}$  preferentially activating only the cytosolic pool of cdk5/p25 complexes (see below).

To determine if taxol may decrease cdk5 activity by directly inhibiting the enzyme, cdk5 was immunoprecipitated from untreated neurons and an *in vitro* kinase assay was

performed as above except that 100 nM taxol was added directly to the reaction mix prior to initiating the reaction by the addition of substrate. Under these conditions, taxol had absolutely no effect on the phosphorylation of histone H1 or tau by cdk5 (Fig. 3b). These data suggest that the reversal of the A $\beta$ -induced increase in cdk5 activity by taxol is not due to a direct inhibition of the kinase by the drug and requires cell signaling events. To examine the relationship between MT stabilization and the inhibitory effect of taxol on A $\beta$ -induced cdk5 activation, neurons were treated with 10-deacetylbaccatin III. After 4 days of treatment, the cells were harvested, cdk5 activity immunoprecipitated and kinase activity assessed using histone H1 as the substrate. In contrast to taxol treatment, 10-deacetylbaccatin III had no effect on inhibiting A $\beta$ -induced cdk5 activation (Fig. 3c).

**Fig. 3** Taxol but not 10-deacetylbaccatin III inhibits A $\beta$ -induced cdk5 activation. Neurons were exposed for 4 days to buffer (Con), 100 nM taxol (T) or 10  $\mu$ M A $\beta_{25-35}$  in the absence (A $\beta$ ) or presence of taxol (T + A $\beta$ ) and cell lysates were prepared. (a) Cdk5 was immunoprecipitated from whole cell lysates and kinase activity was assessed using tau as the substrate. Inset shows representative autoradiogram for the effect of A $\beta_{25-35}$  and taxol treatment on *in vitro* tau phosphorylation. Tau phosphorylation was quantitated from four experiments. \*,  $p < 0.01$  compared with control; #,  $p < 0.001$  compared with A $\beta_{25-35}$  only. (b) Cdk5 was immunoprecipitated from untreated neurons and kinase activity assessed in the absence or presence of 100 nM taxol. Taxol was added directly to the reaction mixture prior to the addition of histone H1 or tau, the radiolabeled products were separated by electrophoresis and the level of phosphorylation determined using a phosphorimager. Results shown are mean  $\pm$  SEM from three experiments. (c) Cells were incubated for 4 days with buffer (Control), 100 nM 10-deacetylbaccatin III (DAB) or 10  $\mu$ M A $\beta_{25-35}$  in the absence (A $\beta$ ) or presence of 100 nM 10-deacetylbaccatin III (A $\beta$  + DAB). Cells were harvested and cdk5 activity assessed as described above using histone H1 as the substrate. Upper panel shows histone H1 phosphorylation and bottom panel shows equivalent levels of cdk5 in each sample.



These results suggest that MT stabilization is necessary for the inhibitory effect of taxol on cdk5 activation by A $\beta_{25-35}$ .

Cdk5 activity is regulated by interaction with specific activator proteins, p35 and p25, that have different subcellular localizations. Due to the presence of an N-terminal myristoylation site, p35 is essential for targeting cdk5 to the plasma membrane (Tsai *et al.* 1994; Dhavan *et al.* 2001). In contrast, a calpain-directed proteolytic degradation of p35 releases p25 from the N-terminal region of p35 that is tethered to the membrane and increases the amount of cytosolic cdk5/p25 complexes (Kusakawa *et al.* 2000; Lee *et al.* 2000; Nath *et al.* 2000). Because the above experiments used an antibody directed against cdk5, we could not determine whether A $\beta_{25-35}$  activated cdk5/p35 or cdk5/p25 complexes nor whether one or both complexes may be inhibited by taxol.

To determine the effect of A $\beta_{25-35}$  and taxol on the activity of cdk5/p35 versus cdk5/p25 complexes, two approaches were taken. In the first approach, cdk5 activity was assessed following immunoprecipitation with antibodies that recognize either the N-terminus (N-20) or C-terminus (C-19) of p35. As p35 and p25 share the same C-terminus, the C-19 p35 antibody will immunoprecipitate both p35 and p25 and provide an assessment of total cdk5 activity. However, the N-20 p35 antibody is directed against an N-terminus region that is lacking in p25 and provides a measure of kinase activity associated with only the cdk5/p35 complex. Therefore, the contribution of the cdk5/p25 complex to total cdk5 activity may be measured indirectly by subtracting the cdk5/p35-specific activity (N-20 antibody) from the total activity (cdk5/p35 + cdk5/p25) obtained following immunoprecipitation with the C-19 antibody.

Neurons were treated with A $\beta_{25-35}$  in the absence or presence of taxol, the cells were harvested in lysis buffer and each whole cell lysate was divided into two  $\times 100$   $\mu$ g aliquots. Each aliquot was then incubated with 2  $\mu$ g of the C-19 or the N-20 p35 antibody, the immune complexes were isolated with protein A Sepharose and cdk5 activity was assessed as described above. Similar to results in Fig. 3a, A $\beta_{25-35}$  treatment activated total cdk5 activity (C-19 p35 antibody) but kinase activity associated with the cdk5/p35 complex (N-20 p35 antibody) did not contribute to the overall increase (Fig. 4a). Indeed, total cdk5 was activated by A $\beta_{25-35}$  about 1.5-fold. However, subtracting the p35-specific activity from total activity indicated that cdk5/p25 complexes were activated by A $\beta_{25-35}$  approximately 2.1–2.3-fold (Fig. 4b). Moreover, taxol significantly inhibited kinase activity associated with the cdk5/p25 complexes but had no effect on the activity of cdk5/p35 complexes (Fig. 4b).

To provide a more direct assessment of the effect of A $\beta_{25-35}$  and taxol on the activity of cdk5/p25 complexes, our second approach exploited the differential compartmentation of cdk5/p35 versus cdk5/p25 complexes. As cdk5/p35 is

primarily membrane-associated whereas cdk5/p25 is cytosolic (Nikolic and Tsai 2000), soluble and particulate fractions of treated neurons were prepared as described in Experimental procedures. Prior to centrifugation, an aliquot of the whole cell lysate was removed to determine total cdk5 activity. Cdk5 present in the whole cell lysate, soluble and particulate fractions was immunoprecipitated with the C-19 p35 antibody and kinase determined as described above. Once again, A $\beta_{25-35}$  activated total cdk5 activity immunoprecipitated from whole cell lysates by 1.5-fold and this activation was completely inhibited by taxol (Fig. 4c). However, cdk5/p25 activity immunoprecipitated from the cytosolic fraction was activated greater than 3-fold by A $\beta_{25-35}$  and this activation was inhibited by about 55% in cells treated with taxol and A $\beta_{25-35}$ . Similar to our results above, A $\beta_{25-35}$  and taxol had no effect on the activity of cdk5/p35 complexes immunoprecipitated from the membrane fraction. Together, these results strongly support that A $\beta$ -induced cdk5 activity is associated primarily with cytosolic cdk5/p25 complexes and that taxol specifically decreases the A $\beta$ -induced activation of the cdk5/p25 complex.

#### Taxol prevents A $\beta$ -induced changes in the ratio of p35/25

Because taxol was specifically inhibiting the activity of cdk5/p25 complexes, we next addressed potential mechanisms for this effect. p35 is a short-lived protein that undergoes relatively rapid degradation by calpain-mediated proteolysis (Lee *et al.* 2000) and via interaction with the proteasome (Patrick *et al.* 1998). Moreover, recent reports suggest that A $\beta$  increases the degradation of p35 to p25 in AD brain (Lee *et al.* 1999; Patrick *et al.* 1999) and cultured primary neurons (Lee *et al.* 2000). Similarly, A $\beta_{25-35}$  treatment induced a significant 1.5-fold increase in the production of p25 in the cortical neurons after 4 days (Fig. 5a) and co-treatment of the cells with A $\beta_{25-35}$  and taxol completely prevented this increase. Thus, decreased p25 production correlated with the effect of taxol on decreasing cdk5/p25 activity.

To determine if taxol was decreasing the turnover of p35, we measured its half-life in cortical neurons treated with vehicle or 100 nM taxol for 4 days. To inhibit protein synthesis, 30  $\mu$ g/mL of cycloheximide was added to the cells (Patrick *et al.* 1998) and the neurons were scraped into lysis buffer at various times between 0 and 480 min following the addition of cycloheximide. Similar amounts of total protein from each time point were separated by SDS-PAGE, the proteins were transferred to nitrocellulose and the presence of p35 and p25 was determined by immunoblot analysis using the C-19 p35 antibody. In control neurons the half-life of p35 was around 140–160 min (Fig. 5b and c), substantially longer than the 20–30 mins that has been reported in cortical neurons cultured for 3 days *in vitro* (Patrick *et al.* 1998) or in transfected COS-7 cells (Patrick *et al.* 1999). Whether this difference is related to the age of the cultures, specific

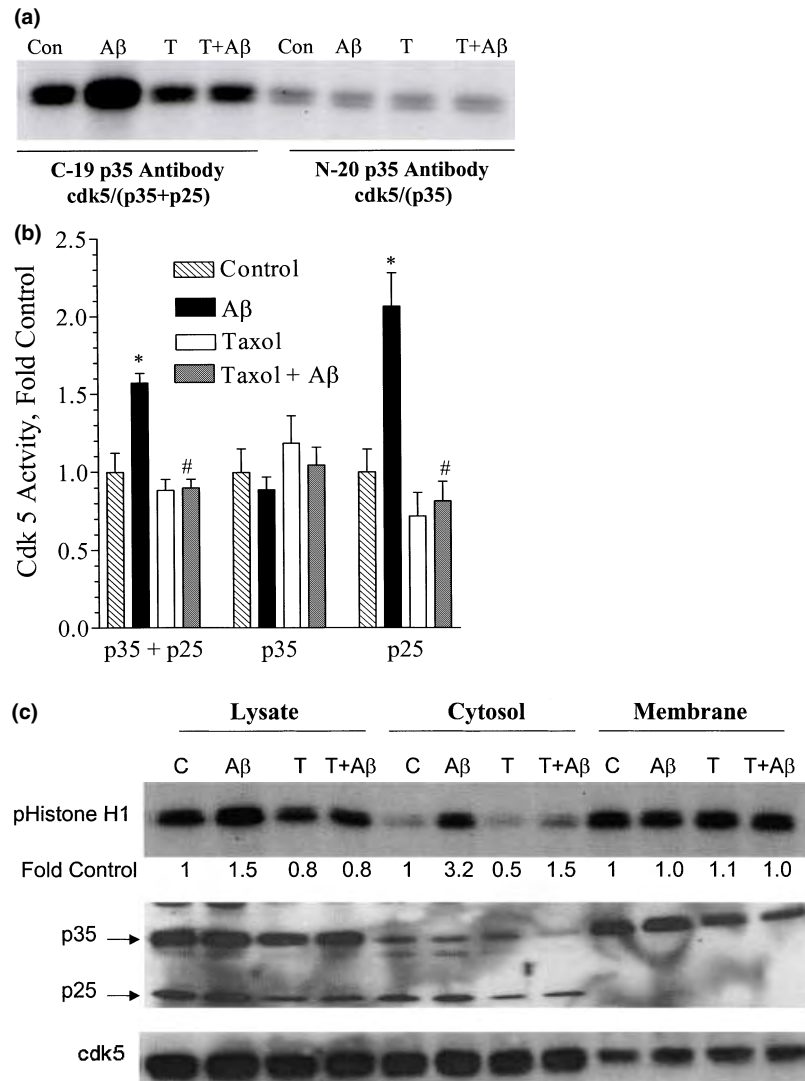


**Fig. 4** Taxol inhibits the activity of cdk5/p25 complexes. (a) Neurons were treated as indicated and the whole cell lysates were divided into  $2 \times 100 \mu\text{g}$  aliquots. Cdk5 was immunoprecipitated from each aliquot with either the C-19 p35 antibody which recovers cdk5/(p35 + p25) complexes or the N-20 p35 antibody which recovers only cdk5/p35 complexes. Cdk5 activity was assayed and phosphorylated histone H1 separated by SDS-PAGE and detected by phosphoimaging. (b) The relative density of histone H1 phosphorylation by cdk5(p35 + p25) and cdk5/(p35) complexes was quantitated from three experiments. Results shown for cdk5/(p25) were obtained by subtracting the relative density of histone H1 phosphorylation obtained for cdk5/(p35)

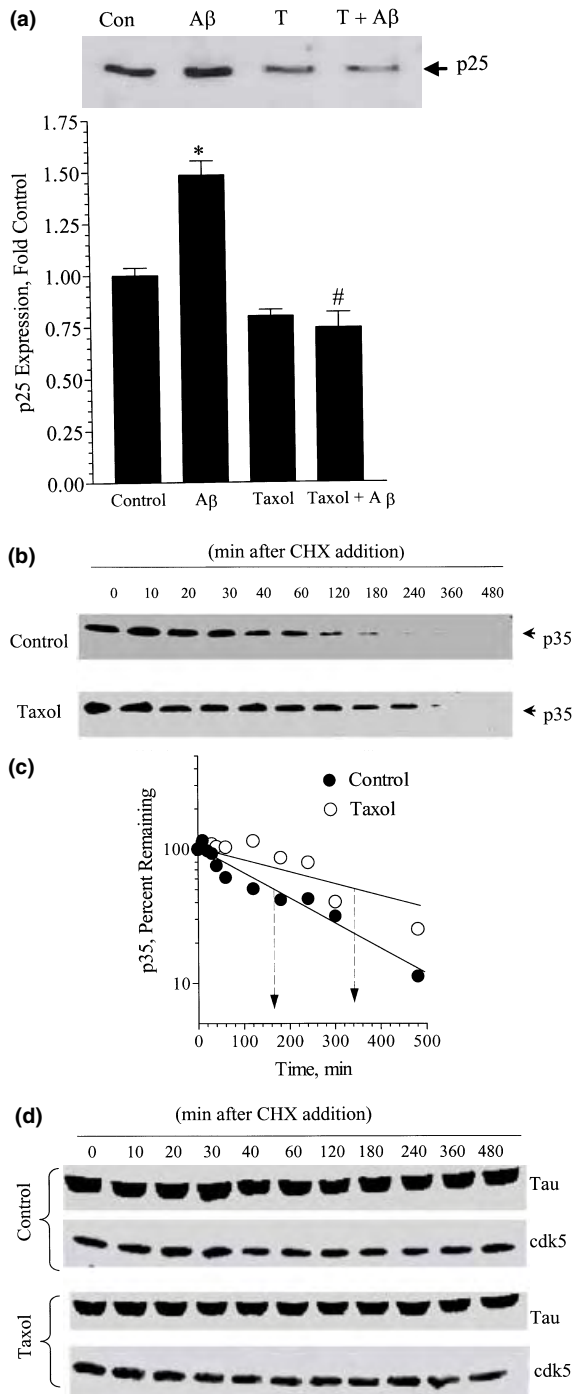
( $5.4 \pm 0.8$ ) from cdk5/(p35 + p25) ( $13.5 \pm 1.6$ ) and expressed as fold control. \*,  $p < 0.01$  compared to control; #,  $p < 0.001$  compared to A $\beta$  only. (c) Neurons were treated as indicated and an aliquot of the total lysate saved. Of the remaining whole cell lysates,  $100 \mu\text{g}$  was separated into cytosolic and membrane fractions by centrifugation. Each fraction was immunoprecipitated with the C-19 p35 antibody and cdk5 activity assessed using histone H1 as the substrate. Upper panel, histone H1 phosphorylation; middle panel, immunoblot of p35 and p25 levels in membrane and cytosolic fractions; lower panel, immunoblot for the level of cdk5 in each sample.

differences in culture conditions, antibodies or cell type is unknown. Nevertheless, addition of  $100 \text{ nM}$  taxol to the cortical neurons for 4 days increased the half-life of p35 to about 320–340 min (Fig. 5b and c). Importantly, using the same cell extracts, taxol had no effect on the half-life of either tau or cdk5, indicating that it was not non-specifically decreasing protein degradation (Fig. 5d). The lack of change

in cdk5 and tau levels also indicates that the increased half-life of p35 in the presence of taxol is not due to differences in protein loading.

Phosphorylation of p35 by cdk5 enhances its degradation via the proteasome and direct inhibition of cdk5 with roscovitine can increase the half-life of p35 (Patrick *et al.* 1998). Therefore, a decrease in cdk5 activity would be





expected to increase the half-life of p35. However, our results indicate that taxol does not directly inhibit cdk5, suggesting that it stabilizes p35 by another mechanism. Although we cannot rule out the possibility that taxol may increase the half-life of p35 by interfering with its accessibility to serve as a substrate for cdk5, the calpain-mediated cleavage of p35 also leads to enhanced formation of p25 (Kusakawa *et al.* 2000; Lee *et al.* 2000). Because taxol stabilized p35 and

**Fig. 5** Taxol increases the half-life of p35 and decreases the formation of p25 by A $\beta$ <sub>25–35</sub>. (a) Neurons were exposed for 4 days to buffer (Con), 100 nM A $\beta$  (A $\beta$ ) or presence of taxol (T + A $\beta$ ), cell lysates were prepared and p25 levels were determined by immunoblot analysis. Inset shows representative immunoblot for the effect of A $\beta$ <sub>25–35</sub> and taxol treatment on p25 expression. p25 expression was quantitated densitometrically from four experiments. \*,  $p < 0.001$  compared with control; #,  $p < 0.001$  compared with A $\beta$  only. (b) Neurons were treated with vehicle or 100 nM taxol for 4 days, 30  $\mu$ g/mL cycloheximide (CHX) was added, and the cells were harvested at the indicated time after CHX addition. Whole cell lysates were subjected to SDS–PAGE (20  $\mu$ g per lane) and the half-life of p35 was measured by immunoblot analysis. (c) Expression of p35 was quantitated by densitometry and the approximate half-life of p35 in control and taxol treated cells is indicated by the arrows. (d) Separate aliquots from the same neuronal lysates used above were subjected to SDS–PAGE and the effect of taxol on the half-life of tau and cdk5 was determined by immunoblot analysis.

decreased p25 formation, we examined the effect of A $\beta$ <sub>25–35</sub> and taxol on calpain activity. Primary cortical neurons were treated with A $\beta$ <sub>25–35</sub> in the absence or presence of taxol for 4 days, cell lysates were prepared and calpain activity was determined fluorometrically (Xie and Johnson 1997). As anticipated, A $\beta$ <sub>25–35</sub> treatment induced an approximate 2-fold activation of calpain (Fig. 6). Although taxol decreased basal calpain activity, it also inhibited calpain activation induced by A $\beta$ <sub>25–35</sub>. As a positive control, the assay was verified by incubating the cell lysate with ALLN, a calpain inhibitor that completely blocked hydrolysis of the substrate.

The inhibition of calpain activity by taxol was not due to decreases in the level of calpain-1 ( $\mu$ -calpain) or calpain-2 (m-calpain) nor to increases in the expression of the endogenous calpain inhibitor, calpastatin (data not shown). It should be noted, however, that 13 different calpains are broadly expressed (Huang and Wang 2001). Importantly, taxol had no effect on endogenous calpain activity when it was added directly to cell lysates prepared from untreated neurons and incubated with the calpain substrate. This result suggests that taxol does not inhibit calpain directly. However, to rule out the possibility that some endogenous proteins or lipids present in the cell lysate were sequestering taxol and preventing it from inhibiting calpain directly, purified calpain-1 was incubated with the peptide substrate plus 5 mM Ca<sup>2+</sup> in the presence and absence of 100 nM taxol. Once again, taxol had no inhibitory effect on calpain-1 activity with the purified enzyme (data not shown). Collectively, these results suggest that a primary point of action of taxol is upstream of calpain activation by A $\beta$ <sub>25–35</sub>.

#### Overexpression of p25 reverses taxol-mediated neuroprotection against A $\beta$ -induced cell death

Transgenic mice overexpressing p25 exhibit cytoskeletal disruptions and increased phosphorylation of neurofilaments

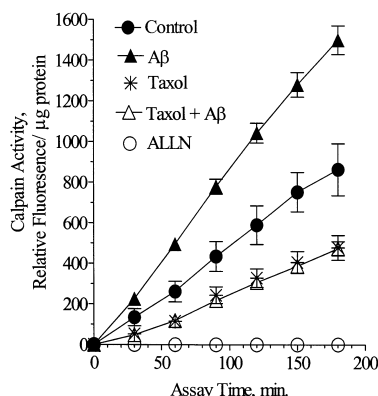


**Fig. 6** Inhibition of A $\beta$ -induced calpain activation by taxol. Neuronal cultures were exposed for 4 days to 10  $\mu$ M A $\beta_{25-35}$  in the absence or presence of 100 nM taxol and cell lysates prepared. Calpain activity was monitored fluorometrically in quadruplicate and the results shown are from four experiments.

and tau (Ahlijanian *et al.* 2000). Moreover, tau phosphorylation by cdk5 decreases MT stability (Lee *et al.* 2001). If MT stabilization by taxol is sufficient to protect neurons against A $\beta$  toxicity, then it should be protective even during ectopic expression of p25 and increased tau phosphorylation. Primary cortical neurons were infected with a recombinant p25 adenovirus and protein expression and cdk5 activity determined over a period of 4 days. Overexpression of p25 was maximal 2 days after infection (Fig. 7a) and increased cdk5 activity about 2-fold using either histone H1 or tau as the substrate (Fig. 7b). Therefore, we examined the effect of p25 overexpression (200 pfu/cell) on the protection against A $\beta_{25-35}$  toxicity by taxol at this time.

Similar to uninfected cells (Fig. 5a), taxol inhibited the A $\beta$ -induced increase in p25 expression (Fig. 7c, upper panel) and cdk5-mediated tau phosphorylation (Fig. 7c, middle panel) in cells infected with the blank virus. In contrast, neither A $\beta_{25-35}$  nor taxol changed p25 expression (Fig. 7c, upper panel) or cdk5-mediated histone H1 phosphorylation (Fig. 7c, middle panel) in neurons infected with the p25 adenovirus. As taxol did not decrease cdk5 activity in cells overexpressing p25, these results also support that the inhibitory effect of taxol on A $\beta$ -induced cdk5 activation requires the disruption of signal transduction events and is not due to a direct inhibition of the kinase by taxol.

A $\beta_{25-35}$  induced a significant level of cell death in neurons infected with blank or p25 adenoviruses (Fig. 7d). However, p25 overexpression only modestly decreased cell viability regardless of the absence or presence of A $\beta_{25-35}$ . The modest effect of p25 expression on increasing the extent of cell death may be due to using these cells 2 days post infection. At this time, the viability of neurons infected with blank virus ( $71 \pm 3.1\%$ ) was similar to uninfected neurons ( $76.6 \pm 2.6\%$ ). Although p25 expression was significantly more effective at inducing cell death 3–4 days post infection,

viability of neurons treated with blank virus alone was also decreasing (data not shown). Importantly, viral infection did not non-specifically alter the response to taxol as the drug also protected against A $\beta_{25-35}$  toxicity in neurons infected with blank virus (compare bars 3 and 7). In contrast, taxol did not significantly inhibit cell death in response to increased p25 expression in the absence (compare bars 2 and 6) or presence (compare bars 4 and 8) of A $\beta_{25-35}$ . Indeed, forced expression of p25 reversed the neuroprotective effect of taxol seen in cells infected with blank virus and treated with A $\beta_{25-35}$  (compare bars 7 and 8). As ectopic expression of p25 had no effect on the stabilization of MTs by taxol (data not shown), these data suggest that MT stabilization alone is not sufficient to overcome the detrimental effect of enhanced cdk5 activity.

#### Systemic administration of a taxol analog mimics the effect of taxol on inhibiting activation of cdk5 by A $\beta_{25-35}$

Unfortunately, identifying the most active compound in cell cultures with regards to MT stabilization, intracellular signaling and neuroprotection is usually not sufficient to overcome the difficulties of showing activity in an intact organism. In this regard, the potential for taxol as a therapeutic agent either for AD or cancers of the central nervous system (CNS) is limited by its lack of penetration across the blood–brain barrier.

The blood–brain barrier is composed of numerous tight junctions between capillary endothelial cells that create a low passive permeability across this barrier and a selective exchange of molecules from the circulation into the CNS (Thiel and Audus 2001). Additionally, the presence of the P-glycoprotein in cells forming the blood–brain barrier permits the rapid efflux of lipophilic molecules such as taxol which limits the effectiveness of this drug in treating tumors of the CNS (Heimans *et al.* 1994; Brouty-Boye *et al.* 1995). Although pharmacologic inhibition of this efflux can increase the brain level of taxol 4-fold (van Asperen *et al.* 1997), transport of essential macromolecules across the blood–brain barrier may also be facilitated by highly selective transporter proteins (Thiel and Audus 2001). The presence of specific small molecule transporters offers the possibility that modification of taxol may circumvent P-glycoprotein-mediated efflux and enhance its permeability across the blood–brain barrier while retaining its MT-stabilizing and neuroprotective properties.

Using combinatorial chemistry and a strategy that exploited the presence of specific transporters for basic amino acids, biotin, amines and monocarboxylic acids, a library of compounds was prepared that modified taxol with these various molecules (Liu *et al.* 2002). From this library, a succinylated taxol derivative (10-succinyl taxol, TX67) emerged as a candidate molecule that efficiently stabilized MTs (Liu *et al.* 2002), bypassed the P-glycoprotein efflux system and has a 150-fold greater permeability than taxol at



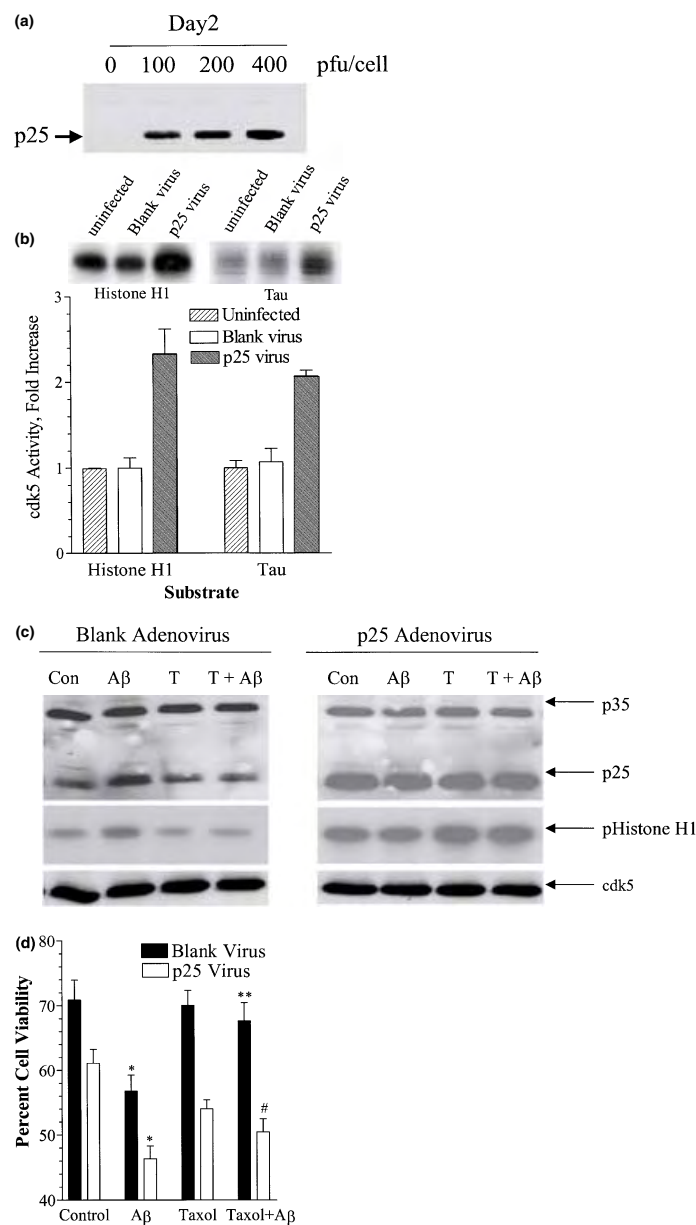


**Fig. 7** Overexpression of p25 reverses the neuroprotective effect of taxol. (a) Neurons were infected with recombinant adenoviruses at 0–400 pfu/cell for 2 days and cell lysates were prepared. Following SDS-PAGE (20  $\mu$ g/lane), p25 was detected by immunoblot analysis. (b) Cell lysates were prepared from uninfected neurons or neurons infected with 200 pfu/cell of blank adenovirus or p25 adenovirus for 2 days. Cdk5 was immunoprecipitated and its activity was assessed using histone H1 or tau as the substrate in an *in vitro* kinase assay. The upper panels show the extent of histone and tau phosphorylation. Band intensity was quantitated using a phosphorimager and expressed as fold-increase relative to basal activity of uninfected cells. The results from three experiments are shown. (c) Neurons were infected with blank or p25 adenoviruses at 200 pfu/cell. After 2 h, the neurons were treated with buffer (Con), 100 nM

taxol (T) or 10  $\mu$ M A $\beta$ <sub>25–35</sub> in the absence (A $\beta$ ) or presence of taxol (T + A $\beta$ ) for 2 days. Cell lysates were prepared and p25 levels were assessed by immunoblot analysis. Cdk5 (C-8 antibody) was immunoprecipitated and its activity assessed using histone H1 as the substrate. Total cdk5 levels (lower panel) were similar between each treatment. (d) Cells infected with blank or p25 adenovirus were treated with 10  $\mu$ M A $\beta$ <sub>25–35</sub> in the absence or presence of 100 nM taxol for 2 days and cell viability was assessed. Values presented are from four experiments. The per cent viability in uninfected neuronal cultures was  $76.6 \pm 2.6$ . \*,  $p < 0.05$  for A $\beta$  compared to respective control; \*\*,  $p < 0.05$  blank virus-taxol compared with blank virus-(taxol + A $\beta$ ); #,  $p < 0.001$  blank virus-(taxol + A $\beta$ ) compared with p25 virus-(taxol + A $\beta$ ).

therapeutically relevant concentrations in a cellular model for the blood–brain barrier (Michaelis *et al.* 2002). Importantly, TX67 also was neuroprotective against A $\beta$  in cultured primary neurons (Table 1). Therefore, we assessed whether systemic administration of TX67 may mimic the effect of taxol on inhibiting A $\beta$ -induced cdk5 activation in acutely dissociated neurons prepared from TX67-treated animals. Adult mice were injected every other day for 16 days with vehicle, 8 mg/kg of TX67 or a similar dose of taxol. To determine the *in vivo* effectiveness of TX67 versus taxol, cultures of acutely dissociated cortical neurons were prepared and the cells were treated *ex vivo* with buffer or 20  $\mu$ M A $\beta_{25-35}$  immediately after their preparation. We used a higher concentration of A $\beta_{25-35}$  in these studies as the acutely dissociated neurons are still partially clumped and represent a mixed population of cells. After 24 h, the cells were harvested, cdk5 was immunoprecipitated and histone H1 phosphorylation was assessed using the *in vitro* kinase assay. Similar to the cultured embryonic cortical neurons, A $\beta_{25-35}$  induced a 1.8-fold increase in cdk5 activity in acutely dissociated neurons obtained from adult animals that received the drug vehicle only (Fig. 8a). Administration of taxol to the animals was ineffective at preventing the A $\beta$ -induced activation of cdk5, consistent with its poor ability to cross the blood–brain barrier (Cavaletti *et al.* 2000). In contrast, TX67 markedly decreased the magnitude of basal cdk5 activity and blocked its activation by A $\beta_{25-35}$  (Fig. 8a and b). Overall, these data provide compelling evidence for proof of principle that taxol analogs may be useful for attenuating the magnitude of some aspects of A $\beta$  signal transduction *in vivo*.

## Discussion

Lee and colleagues originally proposed that MT stabilizing agents may be useful therapeutics for slowing the progression of the neurofibrillary pathology that is one hallmark of advanced AD (Lee *et al.* 1994). In this report, we provide insight into the molecular mechanism by which taxol protects cortical neurons from toxicity by A $\beta$  peptides. Although taxol stabilized MTs in A $\beta_{25-35}$  treated cells, it also decreased A $\beta$ -induced calpain activation, p25 production and activation of cdk5/p25 complexes. Collectively, these results suggest that taxol acts upstream of calpain in regulating the cdk5 pathway.

### The cdk5/p25 complex as a therapeutic target in AD

The induction of tau hyperphosphorylation by cdk5/p25 complexes in cultured cells and transgenic mice suggests that this complex may contribute to the increased amount of hyperphosphorylated tau present in PHFs from AD patients (Dhavan *et al.* 2001). Increased cdk5 activity may also provide a mechanistic link in the etiology of motor neuron dysfunction in amyotrophic lateral sclerosis (Nguyen *et al.*

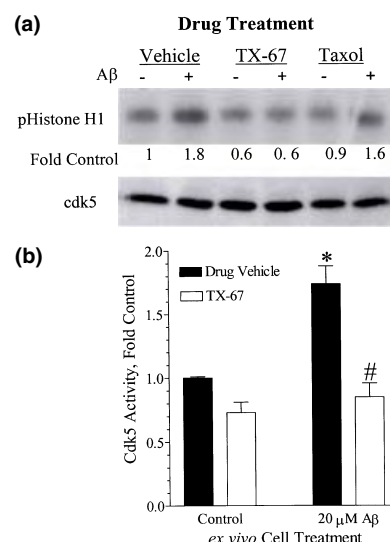


**Fig. 8** Systemic administration of a succinylated taxol analog (TX67) blocks A $\beta$ -induced cdk5 activation. (a) Animals were given intraperitoneal injections of the drug vehicle, 8 mg/kg TX 67 or taxol every other day for 16 days. The animals were killed, cultures of acutely dissociated cortical neurons were prepared and treated with 20  $\mu$ M A $\beta_{25-35}$  for 24 h. Cell lysates were prepared, cdk5 was immunoprecipitated and its activity was assessed using histone H1 as the substrate (upper panel). The amount of cdk5 in each sample was determined by immunoblot analysis (lower panel). Histone H1 phosphorylation was quantitated with a phosphorimager and normalized to the expression level of cdk5 to account for the slight differences in cdk5 levels between samples. Numbers below the upper panel indicate fold histone H1 phosphorylation relative to control neurons obtained from animals receiving the drug vehicle. (a) Quantitation of the effect of TX-67 administration on A $\beta$ -induced histone H1 phosphorylation. Values are from three animals for each treatment. \*,  $p < 0.01$  compared with control neurons from animals receiving the drug vehicle; #,  $p < 0.01$  compared with A $\beta$ -treated neurons from animals receiving the drug vehicle.

2001; Patzke and Tsai 2002b). Thus, the cdk5/p25 complex is emerging as an attractive pharmacological target in neurodegenerative diseases.

Direct inhibition of cdk5 with kinase inhibitors can prevent A $\beta$ -induced cell death of primary hippocampal neurons (Alvarez *et al.* 1999) and our results are consistent with these data. However, taxol did not inhibit cdk5 activity directly but decreased kinase activity, presumably by regulating the formation of p25. These data suggest that the pharmacologic regulation of p25 production may provide an alternative therapeutic approach to regulating cdk5 activity. Although a calpain inhibitor would obviously be attractive for preventing this degradation, calpain is critical to regulating cytoskeletal proteins and numerous metabolic functions in cells. This broad spectrum of bioactivity contributes to the considerable lack of specificity and toxicity that current calpain inhibitors exhibit toward cells (Nakagawa and Yuan 2000; Wang 2000; Huang and Wang 2001).

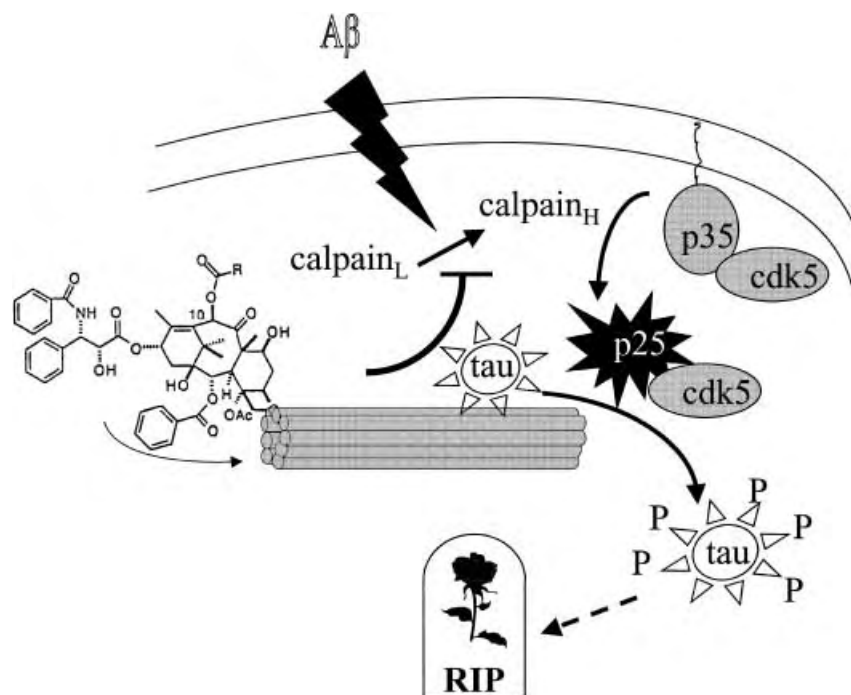


**Fig. 9** Taxol inhibition of the cdk5 pathway occurs at the level of calpain activation by A $\beta$ . See text for details. Calpain<sub>L</sub>-low activity; calpain<sub>H</sub>- high activity. The R group at the C10 position contains an acetyl moiety in taxol and this group is substituted with succinate in TX-67.

A caveat to the potential of cdk5 as a therapeutic target, with respect to AD at least, hinges upon whether enhanced production of p25 and chronic activation of cdk5 activity is a consistent phenomenon in AD brain. Recent studies from post-mortem brain tissue obtained from AD patients suggest that p25 levels may be elevated in this disease (Patrick *et al.* 1999, 2001). Consistent with increased p25 expression, pre-frontal cortex from post-mortem brain of AD patients showed a significant increase in cdk5 activity relative to control patients, when corrected for either the level of cdk5 expression or for neuronal loss (Lee *et al.* 1999). In contrast, others have reported that p25 levels were decreased in post-mortem tissue from AD versus control brain (Taniguchi *et al.* 2001; Yoo and Lubec 2001). One complicating factor that may contribute to these discrepancies is the effect of the post-mortem interval on induction of an artifactual increase in p25 production via calpain-mediated degradation (Kusakawa *et al.* 2000; Taniguchi *et al.* 2001). Thus, a critical assessment using either pharmacologic or genetic manipulation of the cdk5 pathway in animals and examination of its role in the development of neurofibrillary pathology will be required to characterize more fully the role of this pathway in AD.

#### **Taxanes and neurodegenerative disease: the conundrum of multiple mechanisms-multiple outcomes**

Increased tau phosphorylation by cdk5 is sufficient to directly decrease stabilization of MTs and contribute to A $\beta$  toxicity (Evans *et al.* 2000). MT-stabilization by taxol, and presumably taxol analogs, is necessary for neuroprotection against A $\beta$  toxicity as 10-deacetylbaccatin III does not

stabilize MTs and was ineffective at preventing A $\beta$ -induced cell death. Further, MT stabilization is also necessary for the inhibition of the cdk5 pathway by taxol as 10-deacetylbaccatin III did not inhibit the activation of cdk5 by A $\beta_{25-35}$ . However, MT stabilization alone was not sufficient to protect neurons against A $\beta_{25-35}$  toxicity in neurons ectopically expressing p25. Similarly, activation of c-jun N-terminal kinase (JNK) by taxol in breast cancer cells also requires MT binding (Wang *et al.* 1998) and no clear evidence exists that any effect of taxol on cell signaling is necessarily independent of its MT binding properties at therapeutically relevant concentrations (Blagosklonny and Fojo 1999). Together, these data support the hypothesis that the state-of-stability or dynamic instability of axonal MTs represents a signaling pathway within neurons and that the integrity of MT structure may serve as a sensor of the normal homeostasis in cells. A schematic summary of the role of taxanes in regulating A $\beta$  toxicity is presented in Fig. 9. We propose that taxol may minimize A $\beta$  toxicity through distinct but interrelated contributions: (i) its ability to stabilize MTs in the presence of A $\beta$  and (ii) an inhibition of A $\beta$ -induced calpain activation which minimizes proteolysis of p35 to p25, leading to decreased activation of cdk5/p25 complexes and subsequent tau phosphorylation. Finally, as A $\beta$  induces the loss of intraluminal Ca<sup>2+</sup> pools in the endoplasmic reticulum (ER) (Siman *et al.* 2001), the inhibition of calpain by taxol raises the possibility that MT-stabilization may link to minimizing ER stress. We are currently examining the role of taxol and the cdk5 pathway in regulating the activity of ER-resident proteins such as presenilins and caspase 12; the later is

activated by calpain cleavage and is critical to A $\beta$ -induced apoptosis (Nakagawa and Yuan 2000; Yoneda *et al.* 2001).

An important consideration in our approach of using taxol and taxol analogs as neuroprotective agents derives from the likelihood that these compounds may affect other aspects of cell signaling (Blagosklonny and Fojo 1999). Taxol is well recognized as an anti-mitotic agent that induces apoptosis in cancer cells by causing cell cycle arrest at the G2/M transition (Jordan *et al.* 1993; Blagosklonny and Fojo 1999), activating JNK (Wang *et al.* 1998; Amato *et al.* 1998) and inducing phosphorylation of bcl-2 (Blagosklonny *et al.* 1996; Blagosklonny *et al.* 1997). Additionally, in macrophages and monocytes, taxol exerts lipopolysaccharide-like effects at high concentrations (10–30  $\mu$ M) (Ding *et al.* 1990; Manthey *et al.* 1993), which, although therapeutically unsustainable (Blagosklonny and Fojo 1999), may contribute to its apoptotic actions.

It has been reported recently that 100 nM taxol can also induce apoptosis in cortical neurons through a pathway independent of bcl-2 phosphorylation but still requiring activation of a nuclear pool of JNK and phosphorylation of the *c-jun* transcription factor (Figuerola-Masot *et al.* 2001). In contrast, addition of 1–10  $\mu$ M taxol had no effect on neuronal morphology and presumably the viability of hippocampal neurons obtained from wild type or tau-deficient mice (Rapoport *et al.* 2002). Indeed, taxol had no significant effect on the activation of caspase 3 and significantly decreased the A $\beta$ -induced activation of this enzymatic marker of apoptosis (Michaelis *et al.* 1998). Although we have not examined the effect of taxol on neuronal viability under the conditions used by Xia and colleagues (Figuerola-Masot *et al.* 2001), it is possible that the addition of 10% fetal calf serum to the primary cultures used in these studies may provide very strong survival signals upon which the neurons become dependent. Under these growth conditions, taxol may promote apoptosis by stabilizing MTs and decreasing the activity of phosphoinositide 3-kinase (Figuerola-Masot *et al.* 2001).

Similar to our results, a recent study also found that taxol did not induce death in neurons isolated from wild type or tau-deficient animals in the absence of A $\beta$  treatment (Rapoport *et al.* 2002). However, taxol was not protective against A $\beta$  treatment of neurons from wild type animals. Interestingly, neurons from tau-deficient animals were insensitive to A $\beta$ -induced neurite degeneration *unless* the MTs were first stabilized with taxol. These results have led to the proposal that increasing MT stability may not permit cells to compensate for degenerative cues arising from A $\beta$  treatment (Rapoport *et al.* 2002). The reason for the underlying difference between the protective effect of taxol against A $\beta$  peptides in our study versus Rapoport *et al.* (2002) is unclear but both studies support that tau plays a central role in regulating cellular responses to A $\beta$  peptides. Nevertheless, the rather dichotomous effect of taxol on post-mitotic

neurons under different growth conditions raises the issue that the *in vivo* effects of taxol at therapeutically sustainable concentrations (5–200 nM) (Blagosklonny and Fojo 1999) may be influenced by the balance between survival and stress signals that impact on the state-of-stability or dynamic instability of axonal MTs in a given neuronal population.

### The *in vivo* potential of MT-stabilizing agents to minimize neurofibrillary pathology

Numerous lipophilic drugs, including taxol, do not penetrate the blood–brain barrier due to the presence of a P-glycoprotein efflux system, the multidrug resistant protein (MDR1) (Teraski and Tsuji 1995). We circumvented this problem by using a succinylated taxol analog that is not effluxed by P-glycoprotein present in the capillary endothelial cells that form the blood–brain barrier (Michaelis *et al.* 2002). Indeed, neurons obtained from TX67 but not taxol treated animals, showed decreased basal cdk5 activity and were resistant to the A $\beta$ -induced activation of this tau kinase. This outcome suggests that, in contrast to the use of direct inhibitors of cdk5 that interact with the ATP binding domain (i.e. roscovitine), taxol analogs may permit an alternative regulation of cdk5 which may allow the enzyme to respond to cellular signals. In this regard, a basal level of cdk5 activity is associated with enhanced neuronal survival (Li *et al.* 2002).

In summary, our results support the premise that MT-stabilizing agents based upon the taxol backbone can be rationally designed and may have potential usefulness in treating neurofibrillary pathology if they cross the blood–brain barrier, stabilize MTs and attenuate tau kinase activity. If tau phosphorylation by cdk5 is sufficient to destabilize MTs (Evans *et al.* 2000), taxol analogs or other MT-stabilizing agents that are more permeable to the blood–brain barrier (i.e. epothilones) may minimize MT destabilization and prove beneficial in slowing the formation of NFTs during the progression of AD and other tauopathies.

### Acknowledgements

We would like to thank Dr L-H. Tsai for providing p35 cDNA, Dr Peter Davies for the Tau-5 and PHF-1 antibodies, and Dr T. C. He for the pAdTRACK and pAdEASY adenoviral vectors. This work was supported by grants NS38154, NS38745 (RTD), H220528 (MLM) and CA82801 (GG) from the National Institutes of Health and the Institute for the Study of Aging (MLM).

### References

- Ahlijanian M. K., Barrezueta N. X., Williams R. D., Jakowski A., Kowsz K. P., McCarthy S., Coskran T., Carlo A., Seymour P. A., Burkhardt J. E., Nelson R. B. and McNeish J. D. (2000) Hyperphosphorylated tau and neurofilament and cytoskeletal disruptions in mice overexpressing human p25, an activator of cdk5. *Proc. Natl Acad. Sci. USA* **97**, 2910–2915.

- Alvarez A., Toro R., Caceres A. and Maccioni R. B. (1999) Inhibition of tau phosphorylating protein kinase cdk5 prevents beta-amyloid-induced neuronal death. *FEBS Lett.* **459**, 421–426.
- Alvarez A., Munoz J. P. and Maccioni R. B. (2001) A Cdk5-p35 stable complex is involved in the beta-amyloid-induced deregulation of Cdk5 activity in hippocampal neurons. *Exp. Cell Res.* **264**, 266–274.
- Amato S. F., Swart J. M., Berg M., Wanebo H. J., Mehta S. R. and Chiles T. C. (1998) Transient stimulation of the c-Jun – NH2-terminal kinase/activator protein 1 pathway and inhibition of extracellular signal-regulated kinase are early effects in paclitaxel-mediated apoptosis in human B lymphoblasts. *Cancer Res.* **58**, 241–247.
- van Asperen J., van Tellingen O., Sparreboom A., Schinkel A. H., Borst P., Nuijten W. J. and Beijnen J. H. (1997) Enhanced oral bioavailability of paclitaxel in mice treated with the P-glycoprotein blocker SDZ PSC 833. *Br. J. Cancer* **76**, 1181–1183.
- Billingsley M. L. and Kincaid R. L. (1997) Regulated phosphorylation and dephosphorylation of tau protein: effects on microtubule interaction, intracellular trafficking and neurodegeneration. *Biochem. J.* **323**, 577–591.
- Blagosklonny M. V. and Fojo T. (1999) Molecular effects of paclitaxel: myths and reality (a critical review). *Int. J. Cancer* **83**, 151–156.
- Blagosklonny M. V., Schulte T., Nguyen P., Trepel J. and Neckers L. M. (1996) Taxol-induced apoptosis and phosphorylation of Bcl-2 protein involves c-Raf-1 and represents a novel c-Raf-1 signal transduction pathway. *Cancer Res.* **56**, 1851–1854.
- Blagosklonny M. V., Giannakou P., el Deiry W. S., Kingston D. G., Higgs P. I., Neckers L. and Fojo T. (1997) Raf-1/bcl-2 phosphorylation: a step from microtubule damage to cell death. *Cancer Res.* **57**, 130–135.
- Brouty-Boye D., Kolonias D., Wu C. J., Savaraj N. and Lampidis T. J. (1995) Relationship of multidrug resistance to rhodamine-123 selectivity between carcinoma and normal epithelial cells: taxol and vinblastine modulate drug efflux. *Cancer Res.* **55**, 1633–1638.
- Busciglio J., Lorenzo A., Yeh J. and Yanker B. A. (1995)  $\beta$ -Amyloid fibrils induce tau phosphorylation and loss of microtubule binding. *Neuron* **14**, 879–888.
- Cavaletti G., Cavaletti E., Oggioni N., Sottani C., Minoia C., D'Incalci M., Zucchetti M., Marmiroli P. and Tredici G. (2000) Distribution of paclitaxel within the nervous system of the rat after repeated intravenous administration. *Neurotoxicology* **21**, 389–393.
- Dhavan R., Tsai L. H. and Tsai L. H. (2001) A decade of cdk5. *Nat. Rev. Mol. Cell Biol.* **2**, 749–759.
- Ding A. H., Porteu F., Sanchez E. and Nathan C. F. (1990) Shared actions of endotoxin and taxol on TNF receptors and release. *Science* **248**, 370–372.
- Evans D. B., Rank K. B., Bhattacharya K., Thomsen D. R., Gurney M. E. and Sharma S. K. (2000) Tau phosphorylation at serine 396 and serine 404 by human recombinant tau protein kinase II inhibits tau's ability to promote microtubule assembly. *J. Biol. Chem.* **275**, 24977–24983.
- Figuerroa-Masot X. A., Hetman M., Higgins M. J., Kokot N. and Xia Z. (2001) Taxol induces apoptosis in cortical neurons by a mechanism independent of Bcl-2 phosphorylation. *J. Neurosci.* **21**, 4657–4667.
- Goedert M. (1997) The neurofibrillary pathology of Alzheimer's disease. *Neuroscientist* **3**, 131–141.
- Goedert M., Crowther R. A. and Spillantini M. G. (1998) Tau mutations cause frontotemporal dementias. *Neuron* **21**, 955–958.
- He T. C., Zhou S., da Costa L. T., Yu J., Kinzler K. W. and Vogelstein B. (1998) A simplified system for generating recombinant adenoviruses. *Proc. Natl Acad. Sci. USA* **95**, 2509–2514.
- Heimans J. J., Vermorken J. B., Wolbers J. G., Eeltink C. M., Meijer O. W., Taphoorn M. J. and Beijnen J. H. (1994) Paclitaxel (taxol) concentrations in brain tumor tissue. *Ann. Oncol.* **5**, 951–953.
- Huang Y. and Wang K. K. (2001) The calpain family and human disease. *Trends Mol. Med.* **7**, 355–362.
- Ino H., Ishizuka T., Chiba T. and Tatibana M. (1994) Expression of CDK5 (PSSALRE kinase), a neural cdc2-related protein kinase, in the mature and developing mouse central and peripheral nervous systems. *Brain Res.* **661**, 196–206.
- Jordan M. A., Toso R. J., Thrower D. and Wilson L. (1993) Mechanism of mitotic block and inhibition of cell proliferation by taxol at low concentrations. *Proc. Natl Acad. Sci. USA* **90**, 9552–9556.
- Kusakawa G., Saito T., Onuki R., Ishiguro K., Kishimoto T. and Hisanaga S. (2000) Calpain-dependent proteolytic cleavage of the p35 cyclin-dependent kinase 5 activator to p25. *J. Biol. Chem.* **275**, 17166–17172.
- Lee V. M., Daughenbaugh R. and Trojanowski J. Q. (1994) Microtubule stabilizing drugs for the treatment of Alzheimer's disease. *Neurobiol. Aging* **15**, S87–S89.
- Lee V. M., Goedert M. and Trojanowski J. Q. (2001) Neurodegenerative tauopathies. *Annu. Rev. Neurosci.* **24**, 1121–1159.
- Lee K. Y., Clark A. W., Rosales J. L., Chapman K., Fung T. and Johnston R. N. (1999) Elevated neuronal Cdc2-like kinase activity in the Alzheimer disease brain. *Neurosci. Res.* **34**, 21–29.
- Lee M. S., Kwon Y. T., Li M., Peng J., Friedlander R. M. and Tsai L. H. (2000) Neurotoxicity induces cleavage of p35 to p25 by calpain. *Nature* **405**, 360–364.
- Liu Y., Ali S. M., Boge T. C., Georg G. I., Victory S., Zygmunt J., Marquez R. T. and Himes R. H. (2002) A systematic SAR study of C10 modified paclitaxel analogues using a combinatorial approach. *Comb. Chem. High Throughput Screen* **5**, 39–48.
- Maccioni R. B., Otth C., Concha I. I. and Munoz J. P. (2001) The protein kinase Cdk5. Structural aspects, roles in neurogenesis and involvement in Alzheimer's pathology. *Eur. J. Biochem.* **268**, 1518–1527.
- Manthey C. L., Qureshi N., Stutz P. L. and Vogel S. N. (1993) Lipopolysaccharide antagonists block taxol-induced signaling in murine macrophages. *J. Exp. Med.* **178**, 695–702.
- Michaelis M. L., Walsh J. L., Pal R., Hurlbert M., Hoel G., Bland K., Foye J. and Kwong W. H. (1994) Immunologic localization and kinetic characterization of a Na<sup>+</sup>/Ca<sup>2+</sup> exchanger in neuronal and non-neuronal cells. *Brain Res.* **661**, 104–116.
- Michaelis M. L., Ranciat N., Chen T., Bechtel M. R. R., Hepperle M., Liu Y. and Georg G. (1998) Protection against  $\beta$ -amyloid toxicity in primary neurons by paclitaxel (taxol). *J. Neurochem.* **70**, 1623–1627.
- Michaelis M. L., Chen Y., Hill S., Reiff E., Georg G., Kice A. and Audus K. (2002) Amyloid peptide toxicity and microtubule-stabilizing drugs. *J. Mol. Neurosci.* **19**, 101–105.
- Nakagawa T. and Yuan J. (2000) Cross-talk between two cysteine protease families. Activation of caspase-12 by calpain in apoptosis. *J. Cell Biol.* **150**, 887–894.
- Nath R., Davis M., Probert A. W., Kupina N. C., Ren X., Schielke G. P. and Wang K. K. (2000) Processing of cdk5 activator p35 to its truncated form (p25) by calpain in acutely injured neuronal cells. *Biochem. Biophys. Res. Commun.* **274**, 16–21.
- Nguyen M. D., Lariviere R. C. and Julien J. P. (2001) Deregulation of Cdk5 in a mouse model of ALS: toxicity alleviated by perikaryal neurofilament inclusions. *Neuron* **30**, 135–147.
- Niethammer M., Smith D. S., Ayala R., Peng J., Ko J., Lee M. S., Morabito M. and Tsai L. H. (2000) NUDEL is a novel Cdk5 substrate that associates with LIS1 and cytoplasmic dynein. *Neuron* **28**, 697–711.
- Nikolic M. and Tsai L. H. (2000) Activity and regulation of p35/Cdk5 kinase complex. *Meth. Enzymol.* **325**, 200–213.
- Patrick G. N., Zhou P., Kwon Y. T., Howley P. M. and Tsai L. H. (1998) p35, the neuronal-specific activator of cyclin-dependent kinase 5 (Cdk5) is degraded by the ubiquitin-proteasome pathway. *J. Biol. Chem.* **273**, 24057–24064.

- Patrick G. N., Zukerberg L., de Nikolic M., La M. S., Dikkes P. and Tsai L. H. (1999) Conversion of p35 to p25 deregulates Cdk5 activity and promotes neurodegeneration. *Nature* **402**, 615–622.
- Patrick G. N., Zukerberg L., de Nikolic M., La M. S., Dikkes P. and Tsai L. H. (2001) reply: p25 protein in neurodegeneration. *Nature* **411**, 764–765.
- Patzke H. and Tsai L. H. (2002a) Calpain-mediated cleavage of the cyclin-dependent kinase 5 activator p39 to p29. *J. Biol. Chem.* **277**, 8054–8060.
- Patzke H. and Tsai L. H. (2002b) Cdk5 sinks into ALS. *Trends Neurosci.* **25**, 8–10.
- Rapport M., Dawson H. N., Lester I. B., Vitek M. P. and Ferreira A. (2002) Tau is essential to  $\beta$ -amyloid-induced neurotoxicity. *Proc. Natl Acad. Sci. USA* **99**, 6364–6369.
- Scheuner D., Eckman C., Jensen M., Song X., Citron M., Suzuki N., Bird T. D., Hardy J., Hutton M., Kukull W., Larson E., Levy-Lahad E., Viitanen M., Peskind E., Poorkaj P., Schellenberg G., Tanzi R., Wasco W., Lannfelt L., Selkoe D. and Younkin S. (1996) Secreted amyloid beta-protein similar to that in the senile plaques of Alzheimer's disease is increased *in vivo* by the presenilin 1 and 2 and APP mutations linked to familial Alzheimer's disease. *Nat. Med.* **2**, 864–870.
- Selkoe D. J. (2001a) Alzheimer's disease: genes, proteins, and therapy. *Physiol. Rev.* **81**, 741–766.
- Selkoe D. J. (2001b) Clearing the brain's amyloid cobwebs. *Neuron* **32**, 177–180.
- Siman R., Flood D. G., Thinakaran G. and Neumar R. W. (2001) Endoplasmic reticulum stress-induced cysteine protease activation in cortical neurons: effect of an Alzheimer's disease-linked presenilin-1 knock-in mutation. *J. Biol. Chem.* **276**, 44736–44743.
- Sobue K., Agarwal-Mawal A., Li W., Sun W., Miura Y. and Paudel H. K. (2000) Interaction of neuronal Cdc2-like protein kinase with microtubule-associated protein tau. *J. Biol. Chem.* **275**, 16673–16680.
- Spillantini M. G., Murrell J. R., Goedert M., Farlow M. R., Klug A. and Ghetti B. (1998) Mutation in the tau gene in familial multiple system tauopathy with presenile dementia. *Proc. Natl Acad. Sci. USA* **95**, 7737–7741.
- Taniguchi S., Fujita Y., Hayashi S., Kakita A., Takahashi H., Murayama S., Saido T. C., Hisanaga S., Iwatsubo T. and Hasegawa M. (2001) Calpain-mediated degradation of p35 to p25 in postmortem human and rat brains. *FEBS Lett.* **489**, 46–50.
- Teraski T. and Tsuji A. (1995) Controlling transport and metabolism, in *Peptide Based Drug Design* (Taylor M. D. and Amidon G. L., eds), pp. 297–316. Amer. Chem. Soc., Washington, DC.
- Thiel V. E. and Audus K. L. (2001) Nitric oxide and blood–brain barrier integrity. *Antioxid. Redox Signal.* **3**, 273–278.
- Tsai L. H., Delalle I., Caviness V. S. Jr, Chae T. and Harlow E. (1994) p35 is a neural-specific regulatory subunit of cyclin-dependent kinase 5. *Nature* **371**, 419–423.
- Wang K. K. (2000) Calpain and caspase: can you tell the difference? *Trends Neurosci.* **23**, 20–26.
- Wang T. H., Wang H. S., Ichijo H., Giannakakou P., Foster J. S., Fojo T. and Wimalasena J. (1998) Microtubule-interfering agents activate c-Jun N-terminal kinase/stress-activated protein kinase through both Ras and apoptosis signal-regulating kinase pathways. *J. Biol. Chem.* **273**, 4928–4936.
- Xie H. and Johnson G. V. (1997) Ceramide selectively decreases tau levels in differentiated PC12 cells through modulation of calpain I. *J. Neurochem.* **69**, 1020–1030.
- Yoneda T., Imaizumi K., Oono K., Yui D., Gomi F., Katayama T. and Tohyama M. (2001) Activation of caspase-12, an endoplasmic reticulum (ER) resident caspase, through tumor necrosis factor receptor-associated factor 2-dependent mechanism in response to the ER stress. *J. Biol. Chem.* **276**, 13935–13940.
- Yoo B. C. and Lubec G. (2001) p25 protein in neurodegeneration. *Nature* **411**, 763–764.
- Zukerberg L. R., Patrick G. N., Nikolic M., Humbert S., Wu C. L., Lanier L. M., Gertler F. B., Vidal M., Van Etten R. A. and Tsai L. H. (2000) Cdk5 links Cdk5 and c-Abl and facilitates Cdk5 tyrosine phosphorylation, kinase upregulation, and neurite outgrowth. *Neuron* **26**, 633–646.

## ALZHEIMER'S THERAPEUTICS: Neuroprotection

# Overcoming the Blood–Brain Barrier to Taxane Delivery for Neurodegenerative Diseases and Brain Tumors

**Antonie Rice,<sup>1</sup> Mary L. Michaelis,<sup>\*2</sup> Gunda Georg,<sup>3</sup> Yanbin Liu,<sup>3</sup>  
Brandon Turunen,<sup>3</sup> and Kenneth L. Audus<sup>1</sup>**

<sup>1</sup>Department of Pharmaceutical Chemistry, University of Kansas, 226 Simons, 2095 Constant Avenue, Lawrence, KS 66047; and <sup>2</sup>Department of Pharmacology and Toxicology and <sup>3</sup>Medicinal Chemistry, University of Kansas, 1251 Wescoe Hall Drive, Lawrence, KS 66045

Received October 15, 2002; Accepted March 24, 2003

### Abstract

The blood–brain barrier (BBB) effectively prevents microtubule (MT)-stabilizing drugs from readily entering the central nervous system (CNS). A major limiting factor for microtubule-stabilizing drug permeation across the BBB is the active efflux back into the circulation by the overexpression of the multidrug-resistant gene product 1 (MDR1) or P-glycoprotein (P-gp). This study has focused on strategies to overcome P-gp-mediated efflux of Taxol analogs, MT-stabilizing agents that could be used to treat brain tumors and, potentially, neurodegenerative diseases such as Alzheimer's disease. However, taxol is a strong P-gp substrate that limits its distribution across the BBB and therapeutic potential in the CNS. We have found that addition of a succinate group to the C-10 position of paclitaxel (Taxol) results in an agent, Tx-67, with reduced interactions with P-gp and enhanced permeation across the BBB in both *in vitro* and *in situ* models. Our studies demonstrate the feasibility of making small chemical modifications to Taxol to generate analogs with reduced affinity for the P-gp but retention of MT-stabilizing properties, i.e., a taxane that may reach and treat therapeutic targets in the CNS.

**Index Entries:** Blood–brain barrier; CNS drug permeation; microtubule-stabilizing drugs; Taxol; brain microcapillary endothelial cells; neurofibrillary pathology.

### Introduction

The delivery of therapeutic agents into the brain continues to be a challenge for the pharmaceutical industry. Because of the inadequate delivery of these agents to the desired site of action in the brain, many neurological disorders (i.e., brain tumors, Alzheimer's disease, and other brain disorders) have poor responses to drug treatment (Pardridge, 2002). We have previously shown in neuronal cell cultures that the microtubule (MT)-stabilizing drug Taxol protects neurons against amyloid peptide (A $\beta$ ) toxicity (Michaelis et al., 1998, 2002). The potential for

testing protective effects *in vivo* is severely limited by the failure of Taxol and several of its derivatives to enter the brain. Consequently, we have synthesized a large array of MT-stabilizing drugs related to Taxol and tested them for potential to penetrate into the brain. In this paper we discuss the strategies we have tested and the results obtained regarding brain permeability of one promising taxane.

The blood–brain barrier (BBB) regulates the influx and efflux of a wide variety of substances and remains the major obstacle in the delivery of drugs into the central nervous system (CNS). The most common mechanism for drug distribution across the

\*Author to whom all correspondence and reprint requests should be addressed. E-mail: mlm@ku.edu



BBB is by simple passive diffusion; however, once a drug enters the endothelial lining of the BBB by this mechanism, it may either undergo passive diffusion or active transport back out of the cells into the circulation. First identified in tumors, the active efflux transport mechanisms are implicated as major factors in limiting the effective delivery of a number of drugs and drug classes across the BBB (Schinkel, 1999; Taylor, 2002). The transporters responsible for the active efflux of drugs at the BBB include the multidrug-resistant gene product 1 (MDR1) or P-glycoprotein (P-gp), multidrug resistance-associated proteins, and the breast cancer resistance protein. The major efflux pump at the BBB is MDR1 or P-gp (Schinkel, 1999; Taylor, 2002).

P-glycoprotein is a member of the ATP-binding cassette (ABC) family of transport proteins (Gottesman et al., 1996). This transporter is located on the blood side of the capillary endothelial cell and is involved in the efflux of a wide range of substrates that include antineoplastic agents (e.g., vincristine, vinblastine, and Taxol), antiviral compounds (e.g., saquinavir, zidovudine, zalcitabine), opiates, and other therapeutic agents. Various strategies have been devised to circumvent the BBB to increase drug delivery to the CNS. These strategies involve attempts to manipulate either the chemical properties of the agent, opening the BBB by increasing capillary endothelial permeability, or enhancing the driving force for transport by increasing the plasma concentration of a drug (i.e., high-dose chemotherapy, intra-arterial injection) (Taylor, 2002; Siegel and Zylber-Katz, 2002).

The strategy we chose to overcome the BBB efflux mechanisms was to focus on the use of combinatorial chemistry to manipulate chemical structure in order to reduce affinity for P-gp. This type of approach has been used successfully, for example, to generate molecular diversity in chemical structures for the development of new antibacterial agents in order to overcome bacterial drug resistance (Desnottes, 1996). The starting point for our work was to generate and screen newly synthesized analogs of the anticancer agent, paclitaxel or Taxol, for taxanes that have reduced P-gp affinity relative to the parent drug. Taxol, one of the leading anticancer drugs currently on the market for the treatment of ovarian and breast cancer, is very effective in treating tumors but, unfortunately, is also a substrate for the P-gp efflux pump. Because of interactions with P-gp at the BBB, it is almost impossible to infuse Taxol vascularly to treat brain tumors

(Cahan et al., 1994; Brouty-Boye et al., 1995; Lovich et al., 2001; Fellner et al., 2002). Therefore, second-generation taxanes that retain appropriate pharmacological activity and have reduced interactions with P-gp were generated with the primary objective of improving distribution across the BBB. To characterize these new taxanes we have employed a combination of *in vitro* and *in situ* models of the BBB. The goals of the experiments described herein were to (1) determine which newly synthesized taxanes have reduced P-gp interactions and improved permeability properties relative to Taxol, using an *in vitro* model comprised of P-gp-expressing primary cultures of bovine brain microvessel endothelial cells (BBMECs); and (2) determine which newly synthesized taxanes have improved permeability properties relative to Taxol at the BBB, using an *in situ* rat brain perfusion model. Taxol and the taxanes that were employed in the permeability assays here have been shown previously to retain appropriate pharmacological properties with respect to protecting neurons against A $\beta$ -induced toxicity (Michaelis et al., 1998, 2002).

## Materials and Methods

BBMECs were isolated from the gray matter of cerebral cortices by enzymatic digestion and subsequent centrifugation, and seeded into primary culture as described (Audus and Borchardt, 1987; Audus et al., 1996). Uptake and transport studies were performed in pH 7.4 standard buffer solutions, consisting of either Hank's balanced salt solution or phosphate-buffered saline (PBS) supplemented with 0.63 mM CaCl<sub>2</sub>, 0.74 mM MgSO<sub>4</sub>, 5.3 mM glucose, and 0.1 mM ascorbic acid (PBSA). [<sup>3</sup>H]Taxol (sp. act. 10.5 Ci/mmol) was obtained from Moravsek Radiochemicals. Dr. Gunda Georg (Medicinal Chemistry Department, University of Kansas), supplied the Taxol and taxane analogs. Rhodamine 123 (Rho 123) and cyclosporin A (CsA) were obtained from Sigma.

### *Rho 123 Accumulation in the Presence of Taxanes*

BBMECs were grown in 12-well plates to form confluent monolayers and used as described to assay for P-gp as detailed elsewhere (Rose et al., 1998). Briefly, the fluorescent marker Rho 123 was dissolved in PBSA buffer to give a stock concentration of 100  $\mu$ M. The uptake assay was performed in 1 mL of fresh PBSA. An aliquot of Taxol or one of its analogs



was added to each well to give a final concentration of 25  $\mu\text{M}$ . As a positive control, the P-gp inhibitor CsA (5–10  $\mu\text{M}$ ) was used. The negative control was rhodamine (5–10  $\mu\text{M}$ ) alone. The cells were preincubated at 37°C with Taxol or an analog for ~45 min. After this preincubation period, Rho 123 was added to the cells. After a 45-min incubation, the cells were washed in cold PBS and lysed in a NaOH/Triton X-100 solution. The cell lysates were assayed using a fluorescence spectrophotometer. Rhodamine 123 was measured at excitation/emission wavelengths of 500 nm/535 nm and quantified against a standard curve of Rho 123 in the appropriate lysing solution. The protein content was determined using the bicinchoninic acid (BCA) protein assay reagent kit and the results were expressed as total fluorescence accumulation per milligram of cell protein.

### Transport of Taxanes Across BBMEC Monolayers

The BBMECs were grown on 0.4- $\mu\text{m}$  pore polycarbonate membranes essentially as described (Audus and Borchardt 1987; Audus et al. (1996). When they reached confluency, the cells were transferred to side-by-side diffusion chambers to characterize the transport of a small number of promising tritium-labeled compounds by assessing their permeability relative to that of the paracellular marker [ $^{14}\text{C}$ ] sucrose as an index of monolayer confluency. Bidirectional transport was assessed for each of the radiolabeled compounds to determine if polarized transport was observed. All of the studies were performed in 3 mL of stirred PBSA in each donor and receiver chamber at 37°C. The cells were allowed to equilibrate in PBSA for 30 min prior to the experiment. At each time point, 100  $\mu\text{L}$  of sample was taken from the receiver compartment and replaced immediately with an equal volume of PBSA. Apparent permeability coefficients ( $P_{app}$ ) were calculated according to the following equation,  $P_{app} = (V/AC_o) \cdot (dC/dt)$  where  $V$  = volume of the receiver chamber (3.0  $\text{cm}^3$ ),  $A$  = area of the filter (0.636  $\text{cm}^2$ ),  $C_o$  = initial donor concentration, and  $(dC/dt)$  = flux of the test agent.

### In Situ Rat Brain Perfusion of Taxanes

The *in situ* rat brain perfusion technique described by Smith (1996), was employed to determine the BBB permeability of Taxol and the taxane analog Tx-67. Adult male Sprague-Dawley rats (350–400 g) were anesthetized with a mixture containing: 1.5 mL/kg of solution consisting of 37.5 mg/mL ketamine, 1.9 mg/mL xylazine, and 0.37 mg/mL acepromazine.

The rat brain was then directly perfused through the left carotid artery with a buffered physiologic saline containing a tracer (sucrose) as a vascular marker and the sample ( $[^3\text{H}]$  Taxol or  $[^{14}\text{C}]$  Tx-67) for time periods of 30, 60, or 120 s. The perfusion solution was changed to tracer-free fluid for 30 s to clear the labeled compound from the cerebral vessels. After the perfusion, the rat was decapitated and the brain removed for the sampling of various regions. The brain tissue was digested in Solvable for 24 h and the radioactivity quantified via liquid scintillation spectrometry. The capillary permeability-surface area product ( $PA$ ) ( $\text{mL/s/g}$ ) was calculated for both Taxol and Tx-67 by the following equation,  $PA = -F \ln [1 - C^*_{br}(T)/FT C^*_{pf}]$  where  $F$  is the regional cerebral blood flow ( $\text{mL/s/g}$ ),  $C^*_{br}$  represents the concentration of tracer in the brain parenchyma ( $\text{dpm/g}$ ),  $C^*_{pf}$  is the concentration in the perfusion fluid ( $\text{dpm/mL}$ ), and  $T$  is the total perfusion time.

## Results

Rhodamine 123 accumulation was assessed in the presence of Taxol and the new analogs of Taxol. Although it is an indirect assay, our studies revealed that some of the synthetic taxanes appeared to have reduced interactions with P-gp (i.e., no increase in Rho 123 accumulation in the presence of the analogs). Taxol, a known substrate for P-gp, increased rhodamine uptake by 2- to 2.5-fold in the BBMECs. Rhodamine uptake in the presence of Taxol was very similar to that observed in the presence of the positive control, CsA (5  $\mu\text{M}$ ), a known P-gp inhibitor. Accordingly, from the Rho 123 screening of numerous taxanes in multiwell dish formats, we obtained a rather quick analysis of which taxanes were poor substrate for efflux by P-gp. One of the taxanes that had no apparent interactions with P-gp, that is, no effect on Rho 123 uptake by BBMECs, was designated Tx-67, a compound in which a succinate group was added at the C-10 position of Taxol.

We next assessed the actual permeability properties of Tx-67 relative to Taxol. Given that the BBMECs have an apical (a) and a basolateral (b) surface when grown on polycarbonate membranes, our permeation studies included an assessment of whether the permeation was polarized or asymmetric in nature. We used radiolabeled Taxol and Tx-67 for these experiments to provide sensitivity in the nanomolar concentration range. The apparent permeability coefficient for Taxol was greater in the *b* to *a* direction (i.e.,  $b \rightarrow a > a \rightarrow b$ ). We also observed that the

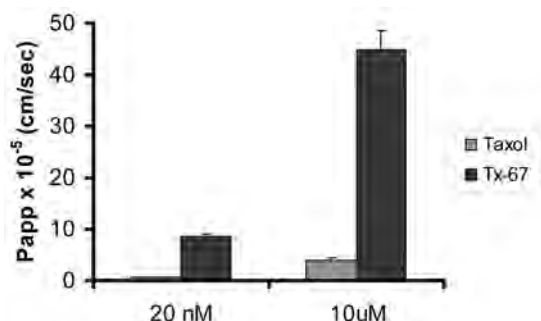


Fig. 1. Concentration dependence of apparent permeability coefficients ( $P_{app}$ ) for Taxol and Tx-67 permeation across primary cultures of BBMEC monolayers at 37°C. The data summarized are the  $P_{app}$  for taxane permeation from the apical (blood) to basolateral (brain) side of the monolayers. The data points are means  $\pm$  S.D. for at least four different monolayers.

analog Tx-67 had enhanced permeation compared to that of Taxol. The apparent permeability coefficient of Tx-67 at any concentration (low or high) was substantially greater than the  $P_{app}$  for Taxol at the highest concentration used (25  $\mu$ M). Moreover, the permeation of Tx-67 was asymmetric but greater in the a to b direction, which suggests greater blood to brain permeation for the new taxane. Fig. 1 shows typical results for Taxol and Tx-67 permeability at 20 nM, a concentration at which the BBMEC P-gp is not saturated, and at 10  $\mu$ M, a concentration at which the transporter is presumed to be saturated and thus the permeability of the monolayers to both agents significantly increased. It is important to note that BBMEC monolayer permeability to radiolabeled sucrose (i.e., a marker for integrity and background monolayer "leakage") was not altered by exposure to either Taxol or Tx-67 under the conditions of these experiments.

In the *in situ* perfusion experiments with [ $^{14}$ C]Tx-67 and [ $^3$ H]Taxol, we observed a substantially greater apparent permeability coefficient for Tx-67 relative to Taxol. It appears that Taxol is not retained in the rat brain tissue, as only minimal amounts (2.5% or less of total control) were detectable in the brain at 120 s. Approximately 6–8% of the total Tx-67 was detectable after 60 s of perfusion. Table 1 lists the  $P_{app}$  determined for Tx-67 and Taxol at each perfusion time.

## Discussion

The initial Rho 123 screening of newly synthesized taxanes showed that some structural modifi-

Table 1  
Apparent Permeability Coefficients for [ $^{14}$ C]Tx-67 and [ $^3$ H]Taxol in *In Situ* Rat Brain Perfusion

Compound	$P_{app} \times 10^7$ cm/s		
	30 s	60 s	120 s
[ $^{14}$ C]Tx-67	8.47	13.71	10.75
[ $^3$ H]Taxol	0.845	1.700	1.574

Time points were for 30, 60, and 120 s (each time point was determined in duplicate experiments).

cations to Taxol generated through combinatorial chemistry approaches lead to compounds that appear to be less avid substrates for P-gp than the parent Taxol. Clearly, Taxol competes with Rho 123 for P-gp, resulting in increased fluorescence using this screening technique. On the other hand, Tx-67 appeared to interact with P-gp to a significantly lesser degree in the same assay. Despite the addition of the succinyl group, Tx-67 retained its MT-stabilizing properties and its effectiveness in protecting neurons against A $\beta$ -induced toxicity, as reported earlier (Michaelis et al., 2002). These findings are consistent with studies in other laboratories that show second-generation taxanes have reduced interactions with P-gp and yet still exhibit potent anticancer activity (Ojima et al., 1996; Ojima and Slater, 1997).

We also determined that the transport of Taxol across BBMEC monolayers was asymmetric and supports previous data that the P-gp is localized on the apical side of the brain (Cordon-Cardo et al., 1989; Tsuji et al., 1992). However, the new taxane, Tx-67, although asymmetric in permeation across the monolayers, showed a much higher permeability, favoring what would be blood to brain distribution in this model. The *in situ* rat brain perfusion data correlated well with our *in vitro* permeability data, showing that Tx-67 permeation across the BBB was in fact substantially greater than the permeation of Taxol into rat brains. Our Taxol data were comparable to perfusion data for other anticancer drugs such as vincristine and vinblastine (Greig et al., 1990).

We have demonstrated that the use of combinatorial chemistry led to synthesis of new taxanes with reduced interactions with P-gp. We have also been able to demonstrate that one of the newly synthesized analogs, Tx-67, appears to cross the BBB both *in vitro* and *in situ* more readily than the parent drug. The Tx-67 permeation studies support our hypothesis that chemical modification of Taxol does enhance its permeability into the brain. In addition, the work

is consistent with literature observations in which small changes in chemical structures can alter interactions with P-gp at the BBB and thereby influence the distribution of the agents into the CNS (Mann et al., 1997). The most significant aspect of these results is that we now have an agent with MT-stabilizing activity and strong neuroprotective actions against A $\beta$  in primary neuronal cultures that can be tested in vivo. Studies are being undertaken to characterize the pharmacokinetic and pharmacodynamic properties of Tx-67 in mice. This is being done in anticipation of testing its therapeutic potential in animal models of both neurodegenerative diseases and brain tumors.

## Acknowledgments

This work was supported by the Institute for the Study of Aging (New York) and an NIH grant (NCI 1 RO1 CA82801).

## References

- Audus K. L. and Borchardt R. T. (1987) Bovine brain microvessel endothelial cell monolayers as a model system for the blood-brain barrier. *Ann. NY Acad. Sci.* **507**, 9–18.
- Audus K. L., Ng L., Wang W., and Borchardt R. T. (1996) Brain microvessel endothelial cell culture systems. *Pharm. Biotechnol.* **8**, 239–258.
- Brouty-Boye D., Kolonias D., Wu C. J., Savaraj N., and Lampidis T. J. (1995) Relationship of multidrug resistance to rhodamine-123 selectivity between carcinoma and normal epithelial cells: taxol and vinblastine modulate drug efflux. *Cancer Res.* **55**, 1633–1638.
- Cahan M. A., Walter K. A., Colvin O. M., and Brem H. (1994) Cytotoxicity of taxol in vitro against human and rat malignant brain tumors. *Cancer Chemother. Pharmacol.* **33**, 441–444.
- Cordon-Cardo C., O'Brien J. P., Casals D., Rittman-Grauer L., Biedler J. L., Melamed M. R., and Bertino J. R. (1989) Multidrug-resistance gene (P-glycoprotein) is expressed by endothelial cells at blood-brain barrier sites. *Proc. Natl. Acad. Sci. USA* **86**, 695–698.
- Desnottes J. F. (1996) New targets and strategies for the development of antibacterial agents. *Trends Biotechnol.* **14**, 134–140.
- Fellner S., Bauer B., Miller D. S., Schaffrik M., Franhanel M., Spruss T., et al. (2002) Transport of paclitaxel (Taxol) across the blood-brain barrier in vitro and in vivo. *J. Clin. Invest.* **110**, 1309–1318.
- Gottesman M. M., Pastan I., and Ambudkar S. V. (1996) P-glycoprotein and multidrug resistance. *Curr. Opin. Genet. Dev.* **6**, 610–617.
- Greig N. H., Soncrant T. T., Shetty H. U., Momma S., Smith Q. R., and Rapoport S. I. (1990) Brain uptake and anticancer activities of vincristine and vinblastine are restricted by their low cerebrovascular permeability and binding to plasma constituents in rat. *Cancer Chemother. Pharmacol.* **26**, 263–268.
- Lovich M. A., Creel C., Hong K., Hwang C. W., and Edelman E. R. (2001) Carrier proteins determine local pharmacokinetics and arterial distribution of paclitaxel. *J. Pharm. Sci.* **90**, 1324–1335.
- Mann H., Ladenheim B., Hirata H., Moran T. H., and Cadet J. L. (1997) Differential toxic effects of methamphetamine (METH) and methylenedioxymethamphetamine (MDMA) in multidrug resistant (mdr1a) knockout mice. *Brain Res.* **769**, 340–346.
- Michaelis M. L., Chen Y., Hill S., Reiff E., Georg G., Rice A., and Audus K. L. (2002) Amyloid peptide toxicity and microtubule-stabilizing drugs. *J. Mol. Neurosci.* **19**, 101–105.
- Michaelis M. L., Ranciat N., Chen Y., Bechtel M., Ragan R., Hepperle M., et al. (1998) Protection against  $\beta$ -amyloid toxicity in primary neurons by paclitaxel (Taxol). *J. Neurochem.* **70**, 1623–1627.
- Ojima I. and Slater J. C. (1997) Synthesis of novel 3'-trifluoromethyl taxoids through effective kinetic resolution of racemic 4-CF<sub>3</sub>-beta-lactams with baccatins. *Chirality* **9**, 487–494.
- Ojima I., Slater J. C., Michaud E., Kuduk S. D., Bounaud P. Y., Vrignaud P., et al. (1996) Syntheses and structure-activity relationships of the second-generation antitumor taxoids: exceptional activity against drug-resistant cancer cells. *J. Med. Chem.* **39**, 3889–3896.
- Pardridge W. M. (2002) Targeting neurotherapeutic agents through the blood-brain barrier. *Arch. Neurol.* **59**, 35–40.
- Rose J. M., Peckham S. L., Scism J. L., and Audus K. L. (1998) Evaluation of the role of P-glycoprotein in ivermectin uptake by primary cultures of bovine brain microvessel endothelial cells. *Neurochem. Res.* **23**, 203–209.
- Schinkel A. H. (1999) P-Glycoprotein, a gatekeeper in the blood-brain barrier. *Adv. Drug Deliv. Rev.* **36**, 179–194.
- Siegel T. and Zylber-Katz E. (2002) Strategies for increasing drug delivery to the brain: focus on brain lymphoma. *Clin. Pharmacokinet.* **41**, 171–186.
- Smith Q. (1996) Brain perfusion systems for studies of drug uptake and metabolism in the central nervous system. *Pharm. Biotechnol.* **8**, 285–307.
- Taylor E. M. (2002) The impact of efflux transporters in the brain on the development of drugs for CNS disorders. *Clin. Pharmacokinet.* **41**, 81–92.
- Tsuji A., Terasaki T., Takabatake Y., Tenda Y., Tamai I., Yamashita T., et al. (1992) P-glycoprotein as the drug efflux pump in primary cultured bovine brain capillary endothelial cells. *Life Sci.* **51**, 1427–1437.



# Single-site chemical modification at C10 of the baccatin III core of paclitaxel and Taxol C reduces P-glycoprotein interactions in bovine brain microvessel endothelial cells

Jared T. Spletstoser,<sup>a</sup> Brandon J. Turunen,<sup>a</sup> Kelly Desino,<sup>b</sup> Antonie Rice,<sup>b</sup> Apurba Datta,<sup>a</sup> Dinah Dutta,<sup>a</sup> Jacquelyn K. Huff,<sup>c</sup> Richard H. Himes,<sup>c,\*</sup> Kenneth L. Audus,<sup>b,\*</sup> Anna Seelig<sup>d,\*</sup> and Gunda I. Georg<sup>a,\*</sup>

<sup>a</sup>Department of Medicinal Chemistry, University of Kansas, 1251 Wescoe Hall Drive, Lawrence, Kansas 66045, USA

<sup>b</sup>Department of Pharmaceutical Chemistry, University of Kansas, Lawrence, Kansas 66047, USA

<sup>c</sup>Department of Molecular Biosciences, University of Kansas, Lawrence, Kansas 66045, USA

<sup>d</sup>Department of Biophysical Chemistry, Biocenter of the University of Basel, Klingelbergstrasse 70, 4056 Basel, Switzerland

Received 24 September 2005; revised 18 October 2005; accepted 19 October 2005

Available online 10 November 2005

**Abstract**—A single-site modification of paclitaxel analogs at the C10 position on the baccatin III core that reduces interaction with P-glycoprotein in bovine brain microvessel endothelial cells is described. Modification and derivatization of the C10 position were carried out using a substrate controlled hydride addition to a key C9 and C10 diketone intermediate. The analogs were tested for tubulin assembly and cytotoxicity, and were shown to retain potency similar to paclitaxel. P-glycoprotein interaction was examined using a rhodamine assay and it was found that simple hydrolysis or epimerization of the C10 acetate of paclitaxel and Taxol C can reduce interaction with the P-glycoprotein transporter that may allow for increased permeation of taxanes into the brain.  
© 2005 Elsevier Ltd. All rights reserved.

Chemotherapy of CNS localized tumors has been limited by the inability of drugs to bypass the blood–brain barrier (BBB) and little progress has been made since the advent of the nitrosoureas.<sup>1</sup> While primary CNS tumors are relatively uncommon, metastatic tumors of the brain outnumber primary lesions at least 10–1.<sup>2</sup> Therefore, the development of agents able to permeate the BBB would provide clinicians with additional options for the treatment of brain localized tumors, especially those with multiple lesions.

Paclitaxel (**1**, Fig. 1) is a microtubule-binding chemotherapeutic agent that causes cell cycle arrest at the G<sub>2</sub>/M phase leading to cellular apoptosis.<sup>3</sup> Paclitaxel is approved for the treatment of breast, ovarian, and non-small cell lung cancers, Kaposi's sarcoma, and is active against a wide variety of cancer cell types.<sup>4</sup>

Paclitaxel does not cross the blood–brain barrier and is not effective against cancers localized in the cranial cavity.<sup>5</sup> The primary mechanism of decreased paclitaxel BBB penetration is active efflux by P-glycoprotein (Pgp), which is a membrane bound protein produced by the multi-drug resistant gene cassette (MDR1). Pgp knockout mice show nearly a fourfold increase in the

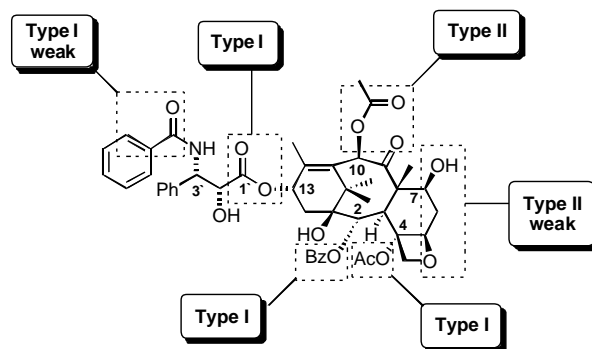


Figure 1. Paclitaxel (**1**) recognition elements for Pgp.

**Keywords:** Paclitaxel; 10-Deacetylpaclitaxel; 10-*epi*-Paclitaxel; P-glycoprotein; Blood–brain barrier.

\* Corresponding authors. Tel.: +1 785 864 4498; fax: +1 785 864 5836; e-mail: [georg@ku.edu](mailto:georg@ku.edu)

concentration of brain paclitaxel levels as compared to normal mice.<sup>6</sup> Paclitaxel has a relatively low toxicity to primary cortical neurons and has been shown to protect them from  $\beta$ -amyloid protein-induced toxicity, which has been implicated in Alzheimer's disease.<sup>7</sup> Thus, if paclitaxel could be modified to evade Pgp, it would provide a potential means for the treatment of brain-related cancers and other CNS diseases.

A series of recognition elements required for Pgp interaction have been described recently by us.<sup>8,9</sup> This analysis identified clusters common to Pgp substrates that consist of hydrogen bond acceptors organized in a defined spatial arrangement, and their relative frequency was correlated with the strength of interaction with Pgp. Two motifs, termed type I and type II, were identified that possess different relative recognition affinities for Pgp. We analyzed paclitaxel (Fig. 1) and identified a strongly and a weakly interacting type II unit, three standard type I units, and one weakly interacting type I unit that consists of an electron-donating heteroatom and a weak  $\pi$ -system in close proximity to one another. The type II unit is considered to have the highest Pgp affinity.

Ojima et al. have demonstrated, using photoaffinity-labeling experiments, that Pgp contains a binding site specific for taxanes.<sup>10</sup> They have also shown that the NCI/ADR-RES (formerly named MCF-7ADR)<sup>11</sup> cell line (a multi-drug resistant breast cancer phenotype known to overexpress Pgp) is very sensitive to substitution of the C10 moiety in 3'-dephenyl-3'-isobutylpaclitaxel analogs,<sup>12</sup> although this effect was not observed when the same modifications were made on paclitaxel.<sup>13</sup> Since the C9 carbonyl-C10 ester motif is a type II unit, we surmised that it might be largely responsible for Pgp interaction. All Pgp inducers carry at least one type II unit and it has been suggested by us that this unit interacts more strongly with the efflux protein.<sup>8</sup> Thus, we reasoned that the chemical modification of this motif through changes of the C10 oxidation state and/or absolute configuration might decrease the affinity of certain taxanes for Pgp. This hypothesis is supported by the recent report that TXD-258 (7-*O*-methyl-10-*O*-methyldeacetaxel) is able to cross the BBB.<sup>14</sup> This analog has a C10 -OMe group in place of the acetoxy group usually found at this position in paclitaxel analogs (this alters the C10 type II ester functionality). We have also found that deletion of the C10 ester unit in certain paclitaxel analogs decreases interaction with Pgp in a concentra-

tion-dependent manner.<sup>15</sup> In the work presented here, we sought to transform the type II interaction to a weaker type I element via C10 ester hydrolysis or by altering the spatial distance between the oxygen heteroatoms through C10 epimerization in paclitaxel and Taxol C.<sup>16</sup>

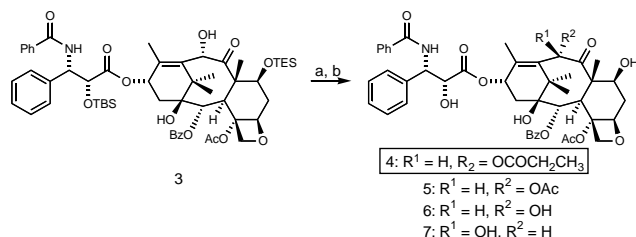
Our group has developed an efficient route to C10 modified taxanes that utilizes a stereoselective hydride addition from the  $\beta$ -face of the baccatin III core to afford the  $\alpha$ -C10 epimeric products 10-*epi*-paclitaxel (**5**) and 10-*epi*-10-deacetylpaclitaxel (**6**) (shown in Scheme 1).<sup>17</sup> Propionyl analog **4** was prepared similarly by reacting **3** with propionic anhydride, followed by HF-mediated deprotection (Scheme 1).

Selective protection of the C2' hydroxyl group of Taxol C (**2**) as the silyl ether furnished **8** in good yield (Scheme 2). Hydrazine-mediated cleavage<sup>18</sup> of the C10 acetate provided the C10 hydroxyl analog **9**, which was regioselectively protected at the C7 hydroxyl group with triethylsilyl chloride to afford **10** in excellent yield. Deprotection of the  $\beta$ -hydroxy taxane **9** provided the 10 $\beta$ -deacetyl-Taxol C analog **11** in 84% yield. Dess–Martin periodinane oxidation of the C10 hydroxy group in **10** occurred smoothly resulting in the C9–C10 diketone **12**.

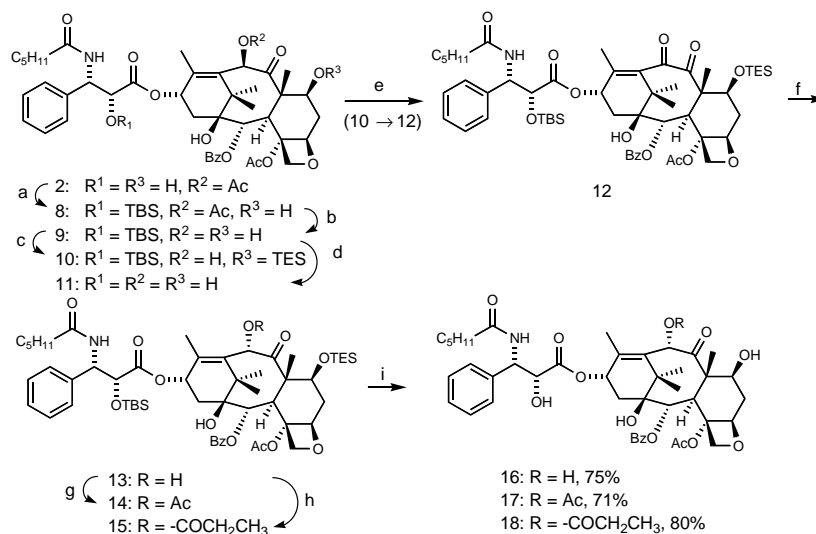
Reduction of **12** using sodium borohydride complexed in diglyme was required to provide sufficient amounts of the  $\alpha$ -C10 compound **13**, as solid sodium borohydride gave mostly the C9–C10 diol resulting from reduction of the C9 carbonyl group. Acetylation and propionylation occurred as expected in good yields affording **14** and **15** in 75% and 85%, respectively, using the corresponding anhydrides. Hydrogen fluoride deprotection furnished target compounds **16**, **17**, and **18** in 75%, 71%, and 80% yield, respectively. All compounds displayed spectroscopic properties in agreement with their structures.

Table 1 displays the effective dose ratios [ED<sub>50</sub>/ED<sub>50</sub>(paclitaxel)] for each compound in a tubulin assembly assay and cytotoxicity studies in the MCF-7 (parental cell line) and NCI/ADR-RES (multi-drug resistant phenotype) cell lines. Our original hypothesis was that the NCI/ADR-RES line would serve as an initial indicator of the Pgp evading potential as this line has been shown to express high levels of MDR-1 and Pgp.<sup>19</sup> Modification of the C10 center did not significantly affect cytotoxicity or tubulin assembly across the range of taxanes. In addition, none of the compounds in Table 1 showed a large increase in cytotoxicity for the multi-drug resistant phenotype. This was unexpected, as we had anticipated significant potency of these compounds in this cell line.

Each analog was evaluated for potential interactions with Pgp relative to the negative (no addition) and positive controls [cyclosporine A (CsA) and paclitaxel, both of which are known Pgp substrates and cause a net increase in cellular rhodamine concentrations] in primary cultures of bovine brain microvessel endothelial cells (BMECs),<sup>20</sup> which we have previously demonstrated to



**Scheme 1.** Synthesis and chemical structures of paclitaxel analogs. Reagents and conditions: (a) (CH<sub>3</sub>CH<sub>2</sub>CO)<sub>2</sub>O, DMAP, 0 °C; 82%; (b) HF/pyridine, pyridine, 0 °C; 75%.



**Scheme 2.** Synthesis of Taxol C analogs. Reagents and conditions: (a) TBSCl, imidazole,  $CH_2Cl_2$ ; 87%; (b)  $N_2H_4 \cdot H_2O$ , EtOH; 89%; (c) TESCl, DMAP,  $CH_2Cl_2$ ; 85%; (d) HF/pyridine, pyridine, 0 °C; 84%; (e) Dess–Martin periodinane,  $CH_2Cl_2$ ; 99%; (f)  $NaBH_4$  (solution in diglyme); 50%; (g)  $Ac_2O$ , DMAP, pyridine, 0 °C; 75%; (h)  $(CH_3CH_2CO)_2O$ , DMAP, pyridine, 0 °C; 86%; (i) HF/pyridine, pyridine, 0 °C.

**Table 1.**  $ED_{50}$  ratios (compound/paclitaxel) for in vitro tubulin assembly and cytotoxicity for compounds 1–2, 4–7, 11, and 16–18<sup>13</sup>

Compounds	Tubulin assembly	MCF-7	NCI/ADR-RES
1	1	1	1
2	2.0	2.2	0.48
4	4.1	2.6	1.1
5	0.8	0.7	1.3
6	3.2	1.4	0.7
7	2.1	7.5	6.6
11	2.2	4.8	3.8
16	1.6	9.2	3.1
17	0.21	3.2	1.6
18	2.1	3.8	2.9

Paclitaxel has a mean  $ED_{50}$  of  $3.23 \text{ nM} \pm 1.84$  and  $1.53 \text{ } \mu\text{M} \pm 1.26$  in the MCF-7 and NCI/ADR-RES lines, respectively.

express Pgp.<sup>21</sup> A compound that does not interact, or interacts weakly, with Pgp should not significantly change the rhodamine level relative to the negative control.

The results with paclitaxel (1) and Taxol C (2) (Fig. 2) demonstrate that compounds containing the  $\beta$ -C10 acetate group strongly interact with Pgp. As is evident, there is a marked loss of interaction when the  $\beta$ -C10 acetate is hydrolyzed (Fig. 2, compounds 7 and 11) for both series. This is likely due to the conversion of the strongly interacting type II unit to a weaker type I motif. The epimerization of the  $\beta$ -OH to the  $\alpha$  configuration does not cause a significant further change in interaction with Pgp in this assay (Fig. 2, compounds 6 and 16). This decreased interaction with the efflux protein is mostly retained upon acetylation of the  $\alpha$ -hydroxyl moiety causing just a slight increase for compound 5 and a decrease for compound 17 in rhodamine accumulation. This is significant as for both series the  $\beta$ -acetate compounds interact appreciably with the Pgp transporter relative to rhodamine. C10  $\alpha$ -substituents reside within the concave ‘cup’ of the baccatin portion of the taxanes.

Thus, it is conceivable that the acetate unit is no longer able to interact with the complementary amino acid residue in the Pgp binding site. Additionally, it is feasible that the epimerization of this unit changes the spatial distance of the outer two electron donors, disrupting or weakening its hydrogen bonding ability. Interestingly, as the size of the  $\alpha$ -substituent increases (Fig. 2, compounds 4 and 18), Pgp interaction is observed at levels near that of the  $\beta$ -acetate compounds or positive controls.

We previously reported that C10-deacetytaxol and C10-deacetytaxol-C7-deoxytaxol interacted appreciably with Pgp in the rhodamine assay at  $10 \text{ } \mu\text{M}$  but not at  $5 \text{ } \mu\text{M}$ .<sup>15</sup> However, C7-deoxytaxol inter-

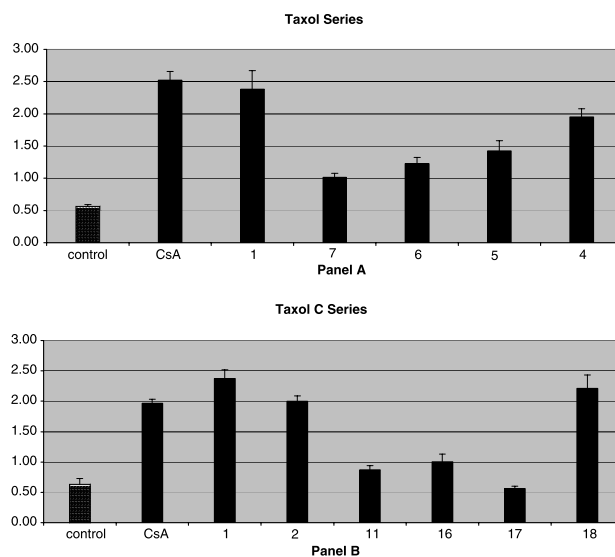


**Figure 2.** Rhodamine uptake results for compounds 4–7 (A, paclitaxel series) and 2, 11, and 16–18 (B, Taxol C series), in BMECs. Paclitaxel and the derivatives were present at a concentration of  $10 \text{ } \mu\text{M}$ . The concentrations of cyclosporin A (CsA) and rhodamine were  $5 \text{ } \mu\text{M}$ .



acted with Pgp at both concentrations. Thus, it seems that the C10 acetate plays a pivotal role in Pgp recognition. It is interesting to note that the compounds presented in this study (5–7, 11, 15, and 17) seem to do little to rhodamine accumulation even at the 10  $\mu$ M concentration.

Although the rhodamine assay is an indirect measurement of Pgp interaction, we have previously established it as a viable indicator of relative BBB permeation by comparison to bidirectional permeation data obtained from BMEC monolayers of related compounds.<sup>20</sup> Further studies regarding these compounds in the BMEC permeation assay are underway.

Although paclitaxel has six purported recognition elements, the simple modification of only one of these groups is sufficient to decrease interaction with Pgp. Although we do not yet know the relative contributions of each recognition element in binding to Pgp, it is clear that the element involving C9 and C10 plays a significant role. This is underscored by observations that certain modifications at C10 resulted in compounds with higher activity against Pgp-overexpressing cancer cell lines<sup>12</sup> or with ability to cross the BBB.<sup>14</sup> We did not find a correlation between our compounds' activity against the NCI/ADR-RES cell line and rhodamine uptake in BMECs. The discrepancy suggests the possibility that other efflux systems may be present in the MDR cell line that recognizes these compounds.<sup>22</sup>

In summary, we have described a novel single point chemical modification of the baccatin portion of taxanes that significantly decreases affinity for the P-glycoprotein transporter system. Additionally, we have begun to elucidate a preliminary structure–activity relationship for Pgp and taxanes with respect to the recognition elements postulated. The concept and data presented illustrate that it might be possible to deliver chemically modified taxanes across the blood–brain barrier. This is in contrast to current strategies for brain delivery of non-CNS permeable drugs, including Pgp inhibition,<sup>5a</sup> and BBB disruption.<sup>1</sup> Long-term application of this research has the potential to lead to effective agents for CNS cancer treatment.

### Acknowledgments

This work was supported by a grant from the National Cancer Institute (CA82801). J.T.S. and B.J.T. would like to acknowledge the Department of Defense Breast Cancer Research Program for predoctoral fellowships (DAMD17-99-1-92530 and DAMD17-02-1-0435). Paclitaxel and Taxol C were generously donated by Tap-estry Pharmaceuticals, Boulder, CO.

### References and notes

- Fortin, D. *Prog. Drug Res.* **2003**, *61*, 127.
- Patchell, R. A. *Cancer Treat. Rev.* **2003**, *29*, 533.
- (a) Woods, C. M.; Zhu, J.; McQueney, P. A.; Bollag, D.; Lazarides, E. *Mol. Med.* **1995**, *1*, 506; (b) Jordan, M. A. *Curr. Med. Chem.: Anti-Cancer Agents* **2002**, *2*, 1.
- Suffness, M.; Wall, M. E. Discovery and Development of Taxol. In *Taxol: Science and Applications*; Suffness, M., Ed.; CRC Press, Inc.: Boca Raton, FL, 1995; pp 3–25.
- (a) Schinkel, A. H. *Adv. Drug Deliv. Rev.* **1999**, *36*, 179; (b) Schinkel, A. H.; Smit, J. J. M.; Telling, O. van.; Beijnen, J. H.; Wagenaar, E.; Deemter, L. van.; Mol, C. A. A. M.; Valk, M. A. Van Der; Robanus-Maandag, E. C.; Riele, H. P. J. Te.; Berns, A. J. M.; Borst, P. *Cell* **1994**, *77*, 491; (c) Schinkel, A. H.; Wagenaar, E.; Mol, C. A. A. M.; Van Deemter, L. *J. Clin. Invest.* **1996**, *97*, 2517; (d) Fellner, S.; Bauer, B.; Miller, D. S.; Schaffrik, M.; Frankhanel, M.; Sprub, T.; Berhardt, G.; Graeff, C.; Farber, L.; Gschaidmeier, H.; Buschauer, A.; Fricker, G. *J. Clin. Invest.* **2002**, *110*, 1309; (e) Kemper, E. M.; van Zandbergen, A. E.; Cleypool, C.; Mos, H. A.; Boogerd, W.; Beijnen, J. H.; van Telling, O. *Clin. Cancer Res.* **2003**, *9*, 2849.
- van Asperen, J.; Mayer, U.; van Telling, O.; Beijnen, J. H. *J. Pharm. Sci.* **1997**, *86*, 881.
- (a) Michaelis, M.-L.; Ranciat, N.; Chen, Y.; Bechtel, M.; Ragan, R.; Hepperle, M.; Liu, Y.; Georg, G. I. *J. Neurochem.* **1998**, *70*, 1623; (b) Michaelis, M. L.; Ansar, S.; Chen, Y.; Reiff, E.; Seyb, K. I.; Himes, R. H.; Audus, K.; Georg, G. I. *J. Pharmacol. Exp. Ther.* **2005**, *48*, 832.
- Seelig, A. *Eur. J. Biochem.* **1998**, *251*, 252.
- (a) Seelig, A.; Landwojtowicz, E.; Fischer, H.; Blatter, X. L. *Methods Princ. Med. Chem.* **2003**, *18*, 461; (b) Seelig, A.; Li Blatter, X.; Wohnsland, F. *Int. J. Clin. Pharmacol. Ther.* **2000**, *251*, 252.
- Ojima, I.; Duclos, O.; Dorman, G.; Simonot, B.; Prestwich, G. D.; Rao, S.; Lerro, K. A.; Horwitz, S. B. *J. Med. Chem.* **1995**, *38*, 3891.
- This cell line has since been renamed NCI/ADR-RES as DNA fingerprinting has shown it is not derived from the MCF-7 cell line: Scudiero, D. A.; Monks, A.; Sausville, E. A. *J. Natl. Cancer Inst.* **1998**, *90*, 862.
- Ojima, I.; Slater, J. C.; Michaud, E.; Kuduk, S. D.; Bounaud, P.-Y.; Vrignaud, P.; Bissery, M.-C.; Veith, J. M.; Pera, P.; Bernacki, R. J. *J. Med. Chem.* **1996**, *39*, 3889.
- Liu, Y.; Boge, T. C.; Victory, S.; Ali, S. M.; Zygmunt, J.; Georg, G. I.; Marquez, R. T.; Himes, R. H. *Comb. Chem. High Throughput Screening* **2002**, *5*, 39.
- For review: Beckers, T.; Mahboobi, S. *Drugs Future* **2003**, *28*, 767.
- Ge, H.; Vasandani, V.; Huff, J. K.; Audus, K. L.; Himes, R. H.; Seelig, A.; Georg, G. I. *Bioorg. Med. Chem. Lett.* **2005**, Manuscript Accepted.
- (a) Hepperle, M. *Isolation, Identification, Preparation, Conformational Aspects and Biological Activities of Taxanes*; University of Kansas: Lawrence, KS, 1995; (b) S  nhilh, V.; Blechert, S.; Colin, M.; Guenard, D.; Picot, F.; Potier, P.; Varenne, P. *J. Nat. Prod.* **1984**, *47*, 131.
- Datta, A.; Vander Velde, D. G.; Georg, G. I. *Tetrahedron Lett.* **1995**, *36*, 1985.
- Datta, A.; Hepperle, M.; Georg, G. I.; Himes, R. H. *J. Org. Chem.* **1995**, *60*, 761.
- (a) Alvarez, M.; Paull, K.; Monks, A.; Hose, C.; Lee, J. S.; Weinstein, J. *J. Clin. Invest.* **1995**, *95*, 2205; (b) Lee, J. S.; Paull, K.; Alvarez, M.; Hose, C.; Monks, A.; Grever, M. *Mol. Pharmacol.* **1994**, *46*, 627.
- Rice, A.; Liu, Y.; Michaelis, M.-L.; Himes, R. H.; Georg, G. I.; Audus, K. L. *J. Med. Chem.* **2005**, *48*, 832.
- Rose, J. M.; Peckham, S. L.; Scism, J. L.; Audus, K. *Neurochem. Res.* **1998**, *23*, 203.
- Sun, H.; Dai, H.; Shaik, N.; Elmquist, W. F. *Adv. Drug Deliv. Rev.* **2003**, *55*, 83.



**[Bis(2-methoxyethyl)amino]sulfur  
Trifluoride, the Deoxo-Fluor Reagent:  
Application toward One-Flask Trans-  
formations of Carboxylic Acids to Amides**

Jonathan M. White, Ashok Rao Tunoori,  
Brandon J. Turunen, and Gunda I. Georg\*

Department of Medicinal Chemistry, University of Kansas,  
1251 Wescoe Hall Drive, Lawrence, Kansas 66045-7582

georg@ku.edu

Received November 10, 2003

**Abstract:** The use of the Deoxo-Fluor reagent is a versatile method for acyl fluoride generation and subsequent one-flask amide coupling. It provides mild conditions and facile purification of the desired products in good to excellent yields. We have explored the utility of this reagent for the one-flask conversion of acids to amides and Weinreb amides and as a peptide-coupling reagent.

Acyl fluorides are versatile functional groups in organic chemistry due to the unique nature of the carbonyl–fluorine bond.<sup>1</sup> Many useful chemical transformations are elicited via this functionality since it possesses greater stability than the corresponding acid chloride toward neutral oxygen nucleophiles, yet is of high reactivity toward anionic nucleophiles and amines.<sup>2</sup> It has been observed that acid fluorides react more like activated esters than acid halides (Cl, Br, I).<sup>2</sup> For example, Fmoc,<sup>3,4</sup> Boc, and Cbz amino acid fluorides<sup>5</sup> were found to be stable, rapid-acting, acylating reagents for peptide bond formation. It is also of note that no significant loss of optical purity is observed during the conversion of acid fluorides to amides.<sup>5,6</sup> These properties make shelf-stable acid fluorides possible and allow for their isolation through organic extraction. It is these characteristics which make them important for further synthetic study.<sup>1</sup>

A variety of techniques are available for the generation of acyl fluorides.<sup>1,2</sup> There are, however, disadvantages associated with these methods, including poor yields, dangerous or toxic chemicals, forcing reaction conditions, and costly reagents. A recently developed alternative, [bis(2-methoxyethyl)amino]sulfur trifluoride, the Deoxo-Fluor reagent (**1**), which was first described by Lal et al. as a thermally stable alternative to the DAST reagent (**2**), overcomes several of these problems (Figure 1).<sup>7,8</sup> The initial investigation of this reagent showcased its utility for the conversion of hydroxy alkanes to the corresponding alkyl fluorides (deoxygenation–fluorination).<sup>8</sup> Ad-

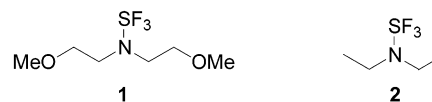


**FIGURE 1.** Structures of Deoxo-Fluor (**1**) and DAST (**2**).

ditional transformations were explored as well, including the conversion of carboxylic acids to acyl fluorides.<sup>7</sup> Based on these observations, we sought to take advantage of the properties of acyl fluorides combined with this new and facile protocol for their preparation. Our efforts have led to a one-flask protocol for the conversion of carboxylic acids to a variety of amides obtained through an intermediate acyl fluoride. A full account of this work is presented herein.<sup>9</sup>

**Conversion of Carboxylic Acids to Amides.** The importance of amides cannot be overstated as they are crucial in the architecture of biological systems and prevalent in natural products and commercial medicines, and their formation is widely utilized in the construction of many molecules/materials. A special group of amides which shows additional versatility are the *N,O*-dimethylhydroxylamides (Weinreb amides).<sup>10</sup> These compounds have become important and widely used building blocks in organic synthesis.<sup>11–14</sup> Accordingly, several methods are available for their formation including the direct conversion of carboxylic acids to amides. Some of these procedures utilize peptide coupling reagents such as BOP,<sup>15,16</sup> DCC,<sup>17</sup> or propylphosphonic anhydride/*N*-ethylmorpholine.<sup>18,19</sup> Einhorn et al. have developed a method for the synthesis of Weinreb amides from carboxylic acids using carbon tetrabromide and triphenylphosphine.<sup>20</sup> Sibi et al. have reported the synthesis of Weinreb amides from carboxylic acids using 2-chloro-1-methylpyridinium iodide (CMPI) or BMPI as the coupling agent.<sup>21</sup> Drawbacks of these methods include expensive coupling reagents and difficult removal of excess reagent and reagent byproducts. Therefore, a continued interest exists in the development of alternative methods for amide formation from carboxylic acids that are operationally simple and allow for easy removal of reagents and reagent byproducts.

In the course of our study, we found that carboxylic acids could be readily converted to the corresponding

\* Corresponding author.

(1) Patai, S. *The Chemistry of Acyl Halides*; Interscience Publishers: New York, 1972.

(2) Carpino, L. A.; Beyermann, M.; Wenschuh, H.; Bienert, M. *Acc. Chem. Res.* **1996**, *29*, 268–274.

(3) Carpino, L. A.; Sadat-Aalae, D.; Chao, H. G.; DeSelms, R. H. *J. Am. Chem. Soc.* **1990**, *112*, 9651–9652.

(4) Kaduk, C.; Wenschuh, H.; Beyermann, M.; Forner, K.; Carpino, L. A.; Bienert, M. *Lett. Pept. Sci.* **1996**, *2*, 285–288.

(5) Carpino, L. A.; Mansour, M. E.; Sadat-Aalae, D. *J. Org. Chem.* **1991**, *56*, 2611–2614.

(6) Bertho, J. N.; Loffet, A.; Pinel, C.; Reuther, F.; Sennye, G. *Tetrahedron Lett.* **1991**, *32*, 1303–1306.

(7) Lal, G. S.; Pez, G. P.; Pesaresi, R. J.; Prozone, F. M.; Cheng, H. *J. Org. Chem.* **1999**, *64*, 7048–7054.

(8) Lal, G. S.; Pez, G. P.; Pesaresi, R. J.; Prozone, F. M. *Chem. Commun.* **1999**, 215–216.

(9) Tunoori, A. R.; White, J. M.; Georg, G. I. *Org. Lett.* **2000**, *2*, 4091–4093.

(10) Nahm, S.; Weinreb, S. M. *Tetrahedron Lett.* **1981**, *22*, 3815–3818.

(11) Sibi, M. P. *Org. Prep. Proced. Int.* **1993**, *25*, 15–40.

(12) Overhand, M.; Hecht, S. M. *J. Org. Chem.* **1994**, *59*, 4721–4722.

(13) Lucet, D.; Le Gall, T.; Mioskowski, C.; Ploux, O.; Marquet, A. *Tetrahedron: Asymmetry* **1996**, *7*, 985–988.

(14) Angelastro, M. R.; Mehdi, S.; Burkhart, J. P.; Peet, N. P.; Bey, P. *J. Med. Chem.* **1990**, *33*, 11–13.

(15) Maugras, I.; Poncet, J.; Jouin, P. *Tetrahedron* **1990**, *46*, 2807–2816.

(16) Shreder, K.; Zhang, L.; Goodman, M. *Tetrahedron Lett.* **1998**, *39*, 221–224.

(17) Braun, M.; Waldmueller, D. *Synthesis* **1989**, 856–858.

(18) Oppolzer, W.; Cunningham, A. F. *Tetrahedron Lett.* **1986**, *27*, 5467–5470.

(19) Dechantsreiter, M. A.; Burkhart, F.; Kessler, H. *Tetrahedron Lett.* **1998**, *39*, 253–254.

(20) Einhorn, J.; Einhorn, C.; Luche, J. L. *Synth. Commun.* **1990**, *20*, 1105–1112.

(21) Sibi, M. P.; Stessman, C. C.; Schultz, J. A.; Christensen, J. W.; Lu, J.; Marvin, M. *Synth. Commun.* **1995**, *25*, 1255–1264.

TABLE 1. Preparation of Amides<sup>a</sup>

Entry	Substrate	Amine	Product	Compound Number	Yield (%) <sup>b</sup>	Reaction Time (hr)
1		HNEt <sub>2</sub>		3	98	2
2				4	74	5
3		HNEt <sub>2</sub>		5	98	2
4		HNEt <sub>2</sub>		6	96	3
5		HNEt <sub>2</sub>		7	93	2
6		HNEt <sub>2</sub>		8	67	2
7			Boc-Pro-Phe-OMe	9	75	8
8			Boc-Val-Gly-OMe	10	87	6
9			Boc-Pro-Gly-OMe	11	77	6

<sup>a</sup> All compounds in Table 1 were prepared via method A (see the Experimental Section, general procedures). <sup>b</sup> Isolated yield.

amides and peptides (Table 1) or Weinreb amides (Table 2) in a one-flask protocol by using the Deoxo-Fluor reagent. This procedure met our goals by providing a straightforward method where the resulting byproducts of the reaction<sup>22</sup> can be easily removed. As shown in Tables 1 and 2, a variety of amides can be prepared from commercially available carboxylic acids. Saturated aliphatic and cyclic acids were cleanly converted to the corresponding amides (entries 1 and 2, Table 1; entries 1 and 3, Table 2). We also prepared the Weinreb amide from *trans*-crotonic acid in good yield (entry 2, Table 2). Benzoic acids with electron-withdrawing and electron-releasing groups (entries 3 and 4, Table 1; entry 5, Table 2) and 2-thiophenecarboxylic acid (entry 5, Table 1; entry

6, Table 2) provided good yields of the amides. This methodology is also applicable to the synthesis of Weinreb amides from amino acids (entries 7–10, Table 2). Carpino has extensively studied and shown many of the advantages of utilizing amino acid fluorides in peptide bond formation.<sup>3–5,23,24</sup> As seen in Table 1 (entries 7–9), dipeptides can similarly be generated utilizing this reagent. The generation of these chiral Weinreb amides and peptides illustrates the amenability of this procedure for a racemization free protocol as determined by optical rotation and chiral HPLC.

**Additional Observations.** In our experimentation, an observation was made related to substrate compat-

(22) Reagent byproducts SO<sub>2</sub> (gas) and HN(CH<sub>2</sub>CH<sub>2</sub>OMe)<sub>2</sub> (liquid bp 170–176 °C) are easily removed under reduced pressure: *Chem. Ber.* **1959**, *92*, 1789–1797.

(23) Carpino, L. A.; Mansour, E. S. M. E.; El-Faham, A. *J. Org. Chem.* **1993**, *58*, 4162–4164.

(24) Carpino, L. A.; El-Faham, A. *J. Am. Chem. Soc.* **1995**, *117*, 5401–5402.

TABLE 2. Preparation of Weinreb Amides

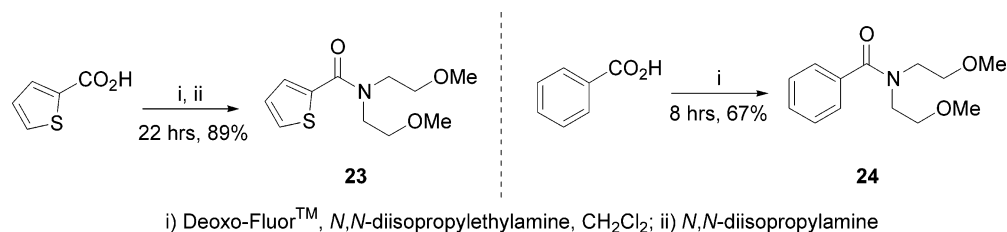
Entry	Substrate	Product	Method <sup>a</sup>	Compound Number	Yield (%) <sup>b</sup>	Reaction Time (hr)
1			B	12	82	3
2			A	13	73	8
3			B	14	85	4
4			B	15	86	8
5			B	16	92	4
6			B	17	76	5
7			A	18	90	6
8			A	19	91	6
9			A	20	86	3
10			A	21	89	5
11			B	22	83	4

<sup>a</sup> All compounds in Table 2 were prepared via method A or B as indicated (see the Experimental Section, general procedures). <sup>b</sup> Isolated yield.

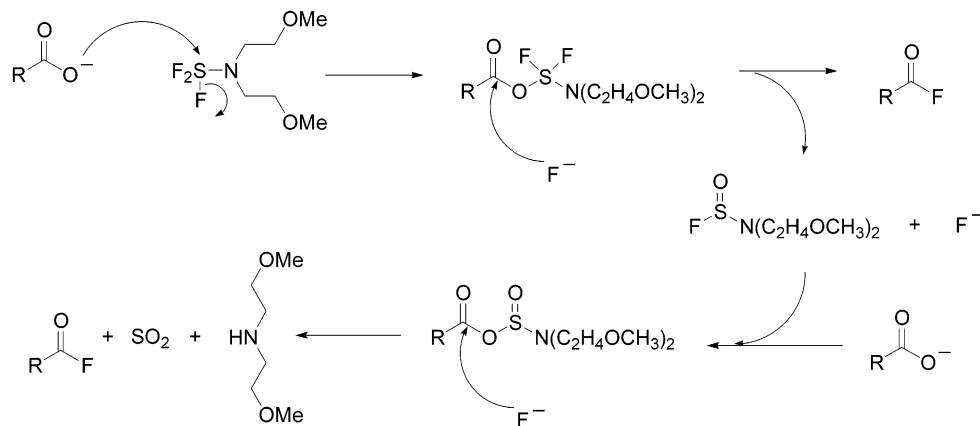
ibility in regards to this method. When we attempted to add *N,N*-diisopropylamine to the corresponding acyl fluoride of 2-thiophenecarboxylic acid, none of the desired diisopropylamide product was formed. Instead, we obtained the bis(methoxyethyl)amide exclusively (Scheme 1, **23**). In a proposed mechanism for acyl fluoride formation utilizing **1** (Scheme 2) the corresponding bis(methoxyethyl)amine is generated along with SO<sub>2</sub>.<sup>33</sup> We propose that in the case of sterically encumbered amines, or a lack of external amine, the bis(methoxyethyl)amine

side product is able to participate in the acylation reaction. This hypothesis was confirmed by treating benzoic acid with the Deoxo-Fluor reagent under our typical conditions for acid fluoride formation (Scheme 1). The reaction mixture was allowed to stir for a period of 8 h without the addition of an external, secondary amine. Upon completion, 67% of the corresponding bis(methoxyethyl)amide (Scheme 1, **24**) was generated. It has been demonstrated with this reagent<sup>7</sup> and DAST<sup>4</sup> that the intermediate acyl fluoride can be readily isolated. Typical

## SCHEME 1



## SCHEME 2



reaction times in these cases are 10–30 min. The resultant product can then be treated with the desired nucleophile in a second step.<sup>3–6</sup> This two step protocol would remedy the side product formation, however, the advantage of the one-flask reaction sequence would be lost.

The use of the Deoxo-Fluor reagent was shown to be a versatile method for acyl fluoride generation and subsequent one-flask amide coupling. It provides mild conditions and facile purification of the desired products and proceeds in good to excellent yields. We have explored the utility of this reagent for the one-flask conversion of acids to amides, Weinreb amides, and as a peptide-coupling reagent. Overall, this method appears to be a robust and easily utilized technique for the aforementioned processes.

## Experimental Section

**General Procedure. Method A.** The carboxylic acid (1 equiv) was dissolved in CH<sub>2</sub>Cl<sub>2</sub> under an argon atmosphere, cooled to 0 °C, and then *N,N*-diisopropylethylamine (1.5 equiv) and [bis(2-methoxyethyl)amino]sulfur trifluoride (1.2 equiv) were added dropwise. After being stirred for 15–30 min (acyl fluoride formation), a solution of the amine (1.5 equiv) in CH<sub>2</sub>Cl<sub>2</sub> was added. This mixture was stirred at 0 °C for an additional 15 min and then allowed to warm to room temperature. Stirring was continued for 3–8 h (monitored by TLC). After completion,

the reaction was diluted with additional CH<sub>2</sub>Cl<sub>2</sub> and sequentially extracted with aqueous saturated sodium bicarbonate, water, and brine. The organic layer was then dried over magnesium sulfate, filtered, and concentrated under reduced pressure. Purification via silica gel column chromatography then provided the final product.

**Method B.** In cases where the substrate was not soluble in CH<sub>2</sub>Cl<sub>2</sub>, *N,N*-dimethylformamide could be used. The same molar ratios were used; however, the workup protocol required dilution of the crude reaction mixture in ether, with sequential extraction using aqueous saturated sodium bicarbonate, water, and brine as before.

**Enantiopurity Determination.** The dipeptides, compounds **9**–**11**, were evaluated on the basis of reported optical rotations (see the Supporting Information for references). The enantiopurity of compounds **18**–**20** and **22** was determined by HPLC analysis. HPLC analysis was conducted using the Chiralcel AD-RH column: solvent, hexanes/2-propanol (95/5); flow rate, 1.00 mL/min; detection 225 nm. Retention times (in minutes) was found as follows: **18** (*R*) 8.2, **18** (*S*) 6.6; **19** (*R*) 7.9, **19** (*S*) 8.7; **20** (*R*) 7.0, **20** (*S*) 6.0; **22** (*R*) 5.6, **22** (*S*) 6.4. Compound **21** could not be resolved under these conditions. The optical purity was >97% for all compounds.

**Acknowledgment.** We thank Professor Apurba Datta for helpful discussions. Support for this work was provided by the National Institutes of Health (CA-084173). J.M.W. is a recipient of the NIH pre-doctoral training grant in dynamic aspects of chemical biology (GM-08454). B.J.T. is a recipient of the Department of Defense Breast Cancer pre-doctoral training grant (DAMD17-02-1-0435).

**Supporting Information Available:** A description of general methods and characterization data for all new compounds (**3**, **4**, **8**, **14**, **16**, **17**, **23**, and **24**). Compounds **5**,<sup>25</sup> **6**,<sup>26</sup> **7**,<sup>27</sup> **9**,<sup>5</sup> **11**,<sup>28</sup> **12**,<sup>29</sup> **13**,<sup>20</sup> **15**,<sup>30</sup> and **18**–**22**<sup>11,20,31,32</sup> have been previously reported. Our spectroscopic data were in agreement with the reported values. Compound **10** is commercially available. This material is available free of charge via the Internet at <http://pubs.acs.org>.

JO035658K

- (25) Yuste, F.; Origel, A. E.; Brena, L. J. *Synthesis* **1983**, 109–110.  
 (26) Kikukawa, K.; Nagira, K.; Wada, F.; Matsuda, T. *Tetrahedron* **1981**, 37, 31–36.  
 (27) Jones, E.; Moodie, I. M. *J. Chem. Soc. C* **1968**, 1195–1196.  
 (28) Mazurov, A. A.; Kabanov, V. M.; Andronati, S. A. *Dokl. Akad. Nauk SSSR* **1989**, 306, 364–366.  
 (29) Trost, B. M.; Lee, C. B. *J. Am. Chem. Soc.* **1998**, 120, 6818–6819.  
 (30) Satyamurthi, N.; Singh, J.; Aidhen, I. S. *Synthesis* **2000**, 375–382.  
 (31) Goel, O. P.; Krolls, U.; Stier, M.; Kesten, S. *Org. Synth.* **1989**, 67, 69–75.  
 (32) Angelastro, M. R.; Burkhart, J. P.; Bey, P.; Peet, N. P. *Tetrahedron Lett.* **1992**, 33, 3265–3268.  
 (33) Hudlicky, M. *Org. React.* **1988**, 25, 513.

## Amino Acid-Derived Enaminones: A Study in Ring Formation Providing Valuable Asymmetric Synthons

Brandon J. Turunen and Gunda I. Georg\*

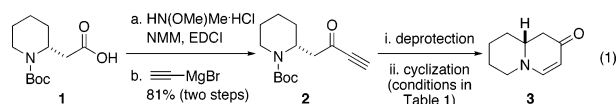
Department of Medicinal Chemistry and Center for Methodology and Library Development, University of Kansas, 1251 Wescoe Hall Drive, Lawrence, Kansas 66045

Received February 7, 2006; E-mail: georg@ku.edu

Cyclic, six-membered enaminones (vinylogous amides) represent a class of molecules that demonstrate unique chemical and biological properties.<sup>1</sup> These compounds serve as multident scaffolds in the stereoselective preparation of alkaloid natural products.<sup>2</sup> Indeed, those that are bicyclic in nature, resembling indolizidine, quinolizidine, and quinolinone alkaloids, are particularly attractive.<sup>3</sup> Since few direct methods exist for accessing bicyclic, asymmetric intermediates of this type, our group initiated the exploration of a new chiral pool approach.<sup>4</sup> While intermolecular 1,4-additions of aliphatic amines to ynones have been known for nearly 40 years,<sup>5</sup> we have found no examples of an intramolecular (6-*endo-dig*) variant. Although 6-*endo-dig* ring closures are classified as favorable transformations<sup>6</sup> in aliphatic systems, very few examples exist with first periodic row elements.<sup>7,8</sup> We disclose herein the results of our investigation of 6-*endo-dig* ring closures of a nonattenuated amine into a pendant ynone.

Executing this enaminone formation strategy, as shown in Figure 1, relied upon production of amino-ynone intermediates. Such substrates could be accessed via  $\beta$ -amino acids, providing both diversity and asymmetry. Of particular interest to us was the mode of intramolecular addition, several of which are possible (Figure 1, inset A–C).<sup>8,9</sup>

To test the feasibility of the reaction, we first targeted known bicyclic enaminone **3** (eq 1).<sup>10</sup> The requisite ynone (**2**) was generated from the commercially available acid **1** via Weinreb amide formation and subsequent addition of ethynylmagnesium bromide (two steps, 81% yield).



A two-tier optimization of both amine deprotection and subsequent cyclization to convert **2** to **3** was next initiated. Early efforts revealed that no enaminone formation occurred under the conditions of acidic amine deprotection. However, when employing TFA to remove Boc, followed by basic aqueous workup, the desired enaminone (**3**) was formed (entry 1, Table 1), albeit in modest yield. This indicated the desired product formed under the conditions of basic workup. In attempts to optimize this transformation, the crude TFA salt derived from deprotection (entry 2) was subjected to *anhydrous* basic conditions, but formation of enaminone **3** was not observed. Under these same conditions, with the addition of water, the enaminone **3** was generated (entry 3), although the yield was still unsatisfactory. When HCl was used in place of TFA, again, no product was observed under anhydrous conditions (entry 4); however, **3** was isolated in good yield and with short reaction times with the addition of water (entries 5 and 6). Conditions found to be optimal were employing either HCl or TMS–I to facilitate deprotection and a solution of K<sub>2</sub>CO<sub>3</sub> in methanol to promote enaminone formation (entries 7 and 8, respectively).

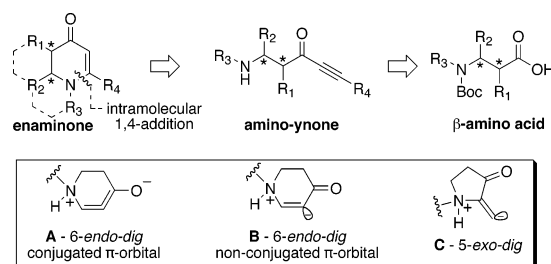


Figure 1. Intramolecular 1,4-addition strategy.

Table 1. Optimization of Deprotection and Cyclization

entry	i. deprotection	ii. cyclization	time	yield <sup>a</sup>
1	TFA, CH <sub>2</sub> Cl <sub>2</sub>	standard workup <sup>b</sup>		30
2	TFA, CH <sub>2</sub> Cl <sub>2</sub>	THF or CH <sub>2</sub> Cl <sub>2</sub> , K <sub>2</sub> CO <sub>3</sub>	20 h	0
3	TFA, CH <sub>2</sub> Cl <sub>2</sub>	CH <sub>2</sub> Cl <sub>2</sub> , H <sub>2</sub> O, K <sub>2</sub> CO <sub>3</sub>	5 h	38
4	4 N HCl/dioxane	THF or CH <sub>2</sub> Cl <sub>2</sub> , K <sub>2</sub> CO <sub>3</sub>	20 h	0
5	4 N HCl/dioxane	CH <sub>2</sub> Cl <sub>2</sub> , H <sub>2</sub> O, K <sub>2</sub> CO <sub>3</sub>	1 h	74
6	4 N HCl/dioxane	THF, H <sub>2</sub> O, K <sub>2</sub> CO <sub>3</sub>	1 h	75
7	4 N HCl/dioxane	MeOH, K <sub>2</sub> CO <sub>3</sub>	15 min	87
8	TMS–I, CH <sub>2</sub> Cl <sub>2</sub>	MeOH, K <sub>2</sub> CO <sub>3</sub>	30 min	95

<sup>a</sup> Isolated yield. <sup>b</sup> CH<sub>2</sub>Cl<sub>2</sub>/sat. aqueous NaHCO<sub>3</sub> (1:1).

Because of the operational simplicity of the HCl protocol (entry 7, Table 1), this method was employed unless the gentler conditions offered by TMS–I (entry 8) were desired.<sup>11</sup> With both deprotection methods, the cyclization environment was held constant (Table 2). With ynones of undefined stereochemistry (compounds **4**–**8**), quinolizidine (**15** and **16**) and indolizidine (**17**–**19**) systems are accessed in excellent yields. Terminally substituted ynones are well tolerated, allowing installation of aliphatic and aromatic substituents adjacent to the ring-fused nitrogen (**15**, **16**, **18**, **19**, and **21**). Using stereodefined substrates (**2**, **9**, **10**, **13**, and **14**), as well as chiral but racemic ynones (**11** and **12**), maintenance of asymmetry was evaluated. The quinolizidine **3** and the pyridinones **20**<sup>12</sup> and **21** are obtained in excellent yields with minimal, if any, loss of optical purity.<sup>13</sup> We next turned to ynone pairs with a built in preference to convert to a more favorable diastereomer (**11** and **12**, **13** and **14**). Both the racemic *trans*- and *cis*-fused quinolinones **22** and **23** can be accessed in excellent yields; however, some diastereomeric interconversion is observed.<sup>14</sup> The hydroxylated pyrrolidine ynones **13** and **14** formed the bicyclic indolizidine core in reasonable yields; however, the stereogenic center adjacent to the amine is compromised. As expected, the pyrrolidine ring with *anti*-substituents (**13**) provided a diastereomeric ratio superior to that with the *syn*-appendages (**14**). With careful addition of TMS–I (**24** and **25**, method 2), this can be minimized, providing improved yields and, more significantly, synthetically useful diastereomeric ratios.<sup>15</sup>

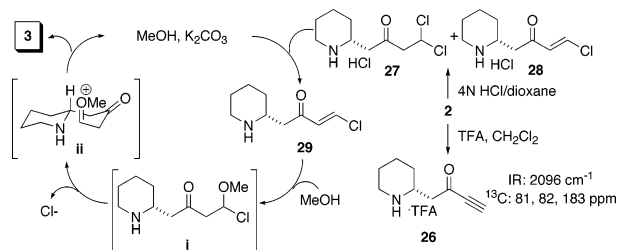
Two experimental observations were made which provided insight into the reaction pathway. The first was that deprotection reagents that incorporate a halogen counteranion (e.g., HCl or TMS–I) improved reaction yields. Comparison of the crude amine



**Table 2.** Ynone to Enaminone Conversion

ynone	enaminone	yield <sup>a,b</sup>	dr or er <sup>c</sup>
2	3	87	er = 97/03 <sup>d</sup>
4	15	87	—
5	16	91	—
6	17	89	—
7	18	87	—
8	19	89	—
9	20	92	er = >95/05 <sup>e</sup>
10	21	96	er = >95/05 <sup>e</sup>
11	22	99	dr = 96/04 <sup>f</sup>
12	23	96	dr = 80/20 <sup>f</sup>
13	24	77	dr = 85/15 <sup>f</sup>
14	25	94 <sup>b</sup>	dr = 96/04 <sup>f</sup>
		60	dr = 60/40 <sup>f</sup>
		70 <sup>b</sup>	dr = 86/14 <sup>f</sup>

<sup>a</sup> Isolated yield. <sup>b</sup> All enaminones were prepared employing method 1 unless indicated by superscript *b*, in these cases, method 2 was used. Method 1: (a) 4 M HCl/dioxane, (b) MeOH, K<sub>2</sub>CO<sub>3</sub>. Method 2: (a) TMS-I, CH<sub>2</sub>Cl<sub>2</sub>, -78 to 0 °C, (b) MeOH, K<sub>2</sub>CO<sub>3</sub>. <sup>c</sup> As determined by the following method. <sup>d</sup> Chiral HPLC. <sup>e</sup> <sup>1</sup>H NMR analysis of Mosher amide derivatives. <sup>f</sup> <sup>1</sup>H NMR.

**Figure 2.** Proposed enaminone formation pathway.

TFA and HCl salts revealed their marked difference in reactivity. The TFA salt (**26**, Figure 2) clearly presented characteristics of the intact ynone. The HCl salt, on the other hand, appeared as a 6:1 mixture of two compounds, the dichloroethane derivative **27** and the vinylogous acid chloride **28**. The second observation was that an oxygen nucleophile (MeOH or H<sub>2</sub>O) was necessary for cyclization regardless of the deprotection method. Under the prescribed reaction conditions, in an NMR tube, it was observed that the mixture of **27** and **28** first converts to only **29** then to enaminone **3**. Although we have no direct evidence, the dependence upon water or methanol may be explained by an addition–elimination sequence via intermediates **i** and **ii** (Figure 2).<sup>16</sup> A similar path can be envisaged from TFA ynone salt **26** via a dimethyl acetal intermediate, bringing to light the dependency on exogenous oxygen nucleophiles with both the TFA and HCl salts.<sup>17</sup>

In summary, we have developed a remarkably simple protocol for preparing valuable synthetic intermediates that previously were only obtainable in a circuitous fashion. Preliminary data in these laboratories indicate that the proposed 6-*endo-dig* mode of cyclization does not occur. Instead, enaminone formation proceeds via an

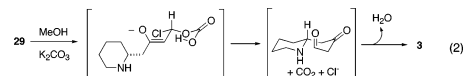
addition–elimination pathway which is controlled by judicious selection of deprotection reagent and reaction solvent. Further investigations concerning the mechanism and synthetic utility of this process are ongoing.

**Acknowledgment.** We thank the National Institutes of Health for their generous support of our programs (NIH CA 90602 and NIH GM069663). We thank Micah Niphakis for preparing **24** and **25** in Table 2 by method 2. B.J.T. was supported by the Department of Defense breast cancer predoctoral fellowship (DAMD17-02-1-0435).

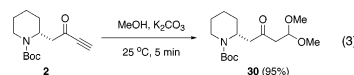
**Supporting Information Available:** Representative experimental procedures, characterization data for all new compounds, and spectra for compounds **2**, **4**–**19**, **21**–**26**, **29**, and **30**. This material is available free of charge via the Internet at <http://pubs.acs.org>.

## References

- (1) For recent reviews, see: (a) Negri, G.; Kascheres, C.; Kascheres, A. J. *J. Heterocycl. Chem.* **2004**, *41*, 461–491. (b) Elassar, A.-Z. A.; El-Khair, A. A. *Tetrahedron* **2003**, *59*, 8463–8480.
- (2) (a) Michael, J. P.; De Koning, C. B.; Gravestock, D.; Hosken, G. D.; Howard, A. S.; Jungmann, C. M.; Krause, R. W. M.; Parsons, A. S.; Pelly, S. C.; Stanbury, T. V. *Pure Appl. Chem.* **1999**, *71*, 979–988. (b) Comins, D. L. *J. Heterocycl. Chem.* **1999**, *36*, 1491–1500.
- (3) Cordell, G. A. *The Alkaloids: Chemistry and Biology*, 60; Elsevier: Amsterdam, The Netherlands, 2003.
- (4) For a scalemic example, see: (a) Slosse, P.; Hootel, C. *Tetrahedron* **1981**, *37*, 4287–4294. For examples in which an intermediate enaminone or related structure is then converted to a bicycle, see: (b) refs 2a and 2b. (c) Back, T. G.; Hamilton, M. D.; Lim, V. J. J.; Parvez, M. *J. Org. Chem.* **2005**, *70*, 967–972.
- (5) Huisgen, R.; Herbig, K.; Siegl, A.; Huber, H. *Chem. Ber.* **1966**, *99*, 2526–2545.
- (6) Baldwin, J. E. *J. Chem. Soc., Chem. Commun.* **1976**, 734–736.
- (7) For attempts with oxygen nucleophiles, see: (a) Suzuki, K.; Nakata, T. *Org. Lett.* **2002**, *4*, 2739–2741. (b) Dreessen, S.; Schabbert, S.; Schaubmann, E. E. *J. Org. Chem.* **2001**, 245–251.
- (8) For a notable exception using carbon nucleophiles which inspired our approach, see: Lavalley, J. F.; Berthiaume, G.; Deslongchamps, P.; Grein, F. *Tetrahedron Lett.* **1986**, *27*, 5455–5458.
- (9) Rudolf, W. D.; Schwarz, R. *Synlett* **1993**, 369–374.
- (10) Comins, D. L.; LaMunyon, D. H. *J. Org. Chem.* **1992**, *57*, 5807–5809.
- (11) Olah, G. A.; Narang, S. C. *Tetrahedron* **1982**, *38*, 2225–2277.
- (12) Comins, D. L.; Zhang, Y.; Joseph, S. P. *Org. Lett.* **1999**, *1*, 657–659.
- (13) Retro-Michael and retro-Mannich-type processes have been reported previously on  $\beta$ -amino ketones. For examples, see: (a) Slosse, P.; Hootel, C. *Tetrahedron* **1981**, *37*, 4287–4294. (b) Morley, C.; Knight, D. W.; Share, A. C. *J. Chem. Soc., Perkin Trans. 1* **1994**, 2903–2907. (c) Harrison, J. R.; O'Brien, P.; Porter, D. W.; Smith, N. M. *J. Chem. Soc., Perkin Trans. 1* **1999**, 3623–3631.
- (14) Diastereomeric conversion in these examples (**22** and **23**) may be explained by simple enolization.
- (15) Studies are underway to clearly determine how this protocol is able to suppress the diastereomeric interconversion.
- (16) Under anhydrous conditions or when a sterically demanding alcohol was employed as solvent (e.g., *s*-BuOH), **29** was recovered and formation of **3** was not observed. An alternative pathway to **3**, suggested by Professor Barry M. Trost, involves addition of a carboxylate anion to **29** (eq 2). The poor solubility of this nucleophile in *s*-BuOH or other anhydrous solvents (THF or CH<sub>2</sub>Cl<sub>2</sub>) could account for these observations.



- (17) When ynone **2** was subjected to reaction conditions, near quantitative conversion to **30** was observed (eq 3).



JA0609046